

Control of Innate Antiviral Immunity by HIV-1

Arjun Rustagi

A dissertation

submitted in partial fulfillment of the
requirements for the degree of

Doctor of Philosophy

University of Washington

2013

Reading Committee:

Michael Gale, Jr., Chair

Michael Emerman

Helen Horton

Program Authorized to Offer Degree:

Pathobiology Group

©Copyright 2013

Arjun Rustagi

University of Washington

Abstract

Control of Innate Antiviral Immunity by HIV-1

Arjun Rustagi

Chair of the Supervisory Committee:

Professor Michael Gale, Jr.

Departments of Immunology, Microbiology, and Global Health

Human immunodeficiency virus 1 (HIV-1) infection continues to be a major public health problem, with 34 million people infected worldwide. Cell-intrinsic innate immune defenses are essential for the control of HIV-1 infection but are subverted by the virus to establish successful infection. Interferon regulatory factor 3 (IRF3) is a central transcription factor of innate immune signaling that is activated by cellular pattern recognition receptors in response to the presence of non-self molecules (e.g. viral RNA or DNA). Activation of IRF3 induces the expression of antiviral and immunomodulatory genes whose products can suppress HIV-1 infection within target cells and regulate the adaptive immune response to infection. We have found that during acute infection HIV-1 evades innate antiviral immunity through the actions of HIV-1 viral protein *u* (Vpu), which interacts with IRF3 and inhibits its activity. While

HIV infection eventually results in proteolytic destruction of IRF3 at later time points of acute infection, we found that inhibition of IRF3-dependent IFN- β transcription by Vpu occurs at early time points. In addition, Vpu blocked both IRF3- and NF κ B-dependent activities at the IFN- β promoter. These findings led us to hypothesize that Vpu blocks IRF3 activation to prevent IRF3 from carrying out the necessary biochemical steps to drive antiviral gene expression. We investigated the process of Vpu regulation of IRF3, and found that IRF3 and Vpu form a stable complex during infection of CD4⁺ T cells with HIV-1. Using truncation and deletion mutants of recombinant IRF3, we mapped the binding epitope for Vpu on IRF3 to a region of IRF3 protein called the IRF association domain. This domain is the site necessary for homodimerization of IRF3 molecules after activation and interaction with transcriptional cofactors. Thus, we hypothesized that Vpu alters IRF3 dimerization and cofactor interaction. Indeed, when we examined the IRF3 activation pathway in the presence of Vpu to identify the site of the Vpu-induced block in IRF3 activity, we found that Vpu inhibited IRF3 dimerization and CBP binding. We predict that Vpu antagonism of IRF3-directed innate immunity is a key step in HIV-1 pathogenesis during acute infection. Further, IRF3 depletion and control of innate antiviral immunity by HIV-1 may correlate with disease progression in HIV-infected patients. To test these predictions, we have developed two novel monoclonal antibodies to human IRF3 to support the study of IRF3 activation and HIV-mediated IRF3 depletion among patient samples in a high-throughput manner. One of these antibodies, AR-1, is specific for activated IRF3. The other, AR-2, detects total IRF3 levels in a flow cytometric assay of blood leukocytes. Use of these new antibodies to study IRF-3 levels during HIV infection could reveal an innate immune correlate of HIV-1 disease progression, while studies to fully define the interaction between Vpu

and IRF3 may reveal novel targets for the development of drugs that preserve IRF3 activity during HIV-1 infection.

Acknowledgments

I thank Mike, for providing me with the resources and guidance needed to succeed, and Brian, whose work formed the basis of my projects and who taught me HIV research methods. I also thank Stacy, whose encouragement helped me weather experimental difficulties, and whose mentorship was critical to my development as a scientist. Finally, I thank my wife Alison, and daughter Sonia, for their love and understanding throughout my graduate training and the necessary time away from them.

TABLE OF CONTENTS

I. INTRODUCTION	1
INNATE IMMUNITY	1
PRR SIGNALING	3
Toll-like receptors.....	4
RIG-I-like receptors	6
Nucleotide-binding domain and leucine-rich repeat-containing proteins.....	8
DNA sensors	9
Sensing of HIV-1	11
IRF FAMILY AND IRF3	13
THE IRF3 ACTIVATION CYCLE	15
IRF3-DRIVEN AND INTERFERON-STIMULATED GENES.....	17
ANTAGONISM OF IRF3 FUNCTION BY VIRUSES	21
MODULATION OF INNATE IMMUNITY BY HIV-1	23
II. DEVELOPMENT OF MONOCLONAL ANTIBODIES AGAINST IRF3	29
ABSTRACT	29
INTRODUCTION.....	29
MATERIAL AND METHODS.....	35
Cells, transfections, and subcellular fractionation	35
Viral stocks and infections.....	36
Monoclonal antibody production and screening.....	36

Immunoblot analysis and fluorescent microscopy.....	37
Flow cytometry.....	37
RESULTS AND DISCUSSION.....	38
CONCLUSIONS.....	54
ACKNOWLEDGMENTS.....	55
ADDENDUM.....	56
III. VPU IS NECESSARY AND SUFFICIENT TO INHIBIT IRF3 FUNCTION	58
ABSTRACT.....	58
INTRODUCTION.....	59
MATERIALS AND METHODS.....	62
Cells and transfections.....	62
Plasmids.....	63
Dual luciferase assay and statistics.....	63
Viral stocks and infections.....	64
Targeted genomics and data analysis.....	64
RESULTS.....	64
DISCUSSION.....	74
CONCLUSIONS.....	75
IV. VPU BINDS IRF3 AND INHIBITS ITS DIMERIZATION AND CBP	77
INTERACTION.....	77
INTRODUCTION.....	77
MATERIALS AND METHODS.....	78

Cells and transfections	78
Plasmids	79
Viral stocks and infections.....	80
Immunoprecipitation and immunoblot	80
RESULTS.....	80
DISCUSSION.....	87
CONCLUSIONS	89
V. CONCLUSIONS AND FUTURE DIRECTIONS.....	90
DEVELOPMENT OF MONOCLONAL ANTIBODIES AGAINST IRF3.....	90
VPU IS NECESSARY AND SUFFICIENT TO INHIBIT IRF3 FUNCTION	91
VPU BINDS IRF3 AND INHIBITS ITS DIMERIZATION AND CBP INTERACTION	93
VI. REFERENCES	99

TABLE OF FIGURES

Figure I-1: Map of signaling pathways downstream of select TLRs (Fig. 3 from [15], used by permission – copyright license # 3190921063703).	5
Figure I-2: Cytosolic sensing of RNA viruses (Fig. 3 from [40], used by permission – copyright license #3166690760831).	8
Figure I-3: The HIV life cycle (Fig. 1 from [71], used by permission – copyright license # 3173480006938).	12
Figure I-4: Schematic of IRF3 functional domains. DBD – DNA-binding domain; NLS – nuclear localization sequence; NES – nuclear export sequence; PRO – proline-rich region; IAD – IRF association domain; SRR – serine-rich region.....	16
Figure II-1: Schematic of IRF3 phosphorylation, dimerization, nuclear translocation, ubiquitination (designated by “Ub”) and degradation that occur during normal activation over a 48-hour time course.	32
Figure II-2: SDS-PAGE followed by immunoblot analysis of IRF3 in SupT1 cells infected with SenV over the indicated time course. Three film exposures are shown for the AR-1 mAb (top), ordered from shortest (first) to longest time of exposure (third). Protein samples were re-run on a separate gel for probing with the AR-2 mAb (bottom). Actin and GAPDH are loading controls. For IRF3, the indicated bands mark resting IRF3 (black arrows).	39
Figure II-3: SDS-PAGE followed by immunoblot analysis of phospho-S396 IRF3, total IRF3, ISG56, and SenV proteins in infected 293T cells at the indicated timepoints. For IRF3, an upper band (black arrow) corresponds to phosphorylated IRF3 (grey triangle).....	40
Figure II-4: Nuclear/cytoplasmic fractionation followed by SDS-PAGE and immunoblot analysis of IRF3 in 293T cells infected with SenV for 18 hrs. Short (top panel) and long (bottom panel) film exposures are shown. Lamin B (nuclear) and GAPDH (cytoplasmic) markers are shown.	41

Figure II-5: SDS-PAGE followed by immunoblot analysis of IRF3 and HIV gag in SupT1 cells infected with HIV _{LAI} (MOI 1) for the indicated timepoints. Black arrow indicates the mature form of HIV gag protein (p24).....	42
Figure II-6: SDS-PAGE followed by immunoblot analysis of extracts of SupT1 cells, wild type (wt) or stably expressing shRNA to IRF3 (IRF3 kd) or non-targeting vector (NTV).....	43
Figure II-7: SDS-PAGE followed by immunoblot analysis of IRF3 in human (SupT1, human PBMC, and 293T), African green monkey (Vero), rhesus macaque, and mouse, using the indicated antibodies.	44
Figure II-8: Sequence alignment using ClustalW of reference protein sequences for IRF3 from human (NCBI Reference Sequence NP_001562.1), rhesus macaque (NP_001129269.1), Vero cell ([222]) and mouse (NP_058545.1), visualized in Jalview. Identical amino acids between at least two species are colored.....	45
Figure II-9: SDS-PAGE followed by immunoblot analysis of IRF3 in 293Ts that were mock transfected or transiently transfected for 36 hrs with BL-CMV-IRF3 or BL-CMV-IRF3 Δ N. For IRF3, the band corresponding to resting full-length IRF3 (grey triangle) and the three bands corresponding to IRF3 Δ N (black arrow) are indicated.	46
Figure II-10: Immunofluorescence analysis of IRF3 (AR-1 mAb, green) and nuclei (DAPI, blue) in TZM-bl cells infected with SenV for 18 hrs.....	47
Figure II-11: ImageStream analysis of IRF3 (AR-1 mAb, green) and nuclei (DAPI, red) in SupT1 cells mock or SenV-infected for 18 hrs. Representative brightfield, red, green, and red/green merge images are shown (top). Analysis of IRF3/DAPI colocalization on the whole population is quantified (bottom). The percentage of cells with similarity values above an arbitrary value of 2 is shown.	49
Figure II-12: Flow cytometry analysis of SupT1 cells using isotype control antibody or AR-1 mAb (IRF3).....	50
Figure II-13: Flow cytometry analysis of IRF3 in SupT1 cells infected with SenV for the indicated timepoints. Mock refers to 0 hrs of infection.	51

Figure II-14: SDS-PAGE followed by immunoblot analysis of IRF3 in the same cells used in Figure II-13.	52
Figure II-15: Native PAGE followed by immunoblot analysis for IRF3 in SupT1 cells infected with SenV for 18 hrs. A rabbit polyclonal antibody or AR-1 mAb was used to detect IRF3. Arrows indicate monomeric IRF3. Short (top) and long (bottom) film exposures are shown.	53
Figure II-16: Native PAGE followed by immunoblot analysis for IRF3 using supernatants from five hybridoma clones. Clone number 1 represents AR-1 mAb, while clone number 2 represents AR-2 mAb. Short and long film exposures of each immunoblot assay are shown as in 4A.	54
Figure II-17: SDS-PAGE followed by immunoblot analysis for IRF3 (AR-1) for loading control.	54
Figure II-18: Immunofluorescence analysis of IRF3 (AR-2 mAb, green) and nuclei (DAPI, blue) in TZM-bl cells infected with SenV for 18 hrs.	57
Figure III-1: NL4-3 Vpu inhibits IFN- β promoter activity. Fold induction of IFN- β promoter (as represented by firefly to renilla luciferase activity ratio) after transfection with IRF3 and Vpu constructs, followed by infection with SenV. White bars represent mock-infected cell lysates; grey bars represent SenV-infected cell lysates. Data represented as mean \pm standard deviation (SD). $N \geq 3$ biological replicates. Two-tailed Student's t -test was used to compare Vpu-transfected samples to vector-transfected for each condition. **** $P \leq 0.0001$; ** $P \leq 0.01$	65
Figure III-2: Q23-17 Vpu inhibits IFN- β promoter activity. Fold induction of IFN- β promoter (as represented by firefly to renilla luciferase activity ratio) after transfection with IRF3 and Vpu constructs, followed by infection with SenV. White bars represent mock-infected cell lysates; grey bars represent SenV-infected cell lysates. Data represented as mean \pm SD. $N \geq 3$ biological replicates. Two-tailed Student's t -test was used to compare Vpu-transfected samples to vector-transfected for each condition. **** $P \leq 0.0001$	66

Figure III-3: Vpu from NL4-3 and WITO inhibit IFN- β promoter activity in a dose-dependent manner. Fold induction of IFN- β promoter (as represented by firefly to renilla luciferase activity ratio) after transfection with a dose response of NL4-3 and WITO Vpu constructs, followed by infection with SenV. The decreased doses represent 2- and 4-fold reductions in Vpu plasmid with vector plasmid added to maintain equal DNA amounts. White bars represent mock-infected cell lysates; grey bars represent SenV-infected cell lysates. Data represented as mean \pm SD. $N \geq 3$ biological replicates. Two-way ANOVA with Bonferroni post-tests was used. **** $P \leq 0.0001$; ** $P \leq 0.01$ 67

Figure III-4: Vpu from NL4-3 and WITO inhibit NF κ B activity. Fold induction of limited promoters (as represented by firefly to renilla luciferase activity ratio) containing five NF κ B binding sites (left) or PRDII sequence (right) after transfection with NL4-3 and WITO Vpu constructs, followed by infection with SenV. White bars represent mock-infected cell lysates; grey bars represent SenV-infected cell lysates. Data represented as mean \pm SD. $N \geq 3$ biological replicates. Two-way ANOVA with Bonferroni post-tests was used. **** $P \leq 0.0001$; *** $P \leq 0.001$ 69

Figure III-5: Vpu from NL4-3 and WITO inhibit IRF3 activity. Fold induction (as represented by firefly to renilla luciferase activity ratio) of limited promoters containing a single IRF3 binding site (left) or the IFN- β promoter with mutated NF κ B DNA-binding site (right) after transfection with NL4-3 and WITO Vpu constructs, followed by infection with SenV. White bars represent mock-infected cell lysates; grey bars represent SenV-infected cell lysates. Data represented as mean \pm SD. $N \geq 3$ biological replicates. Two-way ANOVA with Bonferroni post-tests was used **** $P \leq 0.0001$ 69

Figure III-6: Hierarchical clustering of differentially expressed genes between HIV-1_{JR-CSF} and HIV-1_{JR-CSF A/C} infected samples. Differentially expressed genes are shown as log₁₀(ratio) of infected to mock-infected. Genes whose expression was significantly different in HIV-1_{JR-CSF A/C} relative to mock-infected cells are depicted in the heat map (1.5 fold; $P \leq 0.01$). 71

Figure III-7: Network analysis of the top 25 genes upregulated during HIV-1_{JR-CSF A/C} infection with biological function indicated. Solid arrows indicate direct interaction between those

proteins/genes has been reported, dashed lines indicate indirect interaction (interaction through 1 or more proteins).	73
Figure IV-1: Model of IRF3 protein domains during the activation process (Fig. 4 from [235], used by permission – copyright license #3192260093436).	78
Figure IV-2: Overexpressed Vpu and IRF3 form a stable complex. IP of IRF3 and Vpu using FLAG antibody was performed in 293T cells transfected with FLAG vector or FLAG-IRF3 along with NL4-3 Vpu for 30 hrs. Cells were then infected with SenV (+) or mock infected (-) for 18 hrs prior to harvest. Input cell lysates (left) and FLAG IPed lysates (right) are shown.	81
Figure IV-3: During HIV-1 infection, Vpu and endogenous IRF3 form a stable complex. IP of IRF3 and Vpu using IRF3 antibody or IgG control was performed in SupT1 cells infected for 24 hrs with HIV _{LAI} with or without chloroquine (CQ). For CQ infections, SupT1 cells were pretreated with CQ for 12 hrs prior to infection with HIV _{LAI} , at which point CQ was re-added. Input cell lysates (left) and IPed lysates (right) are shown. IRF3 IP and IgG IP images were taken from the same exposures of the same blots.	82
Figure IV-4: NL4-3 Vpu binds to IRF3 between amino acids 240 and 328. IP of IRF3 mutants and coexpressed NL4-3 Vpu using FLAG antibody was performed in 293T cells transfected with the indicated FLAG-IRF3 constructs along with NL4-3 Vpu for 48hrs. Full-length, wild type (wt) IRF3 has amino acids 1-427, IRF3 5D is full-length and constitutively active, and the amino acids contained in each truncation mutant are indicated. Input cell lysate (left) and IPed lysate (right) are shown.	83
Figure IV-5: Schematic of IRF3 mutants used in Figure IV-4. A summary of the binding results from Figure IV-4 is indicated in the column on the right. The Vpu binding site is indicated in red. DBD, DNA-binding domain; NES, nuclear export sequence; PRO, proline-rich region; RD/IAD, regulatory domain/IRF association domain; SRR, serine-rich region.	84
Figure IV-6: IRF3 multimerization is reduced in cells expressing NL4-3 Vpu. Native and SDS PAGE followed by immunoblot for FLAG (marking IRF3 on native and SDS gels) and Vpu (on SDS gel) was performed in 293 cells infected with SenV (+) or mock infected (-).	

Densitometry of IRF3 dimer during SenV infection (middle band on native blot), as a percentage of pcDNA-transfected cells, is represented in the bar graph (bottom). 86

Figure IV-7: IRF3 interaction with CBP is reduced in cells expressing Vpu. IP using CBP antibody or IgG control was performed in 293 cells transfected with NL4-3 Vpu and FLAG-IRF3 and infected with SenV (+) or mock infected (-). Input cell lysates (left) and IPed lysates (right) are shown. Densitometry of FLAG-IRF3 IPed by CBP antibody during SenV infection, as a percentage of pcDNA-transfected cells, is represented in the bar graph (bottom)..... 87

TABLE OF TABLES

Table I-1: IRF3-driven genes.....	18
Table I-2: A subset of ISGs and their functions	20
Table I-3: Virus-encoded antagonists of innate immunity	22
Table II-1: Summary of new monoclonal antibody properties. TBD, to be determined.....	55
Table III-1: Number of genes annotated with each GO term and the associated <i>P</i> values for genes of a certain GO category to be differentially regulated by HIV-1 \pm Vpu.....	72

ABBREVIATIONS

LPS – lipopolysaccharide

PAMP – pathogen-associated molecular pattern

PRR – pattern recognition receptor

TLR – toll-like receptor

RLLR – RIG-I-like receptor

pDC – plasmacytoid dendritic cell

cDC – conventional (myeloid) dendritic cell

IFN – interferon

HIV-1 – human immunodeficiency virus-1

IRF3 – interferon regulatory factor 3

ss – single-stranded

ds – double-stranded

RNA – ribonucleic acid

DNA – deoxyribonucleic acid

NF κ B - nuclear factor κ -light-chain-enhancer of activated B cells

RIG-I – retinoic acid-inducible gene-I

MDA5 – melanoma differentiation-associated gene 5

LGP2 – laboratory of genetics and physiology 2

CARD – caspase activation and recruitment domain

MAVS – mitochondrial antiviral signaling protein

STING – stimulator of interferon genes

OAS1 – oligoadenylate synthase

NLR - nucleotide-binding domain and leucine-rich repeat-containing proteins

DAI – DNA-dependent activator of IRFs

cGAS – cyclic GMP-AMP synthetase
STING – stimulator of interferon genes
PYHIN – pyrin and HIN-200 domain-containing
Trex1 – 3' exonuclease
DBD – DNA-binding domain
ISRE – IFN-stimulated response element
IAD – IRF association domain
CBP – CREB-binding protein
ISG – interferon-stimulated gene
mAb – monoclonal antibody

I. INTRODUCTION

INNATE IMMUNITY

Until the late 1980s, the concept of the immune system had been one of defense against pathogens mediated primarily by antigen-specific immune cells comprising the adaptive immune response [1]. However, the observation that adjuvants consisting of microbe-derived products (like bacterial lipopolysaccharide, or LPS) were required for immune signaling events that themselves were required for strong adaptive immunity led Charles Janeway to hypothesize that in a layer of the immune system, called the innate immune system, detection of pathogen-associated molecular patterns (PAMPs) by germline-encoded cellular pattern recognition receptors (PRRs) leads to the transmission of signals that provide proper costimulatory signals for adaptive immune cells [1, 2]. This hypothesis has been since supported by numerous studies of PRR agonists and their effects on antigen-presenting cell (APC) costimulatory molecule expression and immune cell activation (reviewed in [3, 4]). Some PRRs are expressed almost exclusively in immune cells (e.g. toll-like receptors, or TLRs) and others are expressed in most tissue cell types (e.g. RIG-I-like receptors, or RLRs) [4], and all the PRR families have expanded greatly since Janeway first published his theory.

Antigen-presenting cells have been further delineated into a diverse family, with cell types tailored to specific roles in innate immunity, such as plasmacytoid dendritic cells (pDCs; producers of systemically-acting interferon), conventional myeloid dendritic cells (cDCs; potent antigen presenters in lymph nodes), monocyte DCs, and tissue-resident dendritic cells (peripheral tissue surveillance and antigen processing) [5]. Further, DC subsets can be distinguished by

surface receptor or other protein expression; for example, CD8 α + DCs (in mice) and the equivalent DNGR-1+/BDCA3+ DCs (in humans) are particularly proficient at cross-presentation of consumed cell debris-associated viral antigens and induction of antiviral T cell responses [6, 7]. Additional immune cell types have been characterized that have effector function but not antigen specificity, such as natural killer (NK) and NKT cells, while the characterization of the macrophage has expanded to include different types that are variously responsible for wound healing, bacterial clearance, and peripheral inflammatory cell (e.g. neutrophil) recruitment.

While an understanding of innate immune effector cells and the PRRs they use provide credence to Janeway's predictions, it has become clear that all nucleated cells have the capacity to respond to pathogens by sensing certain PAMPs of a non-self origin, and in the case of viral PAMPs, producing type I (α and β) interferon (IFN). The effect of type I IFN production in tissues is the activation of the type I IFN receptor, resulting in the induction of hundreds of interferon-stimulated genes (ISGs) in the same or nearby cells that create an antiviral state and promote antigen presentation to immune cells [8, 9]. The antiviral state is established through the actions of antiviral ISG products that may interact directly with viruses or may shut down host protein translation machinery to prevent appropriation by viruses, for example. Production of type I IFN as a result of sensing of pathogen infection by infected target cells or dendritic cells guides the development of adaptive immune cells, including promotion of adaptive antiviral responses by CD8+ and CD4+ T cells [10, 11]. In addition, B and T cells themselves express a varying complement of PRRs that are important for adaptive immune function and cell survival [12, 13]. In summary, innate immune cells and innate immune signaling provide the initial response to microbial infection, with complete pathogen clearance arising from innate immunity-stimulated gene products and appropriate training of the adaptive immune response.

Human immunodeficiency virus-1 (HIV-1) remains a major global health problem and is the leading cause of adult death in sub-Saharan Africa [14]. Despite the advent of highly effective therapy, treatment is not curative, and there is no preventative vaccine. While treatment of HIV-1 infection can reduce morbidity, mortality, and transmission, financial resources are not available to deliver lifelong antiretroviral therapy to all those who need it, so a one-time intervention, i.e. a vaccine, is sorely needed. Major scientific questions still remain about the interactions between the virus and the host innate immune system, and understanding these interactions will be required to better design new therapies and an effective HIV-1 vaccine. Here, I will review the major PRR families and signaling pathways, the role of the transcription factor interferon regulatory factor 3 (IRF3) in innate immunity, and antagonism of innate immunity by pathogens, with special consideration for HIV-1.

PRR SIGNALING

An important aspect of sensing by PRRs is discrimination of self from non-self. PRR signaling and downstream antimicrobial effects must be activated quickly during infection, but are held in check in the absence of true infection to prevent constant inflammation. Thus, PRRs have evolved to sense biochemical structures unique to pathogens. For example, lipopolysaccharide is a structure unique to Gram-negative bacteria, while the presence of double stranded (ds) RNA, single stranded (ss) DNA, or dsDNA in the cytoplasm do not occur in the absence of viral infection. As a result, PRRs demonstrate location and substrate specificity. The PRR families reviewed here include the TLRs, RLRs, NLRs, DNA sensors, and those that have been found to detect HIV-1.

Toll-like receptors

The longest-studied PRRs are the TLRs, with 9 members identified in humans. All TLRs share some basic structural features, including transmembrane domains, extracellular (or endosomal) leucine-rich regions that interact with PAMPs, and cytoplasmic signaling domains that initiate cascades through adaptor molecules [15]. All of the TLRs except TLR3 signal through the adaptor proteins TIRAP/MyD88, while TLR3 and TLR4 signal through TRIF/TRAM [16]. MyD88 signaling leads to the activation of nuclear factor κ -light-chain-enhancer of activated B cells (NF κ B), while TRIF signaling leads to activation of the transcription factors NF κ B (via TRAF6) and IRF3 (via TBK1) [15]. A map of TLR adaptor signaling is displayed in Figure I-1. The MyD88 and TRIF signaling adaptors have Toll-interleukin 1 receptor (TIR) domains that interact with cytoplasmic TLR TIR domains, and these TIR-TIR interactions are essential for TLR function [16].

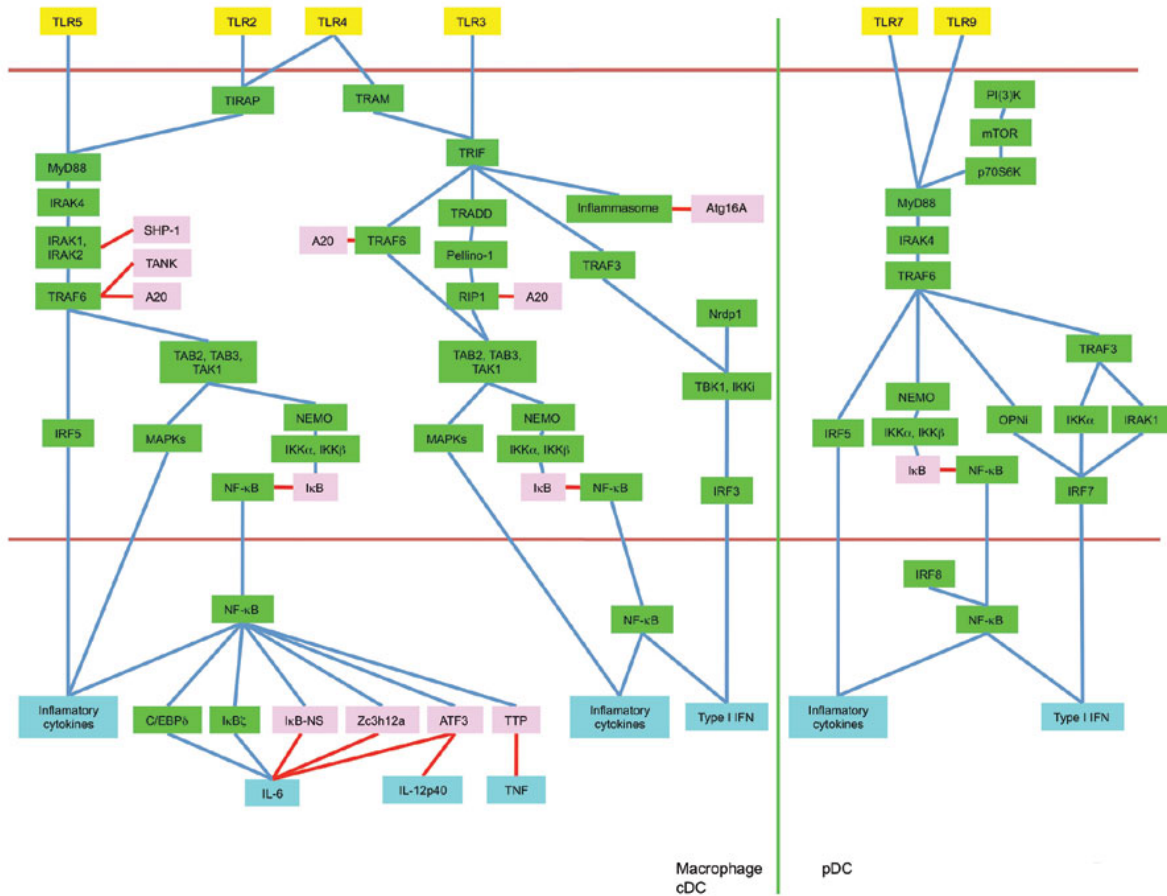


Figure I-1: Map of signaling pathways downstream of select TLRs (Fig. 3 from [15], used by permission – copyright license # 3190921063703).

The TLRs are mainly located on membranes of the cell surface and endosomes of cDCs and other immune cells, with TLR7 and TLR9 being especially highly expressed on pDCs [17, 18]. TLR4 along with MD2 binds LPS on cell surface and signals through MyD88 to NFκB followed by endosomal internalization and signaling through TRAM/TRIF to drive additional NFκB activation as well as interferon regulatory factor 3 (IRF3) activation [15]. TLRs 1, 2, 5, and 6 signal in response to bacterial lipopeptides and drive NFκB activation [15]. TLRs 7 and 9 bind ssRNA and ssDNA respectively, and signal through MyD88 to NFκB and IRF7, while TLR3 binds dsRNA and signals through TRIF to NFκB and IRF3. TLR8 appears to function and

be expressed similarly to TLR7 but is less essential for immunity [19]. TLRs 3, 7, 8 and 9 are all expressed in endosomes, and bind nucleic acid PAMPs derived from phagocytosed cell debris, viruses, and bacteria [15]. There is also evidence that infected pDCs can bring cytosolic PAMPs to the endolysosomal TLRs through autophagy, a process by which endosomes form around cytosolic contents [20]. There is also evidence that pDCs can detect viral RNA PAMPs from neighboring infected cells through exosomal transfer via cell-cell contacts [21, 22].

RIG-I-like receptors

The RIG-I-like receptors (RLRs) are expressed in the cytosol of all nucleated cells. The RLR family consists of three PRRs: retinoic acid-inducible gene-I (RIG-I), melanoma differentiation-associated gene 5 (MDA5), and laboratory of genetics and physiology 2 (LGP2). The RLRs are DexD/H box RNA helicases that bind RNA, hydrolyze ATP, and scan for recognition motifs [23-25]. RIG-I exhibits a preference for shorter dsRNA structures while MDA5 binds longer structures [25]. This property of MDA5 is due to its ability to form long filaments on dsRNA [26]. Structurally, RIG-I and MDA5 contain N-terminal caspase activation and recruitment domains (CARDs) and the helicase domain, and RIG-I but not MDA5 has a C-terminal repressor domain (RD) [27]. LGP2 also contains a helicase domain and RD but lacks the CARD domains, and functions as a regulator of RIG-I and MDA5 signaling [28]. The repressor domain of RIG-I prevents unwanted activation of RIG-I signaling in the absence of appropriate RNA ligand by decreasing CARD exposure to other signaling partners [28, 29].

RIG-I binds to double-stranded RNA that contains a 5' triphosphate, and in the case of hepatitis C virus has sequence specificity for poly-U/UC RNA [28-30]. Upon binding to PAMPs, the RIG-I RD is displaced from the CARDs allowing for their interaction with TRIM25 and 14-

3-3ε, chaperone proteins that promote the relocation of RIG-I from the cytosol to the mitochondrial-associated ER membrane (MAM) [31, 32]. At the MAM, RIG-I CARD interaction with CARD located on the adaptor protein mitochondrial antiviral signaling protein (MAVS) leads to the assembly of a signaling complex that results in the activation of NFκB and IRF3 [33]. The ligand specificity for MDA5 is less clear, though MDA5 signaling also requires MAVS [34, 35]. MDA5 is the RLR that predominantly binds and signals in response to the long forms of the synthetic RNA mimetic poly(I:C) [36]. MAVS itself is essential for signaling after cytoplasmic RNA sensing and downstream interferon production and antiviral immunity [34, 35, 37, 38].

Overall, signaling in response to foreign RNA is complex with multiple sensors feeding into or augmenting the RLR pathway. For example, binding of viral dsRNA to 2'-5' oligoadenylate synthase (OAS1) leads to the activation of RNaseL, which generates RLR ligands from self and viral RNA [39]. Other DexD/H box RNA helicases, HMGB proteins, NOD2 and LRRFIP1 (see below) are reviewed elsewhere [40] for their roles in RNA sensing and additional RNA sensors or proteins that interact with RLR pathways remain to be discovered. Figure I-2 illustrates the various known sensors involved in cytosolic sensing of RNA viruses. Interestingly, RIG-I is also activated by RNA generated as a result of the bacterial infection-induced unfolded protein response [41] and the presence of cytosolic DNA (further described below). While the detection of cytosolic RNA by RLRs is one type of surveillance for infection, the NLR family also includes members that detect PAMPs in the cytosol and can activate innate immune or inflammatory signaling pathways.

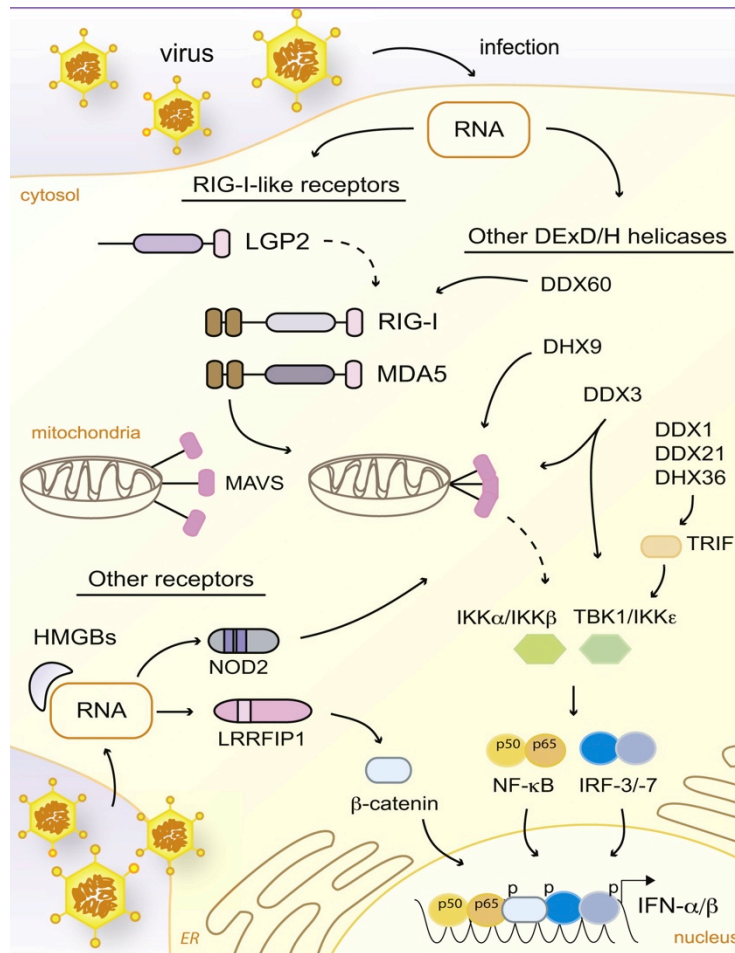


Figure I-2: Cytosolic sensing of RNA viruses (Fig. 3 from [40], used by permission – copyright license #3166690760831).

Nucleotide-binding domain and leucine-rich repeat-containing proteins

The nucleotide-binding domain and leucine-rich repeat-containing proteins (NLRs) are expressed in the cytosol of various cell types including epithelia, APCs, and adaptive immune cells [12]. NLRs represent a diverse family of PRRs, but they all share an ATPase domain and a C-terminal leucine-rich repeat domain [42]. The N-terminal domains vary among the different NLR family members. NOD1 and NOD2 have N-terminal CARD domains, respond to antimicrobial PAMPs in the cytosol (such as bacterial peptidoglycan derivatives or viral ssRNA),

and signal to the activation of NF κ B and IRF3 [43]. The NLRP proteins contain N-terminal pyrin domains and (for those that have known functions) interact with caspase-1 upon activation and thus drive interleukin-1 β production. Signals for NLRP activation include damage or danger-associated molecules (DAMPs), like uric acid, ATP (representing dying cells), reactive oxygen species (suggesting bacterial infection and inflammation), or ion flux (suggesting loss of membrane integrity as could occur during bacterial or viral infection) [42].

DNA sensors

DNA sensing has been known to be accomplished by TLR9 within endosomes in pDCs, which can sense DNA from lysed bacteria or virus. However, there are also widely-expressed sensors for cytosolic DNA that trigger innate immune responses, as revealed by autoinflammatory diseases caused by defects in cytosolic DNA or dNTP clearance [44-47]. The cytosolic DNA sensors discovered to date include IFI16, DNA-dependent activator of IRFs (DAI), RIG-I via RNA polymerase III, DDX41, LRRFIP1, Ku70, and the recently identified cyclic GMP-AMP synthetase (cGAS). DAI binds B-form DNA and activates IRF3 but surprisingly it is not essential for innate immune responses to viral DNA in mice [48]. RNA polymerase III transcribes AT-rich DNA such as the cytosolic DNA analog poly(dA:dT) into poly(rA:rU), which is recognized by RIG-I for signaling through MAVS [49]. However, this pathway is also not essential for sensing of DNA viral infection [49]. DDX41 is a DExD/H helicase family member, like the RLRs, that binds nucleic acids and signals through the adaptor protein stimulator of interferon genes (STING) to activate IRF3 and NF κ B [50]. IFI16 is a pyrin and HIN-200 domain-containing (PYHIN) family member that binds DNA through its HIN domain and can oligomerize with other pyrin domain-containing proteins. Similar to DDX41,

IFI16 signals for the activation of IRF3 in a STING-dependent manner [51]. LRRFIP1 binds DNA through an N-terminal domain and activates β -catenin, which then binds to the C-terminus of IRF3 in the nucleus and enhances transcriptional cofactor interaction [52]. Ku70 is a DNA double strand break repair protein that binds exposed DNA ends in the cytoplasm and signals to the promoter of IFN- λ 1, an antiviral type III interferon [53].

Despite the many DNA sensing mechanisms described above, and while the adaptor STING is essential for the cytoplasmic DNA response [54], no individual DNA-sensing PRR appears to be essential for DNA-dependent type I IFN production in all cell types, and this is still true after the recent discovery of cGAS [55]. Structurally similar to OAS1, cGAS binds DNA in the cytosol and generates the second messenger cyclic hetero-dinucleotide cGAMP, which then binds and activates STING, leading to the activation of IRF3 and production of type I interferon [55-57]. It should be noted that STING itself can bind cyclic di-GMP and DDX41 can bind cyclic di-GMP and cyclic di-AMP directly to drive type I IFN expression [58, 59]. The structure of cGAMP that is produced by mammalian cGAS appears to have an asymmetric phosphodiester linkage $>Gp(2'-5')Ap(3'-5')>$ [60], unlike the symmetric $>Gp(3'-5')Ap(3'-5')>$ structure originally proposed by Wu and colleagues [56]. The symmetric cyclic dinucleotide $>Gp(3'-5')Ap(3'-5')>$ is a bacterial second messenger molecule, while the asymmetric $>Gp(2'-5')Ap(3'-5')>$ appears to be unique to metazoans and thus far exclusively produced by cGAS in response to cytoplasmic DNA binding and used as a second messenger to activate STING [60-62]. Thus, further investigation of the sensing of cytosolic DNA may focus on the generation of asymmetric cGAMP by cGAS during infection by DNA viruses, or retroviruses, that expose viral DNA in the cytoplasm.

Sensing of HIV-1

HIV-1 utilizes the cell surface molecule CD4 as its primary receptor along with CCR5 or CXCR4 as coreceptors [63]. CD4 is expressed most highly on macrophages and certain activated T cells, CCR5 is expressed on macrophages and activated CD4⁺ T cells, and CXCR4 is expressed on naïve CD4⁺ T cells [63]. As a result, CD4⁺ T cells and macrophages are the primary target cells for HIV-1 infection. The life cycle of HIV-1 is depicted in Figure I-3, during which virions deliver viral capsid to the cytoplasm, which then dissociates to expose viral RNA that is then quickly reverse transcribed to DNA using cellular dNTPs. During this cycle, viral nucleic acid in the form of ssRNA (perhaps briefly), RNA:DNA hybrids, ssDNA, and dsDNA could all theoretically be exposed as PAMPs for varying amounts of time to putative cytosolic sensors. The final dsDNA proviral genome translocates to the nucleus and is integrated into the cellular genome, and when activated gives rise to viral mRNA for protein production and genomic RNA for new virions, and these RNA species could also theoretically serve as PAMPs.

It has been reported that the virus presents PAMPs to the cell in the form of capsid structure [64] and nucleic acid [65, 66]. Sensing of incoming capsid structure by TRIM5 signals to the transcription factors AP-1 and NFκB [64], though human TRIM5 has lost this ability in comparison to closely-related primates, while RIG-I binds genomic HIV-1 RNA to trigger IRF3-dependent signaling [66]. The significance of RIG-I sensing of HIV-1 *in vivo* is not yet known. In CD4⁺ T cells *ex vivo* an as yet undefined cytosolic sensor binds reverse transcription intermediates to drive IFN-β expression, caspase activation, and cell death [65], and there is evidence that these nucleic acid PAMPs produced during HIV-1 infection could contain DNA. In particular, constitutively-expressed Trex1 was found to digest ssDNA derived from endogenous

retroelements and prevent their triggering of cytosolic DNA sensors [44], and in the absence of Trex1 HIV-1 is able to trigger IRF3 activation through STING [67]. Another sensor of HIV-1 could be tetherin, an ISG that functions to restrict the release of certain viruses (including HIV-1), but may also serve to sense HIV-1 virion accumulation at the cell surface and activate NFκB [68-70].

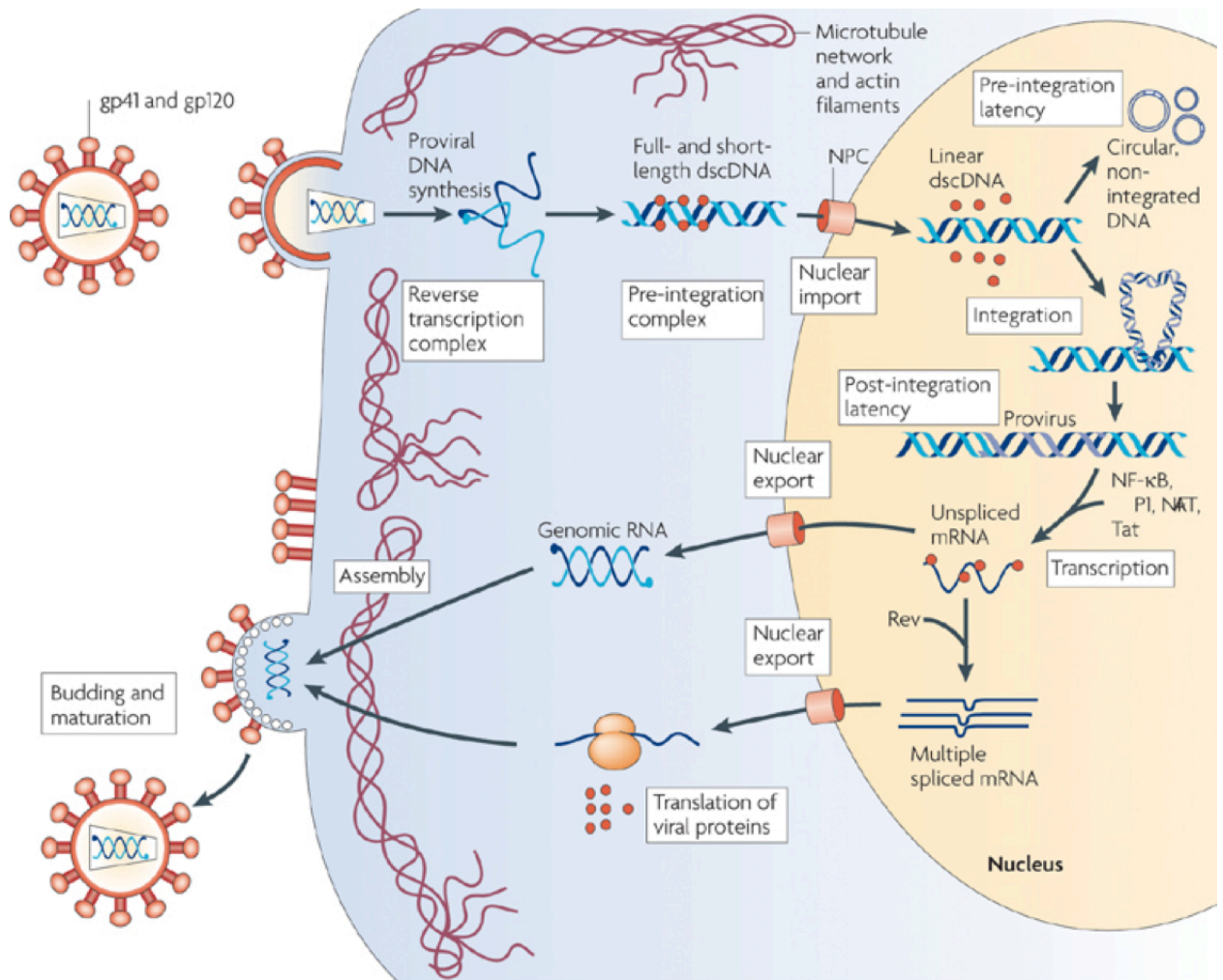


Figure I-3: The HIV life cycle (Fig. 1 from [71], used by permission – copyright license # 3173480006938).

In addition to sensing mechanisms in CD4⁺ T cells and macrophages, the main target cells of infection, there are also sensing mechanisms in cells that are not known to be productively infected with HIV, but still may sense HIV to drive innate immunity. pDCs, via a TLR7-dependent pathway, sense endocytosed HIV-1 virions [72] or infected CD4⁺ T cell debris [73]. Interestingly, HIV-1 virion membrane fusion with the endosomal membrane appears to enhance TLR7 signaling, suggesting that endocytosed virions deliver ssRNA to the cytoplasm which is then delivered from the cytoplasm back to the endosome, as through a process like autophagy [73, 74]. Further, co-culture of HIV-1-infected CD4⁺ T cells with 293T cells (which lack TLR expression) led to activation of IRF3 in the 293T cells, indicating the presence of cytosolic sensing of HIV-associated PAMPs [73]. Conversely, HIV-1-exposed CD4⁺ cDCs are not efficiently infected due to the expression of the restriction factor SAMHD1 (further discussed below) and demonstrate an absence of innate immune signaling in response to HIV-1 [75].

IRF FAMILY AND IRF3

Many PRR signaling pathways converge on IRF3 to induce type I IFN expression. IRF3 is one of 9 members of the IRF family of transcription factors. Most IRFs have constitutively low expression, but their expression is inducible. IRF1 expression can be induced by IFN- γ and other proinflammatory cytokines, while IRF7 can be induced by type I IFN in most cell types but is constitutively expressed in pDCs. On the other hand, IRF3 is constitutively expressed [76, 77]. The IRFs share an N-terminal DNA binding domain (DBD) that contains a helix-turn-helix domain and is well conserved across the family. While the different IRF DBDs have slightly different sequence binding preferences [78], the consensus DNA sequence recognized by these

DBDs is called the IFN-stimulated response element (ISRE) and has the sequence 5'-GAAANNNGAAAG/CT/C-3', where "N" can be any nucleotide [79]. Binding by one IRF may enhance the accessibility of nearby transcription factor binding sites [80]. All of the IRFs except IRF1 and IRF2 have an IRF association domain (IAD) near the C terminus, which allows for homodimer formation (e.g. IRF3), heterodimer formation (e.g. IRF3/IRF7), or other cofactor interaction (e.g. CREB-binding protein; CBP) [76]. Some IRFs, like IRF3 and IRF7, also have C-terminal serine-rich regions containing bioactive phosphorylation sites [79].

The IRFs play varying roles in cell cycle control, development, and innate immunity. IRF1 helps to amplify TLR signaling through an interaction with Myd88 in cDCs [81]. Along with other transcription factor binding sites, IRF1 binding sites are located in the HIV-1 LTR, and IRF1 binding is required to drive HIV-1 genome expression prior to Tat expression [82, 83]. IRF1 activity leads to the expression of the repressors IRF2, which competes with IRF1 for binding to its ISRE sequence but does not signal [84], and IRF8, which blocks IRF1 association with necessary cofactors [82]. IRF1 also has tumor suppressor properties, while IRF2 expression is oncogenic, and the two proteins oppose each other to regulate the cell cycle [85]. IRF4 is expressed in activated lymphocytes and macrophages and either functions to repress, or if bound to partner PU.1 activate, transcription at ISREs [86], while IRF5 is activated by the TLR adaptor MyD88 [87]. IRF6 has no known immune function, but mutations in IRF6 are associated with orofacial development disorders [88].

IRF3, 7, and 9 play major roles in the type I IFN innate immune response. IRF3, as described above, is constitutively expressed in most cells and activated by several PRRs, including the cytoplasmic nucleic acid sensors. Activated IRF3 drives the transcription of IRF3-

dependent genes, including IFN- β , which then drives signaling through the IFN α/β receptor (IFNAR). Activation of IFNAR leads to the formation of a transcriptional complex containing IRF9, which like IRF3 is constitutively expressed. This transcriptional complex, called interferon-stimulated gene factor 3 (ISGF3), drives the transcription of IRF7, which then cooperates with IRF3 to drive the expression of a large set of ISGs. Loss of function of IRF3, 7, or 9 leads to susceptibility to viral infection, while loss of function of IRF3 leads to resistance to bacterial sepsis, due to the role of TLR4 signaling to IRF3 in systemic shock [79].

In addition to its central role in driving the IFN response to PRR signaling, IRF3 activation promotes a pro-apoptotic response [89]. This pathway involves the binding of IRF3 to Bax, translocation of IRF3/Bax to the mitochondria, and the initiation of the intrinsic apoptosis pathway leading to caspase 3 activation [89]. This pathway is important for suppression of viral infection and, if abrogated via IRF3 depletion, leads to chronic viral infection [90]. The IRF3-dependent gene IFIT2 itself drives a similar Bax- or Bak-mediated apoptotic response [91]. In summary, innate immune signaling in response to microbial infection culminates in the actions of members of the IRF transcription factor family. In response to viral infection, the IRFs and in particular IRF3 play a crucial role in the induction of the innate antiviral response, which (as described below) includes expression of type I IFN and other antiviral genes.

THE IRF3 ACTIVATION CYCLE

IRF3 is a 427 amino acid protein with the domain structure indicated in Figure I-4. The C-terminal serine-rich region of IRF3 contains several phosphorylation sites. While IRF3 is phosphorylated in the resting state, activation of IRF3 is characterized by additional phosphorylation, specifically at residues S385, S386, T390, and S396 [92]. Phosphorylation at

S385 or S386 is required for IRF3 dimerization, while phosphorylation at S396 is required for IRF3 dimerization, translocation to the nucleus, and association with CREB-binding protein (CBP)/p300, histone acetyltransferases necessary for IRF3 transcriptional activity [93, 94]. Activation-specific phosphorylation is governed by the I κ B kinase-related protein kinases TBK1 and IKK ϵ [95, 96], which are activated downstream of TRIF-, MAVS-, or STING-dependent PRR signaling [96-98]. After phosphorylation, IRF3 dimerizes, and this has been proposed to occur as a result of charged repulsion of the C-terminal phosphorylation domain from the IAD, exposing the IAD for IAD-IAD interaction between two IRF3 molecules [99]. IRF3 then translocates to the nucleus, and any binding partners required for this process are unknown. Once in the nucleus, IRF3 molecules interact with the cofactor CBP/p300, and then bind cooperatively to promoters containing the IRF3 ISRE sequence 5'-GAAAC/GC/GGAAANT/C-3' leading to IRF3-dependent gene transcription [78]. Dimerized IRF3 binds to two ISRE sequences often in close proximity to each other and the tight packing of the IRF3 homodimer at these binding sites may be important for deformation of DNA and facilitation of transcription initiation complex formation [100].

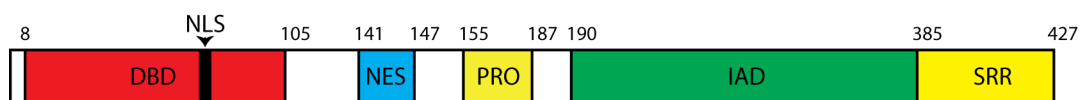


Figure I-4: Schematic of IRF3 functional domains. DBD – DNA-binding domain; NLS – nuclear localization sequence; NES – nuclear export sequence; PRO – proline-rich region; IAD – IRF association domain; SRR – serine-rich region.

After IRF3 has performed its duty in transcription of innate immune genes, its activity is shut down. Thus, if the innate immune response is successful in clearing the cell of the infectious agent and IRF3-activating signals cease, the cell can return to a normal metabolic state and stop

type I IFN and proinflammatory cytokine secretion to nearby cells. For example, the transcription factor MafB blocks recruitment of cofactors to IRF3 in the nucleus [101], while the activation of caspase-8 by RLR signaling leads to caspase-8-mediated cleavage of IRF3, preparing it for ubiquitination [102]. RBCK1 is the virus-inducible E3 ubiquitin ligase that ubiquitinates phosphorylated IRF3, a process that requires Pin1 and leads to proteasome-dependent degradation of IRF3 [103, 104]. SUMOylation of IRF3 has also been implicated in IRF3 turnover and therefore regulation of IRF3 function [105]. Overall, as IRF3 mRNA is highly stable and constitutively expressed, any decrease in total IRF3 levels due to activation and depletion can be rectified within hours [106].

IRF3-DRIVEN AND INTERFERON-STIMULATED GENES

The archetype IRF3-dependent gene is the antiviral cytokine IFN- β , which employs a well-understood virus-inducible enhancer element located -102 to -47 bp from the transcription start site of the IFN- β gene [107]. Strong activation of this enhancer, which is only basally activated in resting cells [108], involves the cooperation of several transcription factors: NF κ B (composed of subunits p50 and p65/RelA), an IRF3 dimer, an IRF7 dimer, and AP-1 (composed of subunits ATF-2 and c-Jun)[109]. These DNA-binding proteins are stabilized on the DNA by interactions with CBP/p300 in a structure called the enhanceosome [107], in which each component mediates an essential activity to drive gene expression [110]. IRF7, like IRF3, binds to IFN-stimulated response element (ISRE) sequences in gene promoters, but its DBD sequence stringency is less than that for IRF3, so it induces a broader ISG response [78]. Thus there are 8 DBDs in very close proximity, binding to most nucleotides in a 51-base stretch of DNA. This complex gene enhancer architecture is governed by evolutionary sequence conservation [109].

IRF7 is expressed at low levels prior to type I IFN signaling, but IFN- β transcription at early timepoints in response to RNA and DNA viral infection is dramatically reduced in the absence of IRF7, suggesting that enough IRF7 is basally expressed to support the earliest activation of the IFN- β promoter by IRF3 [111]. IRF3 and IRF7 are sufficient to drive virus-dependent IFN- β production in the absence of NF κ B and AP-1, while NF κ B and AP-1 may be responsible for the weak basal promoter activity [112].

In addition to IFN- β , IRF3 directly drives the expression of several other genes by binding to an ISRE in their promoters. These genes include several genes with known antiviral function, such as viperin, IFIT1, IFIT2, IFIT3, ISG15, and IFITM3, as well as IFN- α subtype 4, and also other ISGs [113, 114]. IRF3 also directly induces the expression of immunomodulatory molecules like CCL4/MIP-1 β and CCL5/RANTES, as well as the DNA sensor IFI16 [114, 115]. For some genes like IFIT2, IRF3 activation alone is sufficient to drive expression, while CCL5 expression involves cooperation of IRF3 with NF κ B [114]. The functions of these and other select genes directly stimulated by IRF3 are listed in Table I-1.

Table I-1: IRF3-driven genes

Gene name	Function	Reference
CCL4 (MIP-1β)	Proinflammatory cytokine, immune cell activation and chemotaxis	[114]
CCL5 (RANTES)	Proinflammatory cytokine, immune cell activation and chemotaxis	[114, 115]
CXCL10	Proinflammatory cytokine, immune cell activation and chemotaxis	[114]
IFI16	Sensor of intracellular DNA	[51, 114]
IFIT1 (ISG56)	Inhibition of protein translation by phosphorylation of eIF3, viral triphosphate-RNA binding	[113, 114, 116-118]

IFIT2 (ISG54)	Viral, AU-rich RNA binding, association with IFIT1	[114, 118, 119]
IFIT3 (ISG60)	Association with IFIT1/IFIT2 other functions unknown	[114, 118, 119]
IFITM3	Disrupts cellular cholesterol homeostasis and inhibits viral entry by blocking viral membrane fusion with plasma membrane	[114, 120, 121]
IFN-α4	Type I interferon, ligates IFNAR	[114]
IFN-α5	Type I interferon, ligates IFNAR	[114]
IFN-β	Type I interferon, ligates IFNAR	[114, 122]
ISG15	Attached to proteins in a process similar to ubiquitination; activates PKR	[113, 114, 118, 123]
ISG20	3'-5' RNA exonuclease	[114, 124, 125]
MHC class I	Viral antigen presentation	[113, 114]
OAS1	RNA binding, RNaseL activation, RIG-I activation	[39, 118]
Viperin/RSAD2	Inhibition of lipid raft synthesis, regulation of cellular metabolism	[114, 118, 126, 127]
ZAP	Viral mRNA degradation	[128, 129]

Once IFN- β is transcribed, translated, and secreted, it binds to IFNAR on the same or nearby cells. Ligation of IFNAR by extracellular IFN- β results in the phosphorylation of associated kinases Jak1 and Tyk2 at the IFNAR cytoplasmic domain, resulting in recruitment and phosphorylation of STAT1 and STAT2 [130, 131]. STAT1/STAT2 heterodimers dissociate from the membrane signaling complex and associate with cytosolic IRF9 to form a trimeric complex called ISGF3 [132]. This complex binds ISRE sites in gene promoters in the nucleus and drives transcription of ISGs, most importantly IRF7. IRF7 is then expressed in the cytosol and when activated functions as a homodimer or in a heterodimeric complex with IRF3 to drive a large set of ISGs, including IFN- β and all IFN- α subtypes, broadening the antimicrobial response

[133]. The differential abilities of IRF3 and IRF7 to drive transcription of genes of host defense is highlighted by the respective ISRE sequences they recognize, as IRF7 DNA binding sequence is less restricted than that for IRF3 [78].

The sets of genes driven by ISGF3 and IRF7 comprise hundreds of unique ISGs, include several genes whose transcription is also driven by IRF3. While relatively few have been functionally characterized, most are either PRRs, involved in PRR signaling, or effector enzymes with direct antiviral activity [134]. ISGs may also modify existing cellular proteins; for example, the TRIM family contains many ISGs, some of which ubiquitinate, SUMOylate or ISGylate host proteins with varying effects on the antiviral response [135, 136]. A summary of select human ISGs with known functions enriched for those with anti-HIV-1 activity (and not listed in Table I-1) is displayed in Table I-2.

Table I-2: A subset of ISGs and their functions

Gene name	Function	Reference
APOBEC3G	Deaminates retroviral reverse transcription intermediate DNA	[137-139]
cGAS	Senses intracellular DNA	[55, 134]
Herc5	Inhibits HIV-1 assembly	[140]
IFITM1 and 2	Inhibits viral entry by blocking viral membrane fusion with plasma membrane	[121, 134]
IRF1	ISRE binding, signal amplification	[81, 134]
IRF2	Attenuates IRF1 activity	[84, 134]
MDA5	PRR for cytoplasmic dsRNA	[34, 134]
PKR	Phosphorylates eIF2 α , inhibiting translation	[141]
RIG-I	PRR for cytoplasmic dsRNA	[34, 134]
Schlafen 11	Depletes tRNA pool, disadvantaging HIV-1 protein translation due to codon bias	[142]

Tetherin/BST2	Restricts enveloped virus release by tethering virions to the cell membrane, activates NFκB	[68-70]
TRIM21	Inhibits normal IRF3 degradation	[143]
TRIM28/KAP1	Deacetylates HIV-1 integrase, inhibiting proviral integration	[144]
TRIM5α	Destabilizes incoming retroviral capsid, activates NFκB	[64, 136, 145]

ANTAGONISM OF IRF3 FUNCTION BY VIRUSES

While IRF3-dependent gene induction is attenuated by ubiquitination and proteasome-dependent degradation of IRF3 protein, in the context of Sendai virus (SenV) infection, the proteasome inhibitor MG132 does not fully rescue IRF3 degradation, while the protein synthesis inhibitor cycloheximide appears to rescue IRF3 degradation better than MG132 [146]. This suggests that a protein synthesized during SenV infection promotes IRF3 degradation, highlighting the phenomenon observed for many viruses whereby IRF3 signaling is antagonized by viral factors. Inhibition of innate immunity by viruses occurs via a variety of mechanisms, with virus-induced blocks observed in PAMP sensing, PRR signaling, IRF3 activation, IFN-β signaling, and the function of specific ISGs. For example, Kaposi's-sarcoma associated herpesvirus (KSHV) encodes viral proteins with high homology to host IRF family members (vIRFs) that can act as decoys to interrupt antiviral signaling [147], while the West Nile Virus protein NS5 prevents signaling by IFN through IFNAR [148]. Many instances of viral antagonism of innate intracellular immunity have been reported, and a selection of these viruses and the antagonists they encode is displayed in Table I-3.

Table I-3: Virus-encoded antagonists of innate immunity

Virus	Antagonist encoded	Effect on host cell	Reference
Bocavirus	NP1	Binds to IRF3 DBD, blocking binding to IFN- β promoter	[149]
Borna disease virus	Phosphoprotein P	Competes with IRF3 for TBK1 binding, preventing IRF3 phosphorylation	[150]
Bovine viral diarrhea virus	Npro	Ubiquitinates IRF3, targeting it for proteasomal degradation	[151]
Dengue virus	NS2B3	Cleaves STING, blocking IFN induction	[152]
Ebola	VP35	Binds dsRNA, masking PAMPs from RLRs; inhibits IRF3 activation downstream of MAVS	[153, 154]
Epstein-Barr virus (EBV)	BRLF1	Inhibits IRF3 and IRF7 mRNA transcription and protein expression	[155]
EBV	BGLF4	Phosphorylates IRF3 in a the proline-rich region, inhibiting IRF3 activation	[156]
Hepatitis C virus	NS3/4A	Cleaves MAVS, preventing RLR signaling; cleaves TRIF, preventing TLR3 signaling	[97, 157-160]
Herpes simplex virus 1	ICP0	Degrades IFI16, preventing sensing of nuclear viral DNA; sequesters IRF3 and CBP away from chromatin	[161, 162]
HIV-1	Vpu	Targets tetherin and CD4 for sequestration and degradation, and displaces tetherin from virions, enhancing virus release; Targets IRF3 and prevents IRF3-driven gene induction	[163-168], Chapters III, IV
HIV-1	Vif	Targets APOBEC3G for degradation, preventing hypermutation of reverse transcribed DNA	[137, 169]
HIV-1	Protease	Targets RIG-I for lysosomal degradation	[170]
Human herpesvirus 6	IE1	Prevents IRF3 activation	[171]
Kaposi's sarcoma herpes	RTA	Ubiquitinates IRF7, targeting it for proteasomal degradation	[172]

virus (KSHV)			
KSHV	vIRF-1	Sequesters CBP/p300 away from IRF3, preventing IRF3-driven gene transcription	[173]
KSHV	vIRF-2	Prevents induction of IRF3-driven genes as well as ISGF3-dependent ISGs	[174]
KSHV	vIRF-3	Binds to DBD or IAD on IRF7, preventing DNA binding	[175]
Respiratory syncytial virus	NS1	Binds to IRF3, preventing CBP interaction	[176]
Rhesus cytomegalovirus	Virion component	Prevents IRF3 activation after virus entry	[177]
Rotavirus	NSP1	Targets IRF3 for proteasomal degradation	[178]
Varicella-zoster virus	ORF61	Binds and targets activated IRF3 for proteasomal degradation	[179]
West Nile virus	NS5	Prevents STAT1 phosphorylation, preventing IFNAR signaling	[148]

MODULATION OF INNATE IMMUNITY BY HIV-1

Heterosexual transmission of HIV-1 is inefficient, and this may be due to innate immunity at the mucosal barrier which successfully defends viral infection [180]. In acute infection, sequencing and phylogenetics of early viral genomes indicate that a single founder viral RNA genome can be identified as having broken through the mucosal barrier and that this virus is tropic for CD4+ T lymphocytes [181], suggesting that the initial target cell is a mucosal CD4+ T cell. The ability of that cell to mount an antiviral immune response, and conversely the ability of the virion to evade antiviral defenses, will determine whether the virus is able to establish a focus of infection in the epithelium, recruit additional target cells and infect them, and spread to lymphoid tissue reservoirs throughout the body.

Due to several mechanisms of evasion of host immunity, including integration and latent infection, envelope protein epitopes that vary and are glycosylated, mutation of proteins and epitopes for CD8⁺ T cell recognition, and evasion of detection and innate immune signaling by APCs, HIV-1 infection is incurable without allogeneic bone marrow transplant in adults or combination antiretroviral therapy in neonates or acutely infected individuals [182-184]. One of the reasons cDCs and macrophages, cell types that express an especially broad complement of PRRs, are unable to sense HIV-1 and mount an effective antiviral response is that expression of the host factor SAMHD1 prevents them from becoming efficiently infected. With only low levels of infection, these cells are less able to process and present viral antigens. The mechanism for this host restriction by SAMHD1 occurs in part through SAMHD1-mediated decrease of the cytosolic free dNTP pool, preventing viral DNA synthesis during reverse transcription [185]. HIV-2 encodes the protein Vpx, which targets SAMHD1 for degradation and enables HIV-2 to infect cDCs and macrophages more efficiently [186].

SAMHD1 itself is not an ISG [187]; rather, its activity is inhibited by phosphorylation, which can be relieved by IFN treatment [188]. This phosphorylation of SAMHD1 does not alter cellular dNTP levels, suggesting a more complex mechanism for SAMHD1 antiviral activity [189]. The enzyme is expressed at very low levels in the primary HIV-1 target cell, CD4⁺ T cells, but in resting CD4⁺ T cells, which are non-permissive to HIV-1 infection, supplementation of HIV-1 infection with Vpx leads to an increase in viral reverse transcription and gene expression, indicating a role for SAMHD1 in viral restriction [190]. SAMHD1 is phosphorylated and inactivated in dividing cells, including activated CD4⁺ T cells, which are permissive to HIV-1 [188, 189]. Inactivating mutations in both SAMHD1 and Trex1 are linked to the autoinflammatory disease Aicardi-Goutieres syndrome [44-47]. Trex1 is an ISG that digests

cytosolic DNA generated by endogenous retroelements, which are products of ancient retroviruses, thus preventing constant activation of cytosolic IRF3-dependent DNA sensors [44]. In the absence of Trex1, HIV-1 is able to stimulate type I IFN and the downstream antiviral effects, which limits HIV-1 infection. Thus, Trex1 is a restriction factor that works well enough to prevent immune induction by DNA from endogenous retroelements but perhaps too well to allow initial sensing of exogenous HIV-1 reverse transcription products. The HIV-1 PAMP that activates cytosolic DNA sensors has not yet been defined.

Other HIV-1 restriction factors are also ISGs and include TRIM5 α , which recognizes and disassembles incoming capsid [145, 191]; IFITM proteins, which prevent viral membrane fusion [121, 192]; tetherin, which prevents viral escape from infected cells [68-70]; APOBEC3G, a member of a family of deaminases that mutates reverse transcribed DNA [137-139, 169]; and schlafen 11, which depletes the cytosolic tRNA pool to preferentially inhibit viral codon-biased translation [142]. Mechanisms to avoid the effects of the IFITM proteins or schlafen 11 have not yet been defined, while the other molecules are all known to be antagonized or evaded by HIV-1. Human TRIM5 α does not recognize HIV-1 capsid very well, as it has evolved in humans to better recognize a now extinct retrovirus [193]. Tetherin is antagonized by Vpu to promote virus release [68], while APOBEC3G is targeted by Vif to prevent HIV-1 genome hypermutation [169]. In addition, RIG-I is both a PRR upstream of IFN production and an ISG, and is antagonized by the viral protease [170]. Together, the restriction factors described here block HIV-1 at various stages of its life cycle, and the virus has evolved strategies to avoid restriction.

Given the ability of HIV-1 to evade innate immunity, IRF3 function has been investigated during HIV-1 infection, resulting in reports that HIV-1 caused the degradation of

IRF3 in the absence of physiological IRF3 activation and activation-induced turnover [106, 194]. This ability of HIV-1 to block innate immune signaling may be important in the early replication and spread of the virus. In the first report of IRF3 antagonism by HIV-1, Okumura and colleagues found that Vif and Vpr both contributed to IRF3 depletion [194]. In subsequent work, Doehle and colleagues found that Vpu-deficient strains of HIV-1 allowed for the induction of an IRF3-dependent set of genes, while Vpu-expressing strains did not, suggesting that Vpu plays a role in antagonism of IRF3 function [167]. In particular, Vpu blocked the ability of SenV to induce the IFN- β promoter in promoter luciferase assays. Further, we found that Vpu colocalized with IRF3 and lysosomal markers, and that lysosome inhibitors rescued IRF3 during infection [168]. These findings suggest that IRF3 is degraded during HIV-1 infection, and that Vpu mediates a block in IRF3-dependent signaling and lysosome-mediated destruction of IRF3, though this latter finding has been called into question by Hotter and colleagues [195] and warrants further investigation.

Vpu has also been proposed to inhibit the activation of the IFN- β promoter by blocking tetherin-driven NF κ B signaling [195]. In addition, Vpu has been implicated in the suppression or “downregulation” of ligands recognized by NK cells on infected cells, thus allowing HIV to evade NK-cell mediated killing [196, 197]. These results describing evasion of IRF3- and tetherin-mediated innate immune induction do not rule out the contribution of other viral genes to antagonism of innate immunity, nor, until more is known about the HIV-1 PAMP, do they clarify the relationship between timing of viral-encoded antagonists and sensing of HIV-1. Thus, further exploration of the ability of HIV-1 to antagonize IRF3 during infection, and the role(s) of Vpu or other genes in this antagonism, is needed.

Despite evidence that HIV-1 counteracts the induction of interferon by evading PRR detection, type I IFN in patient sera is strongly elevated during the early days and weeks of infection [180], and is elevated during chronic infection [198]. The source of the acute IFN is likely pDCs recruited to infectious foci in the mucosa [199], especially since type I IFN production by rarely-infected cDCs is inhibited [200]. Though, seeding of infection to gut-associated or other lymphoid tissue (either during direct transmission to the rectal mucosa, from dissemination after vaginal mucosal infection, or lymphoid tissue seeding after parenteral transmission) and abortive infection of resting CD4+ T cells could also be a major interferon source *in vivo* [65, 198]. The subsequent chronic activation of pDCs and type I IFN production is associated with an immune exhaustion and dysfunction phenotype that precipitates opportunistic infections during advanced HIV disease [201], and chronic innate immune activation does not occur in natural hosts of retroviral infection [202, 203]. The sensing by pDCs of HIV-1 virions or infected cell debris through TLR7 or cytosolic sensors likely contributes to chronic pDC activation *in vivo*, though IRF3 may only influence cytosolic sensing. As such, antagonism of innate immune signaling by HIV-1 through IRF3 or other mechanisms in acute infection may be effective enough to evade innate immunity and promote viral spread, but not enough to prevent systemic interferon and chronic immune activation that is a hallmark of AIDS.

Investigation of innate immune induction and antagonism by HIV-1 during acute infection may provide the best opportunities to intervene before replication and spread of the virus to therapeutically inaccessible tissue reservoirs. Indeed, modeling of heterosexual transmission and disease progression suggest that for interventions during chronic infection, antiretroviral treatment coverage levels of 95-99% are needed [204], which is a profound

economic challenge, so strategies need to be targeted to prevention or acute infection, where innate and mucosal immunity play major roles.

The innate immune system plays a crucial role in the early detection of microbial infection, induction of antimicrobial effector genes, and training of the adaptive immune response. PRRs recognize microbial PAMPs and initiate signaling cascades that activate critical transcription factors including IRF3. In the context of HIV-1 infection, several genes upregulated by the innate immune response restrict viral replication, and the virus has developed mechanisms to evade these factors. One of these mechanisms involves inhibition of IRF3 function. In the following chapters, I will describe new antibodies I developed to study human IRF3, as well as studies I performed to characterize the mechanism of HIV-1 Vpu-mediated inhibition of IRF3 function.

II. DEVELOPMENT OF MONOCLONAL ANTIBODIES AGAINST IRF3

The following project was published as [205]:

Rustagi, A., Doehle, B.P., McElrath, M.J., and Gale Jr., M. Two new monoclonal antibodies for biochemical and flow cytometric analyses of human interferon regulatory factor-3 activation, turnover, and depletion. *Methods*, 2013. 59(2): 225-32.

The figures in this chapter are used by permission – copyright license #3158620139746.

ABSTRACT

Interferon regulatory factor 3 (IRF3) is a master transcription factor that drives the host intracellular innate immune response to virus infection. The importance of IRF3 in innate immune responses is highlighted by the fact that pathogenic viruses have developed strategies for antagonism of IRF3. Several tools exist for evaluation of viral regulation of IRF3 activation and function, but high-quality monoclonal antibodies that mark the differential activation states of human IRF3 are lacking. To study IRF3 activation, turnover, and depletion in a high-throughput manner in the context of virus infection, we have developed two new monoclonal antibodies to human IRF3. These antibodies detect IRF3 in virus-infected cells in a wide variety of assays and provide a new tool to study virus-host interactions and innate immune signaling.

INTRODUCTION

IRF3 is a transcription factor critical to the intracellular immune response to microbial infection [206]. Microbial infection of human cells is sensed by pattern recognition receptors

(PRRs) that recognize microbial pathogen-associated molecular patterns (PAMPs). The expression of PRRs varies among cell types, but a full complement of these receptors includes those that sense microbial DNA, RNA, or cell wall components (reviewed in [207]). Microbial DNA is sensed in endosomes (by certain Toll-like receptors, or TLRs) or in the cytoplasm, such as through the Interferon-stimulating DNA (ISD) pathway [208]. While the molecules directly involved in sensing of ISD in human cells have not been fully defined, the cytosolic proteins IFI16 [51] and AIM2 [209] have been implicated, and transcription of DNA into RNA in the cytoplasm by RNA polymerase III can trigger RNA sensors [49, 210]. Pathogen-associated RNA in turn is sensed in endosomes (by certain TLRs) or the cytoplasm (by RIG-I-like receptors, or RLRs).

Downstream of PRRs, signaling cascades lead to the transcription of genes that mediate an antimicrobial state. In response to infection by RNA viruses, TLR3 and the RLRs have been shown to recognize double-stranded RNA, while TLR7 recognizes single-stranded RNA. TLR3 and the RLRs activate an antiviral state within the cell by initiating signaling cascades that require the adaptor proteins TRIF and MAVS, respectively, leading to the activation of IRF3. It should be noted that direct sensing of ISD, as can occur during DNA virus or bacterial infection, also results in IRF3 activation [58, 208]. When activated, IRF3 directly drives the transcription of several genes with key antiviral functions. These genes include antiviral effectors such as viperin, ISG54, and the IFITM family of proteins, as well as pro-inflammatory cytokines like interferon- β (IFN- β) and CCL-5/RANTES [114]. Signaling by IFN- β , both in an autocrine and paracrine manner, leads to the expression of hundreds of interferon-stimulated genes (ISGs) [113]. ISG products inhibit viral replication through a diverse set of mechanisms, but most ISGs have yet to be characterized. In order to support replication, viruses have developed mechanisms

to block the induction of the innate antiviral response, the function of specific ISGs, or both. Viral strategies that block IRF3-dependent gene induction modify the normal expression, activation state, or function of IRF3, and are linked to pathogenic outcome of infection.

IRF3 is constitutively expressed in virtually all cells [77]. The IRF3 mRNA encodes a ~55 kDa protein that contains a DNA-binding domain, nuclear export signal, IRF-interacting domain, and a C-terminal serine-rich region [99, 211]. This serine-rich region contains several phosphorylation sites. While some of these serine residues are phosphorylated in the resting state, activation of IRF3 is characterized by additional phosphorylation, specifically at residues S385, S386, T390, and S396 [92]. Activation-specific phosphorylation depends on the actions of the protein kinases TBK1 and IKK ϵ [95]. After phosphorylation by either protein kinase, IRF3 dimerizes and translocates to the nucleus, driving IRF3-dependent gene transcription. Phosphorylation at S385 or S386 is required for IRF3 dimerization, while phosphorylation at S396 is required for IRF3 association with CREB/p300, a cofactor necessary for IRF3 transcriptional activity [93, 94]. Ubiquitination of IRF3, which requires Pin1 and RBCK1, leads to proteasome-dependent degradation of IRF3 thus ending IRF3-dependent signaling [103, 104]. The IRF3 activation cycle is depicted in Figure II-1.

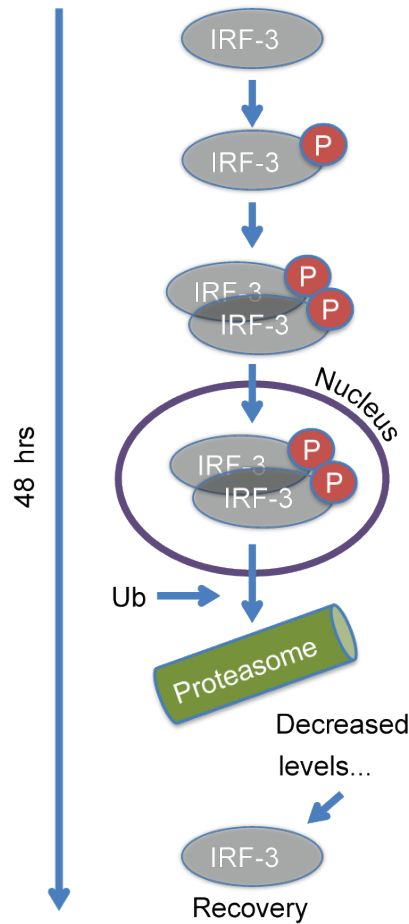


Figure II-1: Schematic of IRF3 phosphorylation, dimerization, nuclear translocation, ubiquitination (designated by “Ub”) and degradation that occur during normal activation over a 48-hour time course.

Given the central role that IRF3 plays in the stimulation and promotion of the antiviral state, a variety of tools have been developed to examine aspects of the normal IRF3 activation cycle. Phosphorylation of IRF3 can be detected by phospho-specific antibodies, while dimerization can be observed directly using native gel electrophoresis [212]. Upon IRF3 activation, nuclear translocation can be reliably detected using nuclear/cytoplasmic fractionation analysis [115] or by immunostaining of cells and microscopic imaging [34]. Degradation of IRF3 can be assessed by measuring ubiquitination of IRF3 [104] and by assessing IRF3 levels during

viral infection in cells treated with proteasome or lysosome inhibitors [213]. As noted above, when activated and present in the nucleus, IRF3 drives gene transcription, and this transcriptional activity can be observed in cells through the use of luciferase (luc)-reporter constructs containing IRF3-target gene promoters. Promoters used in luc-reporter constructs include the ISG56/IFIT1 promoter, the full IFN- β promoter, the interferon-stimulated response element (ISRE), or the PRDIII sequence (the IRF3 binding site encoded within the IFN- β promoter) [157, 213]. IRF3 dependent gene transcription can also be monitored directly by measuring the transcriptional activity of known IRF3 responsive genes [114] or by direct detection of protein abundance changes through immunoblot assays.

The above methods used to analyze IRF3 function have all been used to evaluate viral antagonism of IRF3 in a variety of virus infection systems, both in vivo and in vitro. Similar to other viruses, human immunodeficiency virus-1 (HIV-1) replication is inhibited by signaling-competent IRF3 in T cells and macrophages [106]. To counter these antiviral actions of IRF3, HIV-1 directs the virus-induced degradation of IRF3 [106, 194], which occurs in a viral protease-independent process but independently of IRF3 activation. Interestingly, this degradation of IRF3 suppresses the innate immune effector function of the infected cell, thus supporting viral replication and spread while enhancing permissiveness to secondary viral challenge and superinfection. HIV-1 degradation of IRF3 and suppression of innate immune defenses therefore supports HIV persistence and may contribute to the development of AIDS [106, 194]. Other examples of direct inhibition of IRF3 have been observed: rotavirus directs the proteasome-dependent degradation of IRF3 through the action of rotavirus nonstructural protein 1, resulting in decreased IRF3 dimer formation, decreased nuclear translocation, and decreased IRF3-dependent gene transcription [178], while the bovine viral diarrhea virus protein Npro

targets IRF3 for ubiquitination [151]. A variety of viruses promote the indirect inhibition of IRF3 by affecting other molecules involved in the upstream signaling cascades required for activation. In hepatitis C virus-infected cells, IRF3 activation is indirectly inhibited [157], due to cleavage of the upstream RLR adaptor protein MAVS by the viral protease NS3/4A [97, 158, 159]. Additionally, Borna disease virus phosphoprotein P competes with IRF3 for TBK1 binding, thus preventing IRF3 phosphorylation [150], while Kaposi's sarcoma herpes virus encodes a protein that sequesters IRF3 binding partners thus preventing transcriptional complex formation [173].

Tools used to evaluate IRF3 function can be applied to examine both direct and indirect viral antagonism of innate immunity. To evaluate the downstream effects of IRF3 antagonism on IRF3-dependent gene induction in a high-throughput manner, plasmid constructs encoding viral proteins suspected of being IRF3 antagonists can be expressed in transfected cells along with luciferase reporter constructs employing IRF3-target gene promoters. Cells can then be treated with an IRF3 activator, such as the RNA mimetic poly:I:C or the mouse paramyxovirus Sendai virus, allowing evaluation of the relative strength of IRF3 activation via promoter-luciferase signal in the presence and absence of the suspected IRF3 antagonist [157]. As a result of this and other approaches, several viral antagonists of IRF3, including the aforementioned viral regulators, have been revealed [214].

Recent advances in specialized applications of microscopy (Cellomics, [215]) and flow cytometry (Amnis ImageStream, [73]) allow for the quantification of nuclear translocation of transcription factors (and therefore activation) in populations of cells. However, a conventional flow cytometry assay that allows for analysis of IRF3 activation and degradation has not been described. Such an assay would provide a method for study of heterogeneous infected cell

populations like human peripheral blood cells or mucosal lymphocytes using widely available instrumentation. For example, the relative degree of IRF3 depletion in HIV-infected patient cells is unknown, and may correlate with viral pathogenesis. Additionally, small molecules that activate IRF3 may enhance antiviral immunity in patients, and such molecules could be screened on human immune cells in a high-throughput manner. Several antibodies specific to human IRF3 are commercially available, and we tested many of these prior to initiating the study.

Problematically, we found that a limited subset of commercial anti-IRF3 antibodies is actually suitable for flow cytometric analysis of total intracellular IRF3 levels in the multiple cell types examined. Of these commercially-available antibodies, none have been reported to detect activated IRF3 by flow cytometry. Furthermore, for high-throughput analyses of IRF3 depletion or activation, acquisition of large quantities of commercial antibodies is prohibitively expensive. To these ends, we have developed two monoclonal antibodies against human IRF3 that now facilitate a novel flow cytometric assay of IRF3 expression and activation status, and will provide new tools for conventional analyses of IRF3 in virus-infected cells.

MATERIAL AND METHODS

Cells, transfections, and subcellular fractionation

SupT1 cells, THP-1 cells, CEM-ss cells, and PBMCs were cultured in cRPMI: RPMI 1640 media supplemented with 10% heat-inactivated FBS, L-glutamine, sodium pyruvate, and antibiotics, as described previously [106]. TZM-bl [216] and Vero cells were cultured in cDMEM: DMEM supplemented with 10% heat-inactivated FBS, L-glutamine, HEPES, sodium pyruvate, MEM non-essential amino acids, and antibiotics. GHOST [217] R3/X4/R5 cells were cultured in cDMEM supplemented with 500 µg/mL G418, 100 µg/mL hygromycin, and 1 µg/mL

puromycin. Transfection of cells was performed using the calcium phosphate method or using Fugene6 transfection reagent (Roche) according to the manufacturer's suggested protocol. Plasmids pBL-IRF3 and pBL-IRF3 Δ N have been described previously [213]. SupT1 cells stably expressing lentiviral vectors (Sigma) containing shRNA to IRF3 or nontargeting vector were generated according to the manufacturer's suggested protocol. Nuclear and cytoplasmic fractionation was performed using standard methods previously described [115].

Viral stocks and infections

HIV-1_{LAI} was propagated using CEM-ss cells grown in cRPMI and standard procedures as described previously. Mock infections represent addition of CEM-ss cell conditioned media. HIV-1 was titered on TZM-bl and GHOST cells to determine concentration of infectious virus. Sendai virus (SenV) strain Cantell was obtained from Charles River Laboratory.

Monoclonal antibody production and screening

Mice were immunized with His-tag purified IRF3 and splenocytes were fused with the FOX-NY myeloma cell line and cultured under hybridoma selection using cRPMI plus AAT (adenine/aminopterin/thymidine, Sigma). Hybridoma supernatants were screened against input protein by ELISA, then by overexpressed and endogenous human IRF3 by SDS-PAGE and immunoblot, and strong candidates were selected for confirmatory testing by immunofluorescence on TZM-bl cells infected with 200 hemagglutination units (HAU)/mL SenV. For antibody purification, hybridoma cells were weaned off of drug selection into serum-free media (Gibco), inoculated into a CELLline bioreactor (BD Biosciences) and antibody was purified from the supernatant by thiophilic adsorption (Pierce). Purified antibody was subtyped using an IsoStrip mAb typing kit (Roche).

Immunoblot analysis and fluorescent microscopy

Sodium dodecyl sulfate-polyacrylamide gel electrophoresis (SDS-PAGE) and immunoblot analysis were performed using standard procedures as described previously [34]. Native PAGE was performed using buffers and procedures adapted from [218] to use pre-cast TGX gels (Bio-Rad). Native gels were run for 30 min at 30 mA. The following antibodies were used in the study: Rabbit (Rb) α ISG56 (a gift from G. Sen), Mouse (m) α HIV-1 p24, Goat (Gt) α B-actin (Santa Cruz), Rb total α IRF3 (a gift from M. David, [219]), Rb α IRF3-p (Cell Signaling), Rb α Lamin B (Abcam), Rb α GAPDH (Santa Cruz), Rb α SenV (a gift from I. Julkunen). For immunoblot detection the appropriate HRP-conjugated secondary antibody was used (Jackson ImmunoResearch) followed by treatment of the membrane with ECL Plus reagent (GE Amersham) and imaging on X-ray film. For immunofluorescence imaging, TZM-bl cells were seeded in 8-well chamber slides prior to infection. Prior to staining, cells were washed with PBS, fixed in 3% formaldehyde, incubated in 0.1% Triton X-100, and blocked with 10% fetal bovine serum. The slides were then sequentially stained with the appropriate dilutions of primary antibodies, followed by incubation with AlexaFluor488-conjugated secondary antibody (Jackson ImmunoResearch) along with DAPI before mounting with ProLong Gold (Invitrogen). Samples were imaged on a Nikon TE2000-E microscope and images were processed with NIS Elements software.

Flow cytometry

For Amnis Imagestream analysis, SupT1 cells were fixed and stained using procedures adapted from Amnis. Cells were fixed in 3% formaldehyde and stained with primary antibody in 0.1% Triton X-100/1% BSA followed by secondary staining with DyLight 488-conjugated

secondary antibody (Jackson ImmunoResearch). For quantitation of colocalization, ~2,500 cells per condition were analyzed. For conventional flow cytometry, antibody was directly conjugated to fluorophore using a Molecular Probes protein labeling kit (Invitrogen).

RESULTS AND DISCUSSION

We identified several hybridoma clones producing anti-IRF3 antibodies that recognized both recombinant IRF3 and endogenous IRF3 within SupT1 and 293T cells. Monoclonal antibody (mAb) to IRF3 was purified from a clone that exhibited high reactivity to IRF3 and was designated AR-1. SenV is a potent viral agonist of IRF3 that induces RIG-I signaling in human cells, and we used SenV infection as an activator of IRF3. SDS-PAGE and immunoblot analysis using the AR-1 mAb demonstrates IRF3 activation, turnover, and recovery over a 48-hour timecourse in SupT1 cells infected with 200 HAU/mL SenV (Figure II-2, top). The AR-1 mAb detects resting IRF3 (indicated by the arrows; Figure II-2), which migrates more quickly compared to active IRF3 on an SDS-PAGE gel. This IRF3 isoform and the other IRF3 bands visible at 0 hrs of infection have been phosphorylated heterogeneously [92] at non-activation-specific serine residues. The kinetics of IRF3 activation during SenV infection reveal the appearance of more slowly-migrating AR-1 mAb-reactive bands, or “laddering,” which indicates phosphorylation of IRF3 at various activation-specific residues. Such phospho-IRF3 species are most apparent at 16 and 24 hrs post SenV infection. As a result of being modified by phosphorylation in response to SenV infection, the amount of the resting IRF3 isoform (arrows; Figure II-2) decreases through 24 hrs and then recovers by 48 hrs post infection. The depletion and recovery of IRF3 are mediated by degradation of activated IRF3 and *de novo* synthesis of the pool of resting IRF3, respectively. Though IRF3 activation can be driven by non-viral stimuli, all

upstream events that signal to IRF3 impart IRF3 phosphorylation at activation-specific residues, leading to activation of its transcriptional activity. Indeed, we found that the AR-1 mAb could detect activated IRF3 by SDS-PAGE and immunoblot analysis of extracts from THP-1 cells (a human monocyte cell line that displays a macrophage-like phenotype upon differentiation with phorbol esters) that were stimulated by treatment with ISD, polyI:C, or HCV PAMP RNA [29] (data not shown).

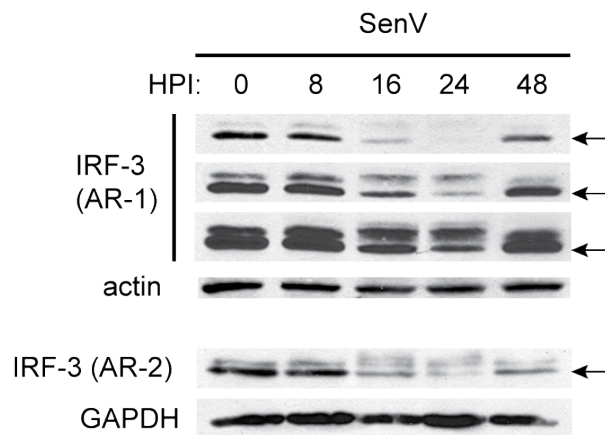


Figure II-2: SDS-PAGE followed by immunoblot analysis of IRF3 in SupT1 cells infected with SenV over the indicated time course. Three film exposures are shown for the AR-1 mAb (top), ordered from shortest (first) to longest time of exposure (third). Protein samples were re-run on a separate gel for probing with the AR-2 mAb (bottom). Actin and GAPDH are loading controls. For IRF3, the indicated bands mark resting IRF3 (black arrows).

To determine whether the appearance of IRF3 laddering represents IRF3 activation-induced phosphorylation detected by the AR-1 mAb, we conducted anti-IRF3 phospho-S-396-specific antibody immunoblot assay of IRF3. For this analysis we assessed 293T cells infected with SenV and compared the resulting pattern of IRF3 abundance with that detected by the AR-1 mAb when used to probe the same blot. Our results show that the AR-1 mAb detects both non-activated and activated/phosphorylated IRF3 isoforms (Figure II-3). The strongest-appearing S-

396-phospho-IRF3 bands (denoted by the grey triangle in Figure II-3) correspond to the slowest mobility bands visible on the AR-1 blot and are indicative of active IRF3 (black arrow, Figure II-3). ISG56 is an IRF3-dependent gene product, and is expressed after IRF3 activation or IFN treatment of cells (Figure II-3). Immunoblot assay of nuclear/cytoplasmic fractions of 293T cells infected with SenV for 18 hrs demonstrates translocation of activated IRF3 to the nucleus as detected by the AR-1 mAb (Figure II-4), as well as the presence of the resting IRF3 isoform (black arrow) in the cytoplasm. Moreover, AR-1 mAb immunoblot analysis revealed the presence of several high mass/putative phosphorylated IRF3 species in the nuclear fraction of infected cells. Thus, the AR-1 mAb provides a sensitive and specific immunoreagent for assessing IRF3 abundance and activation and can detect both resting and active isoforms of IRF3 by immunoblot assay of denatured protein.

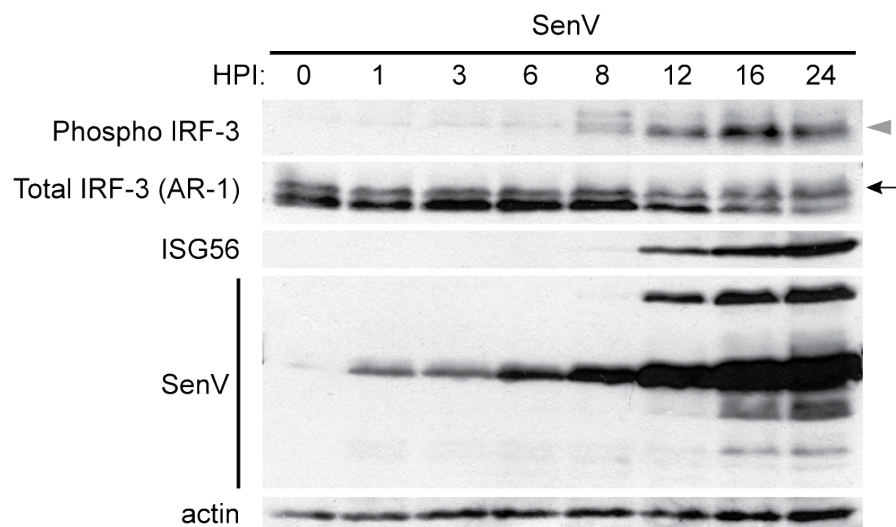


Figure II-3: SDS-PAGE followed by immunoblot analysis of phospho-S396 IRF3, total IRF3, ISG56, and SenV proteins in infected 293T cells at the indicated timepoints. For IRF3, an upper band (black arrow) corresponds to phosphorylated IRF3 (grey triangle).

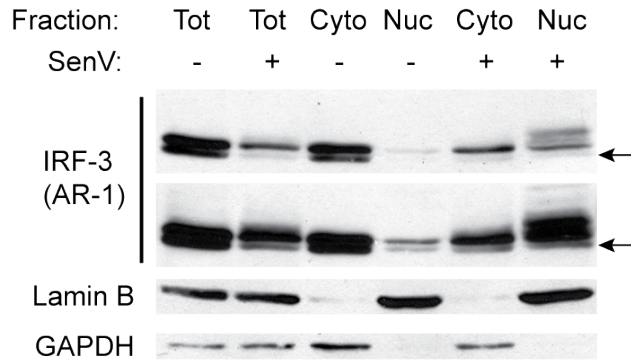


Figure II-4: Nuclear/cytoplasmic fractionation followed by SDS-PAGE and immunoblot analysis of IRF3 in 293T cells infected with SenV for 18 hrs. Short (top panel) and long (bottom panel) film exposures are shown. Lamin B (nuclear) and GAPDH (cytoplasmic) markers are shown.

We previously reported that HIV-1 directs a robust blockade of IRF3 function through the direct targeting and destruction of IRF3 [106]. Infection of SupT1 T cells with HIV_{LAI} and analysis by immunoblot with the AR-1 mAb recapitulates this phenotype. We probed infected cell lysate with the AR-1 mAb and demonstrated HIV-1-mediated degradation of IRF3 by 24 and 48 hours post infection, which is concomitant with viral replication and viral protein accumulation (Figure II-5). Importantly, no laddering of IRF3 was observed upon HIV-1 infection of cells (Figure II-5), consistent with previous reports that HIV-1-induced degradation of IRF3 occurs independently of IRF3 activation and is not mediated by IRF3 activation-induced turnover [106, 194]. Thus, the AR-1 mAb can effectively measure HIV-1 suppression of IRF3 in T cells.

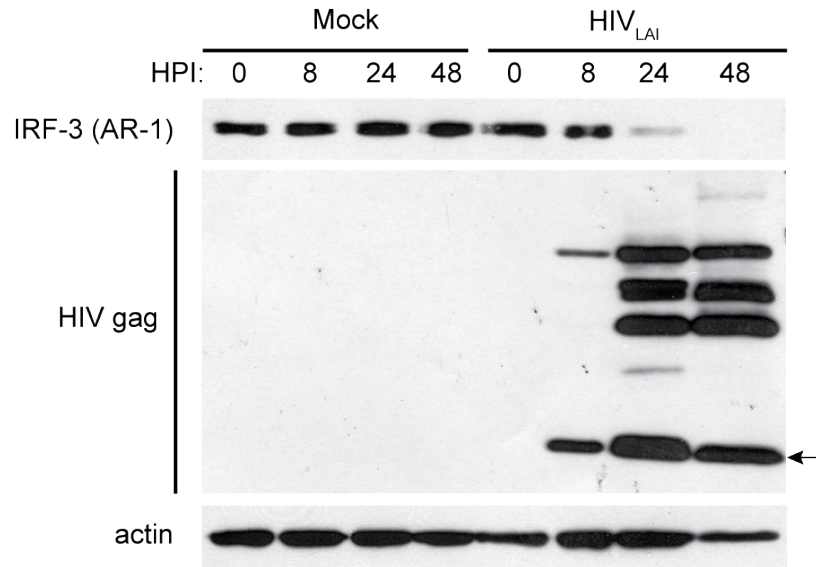


Figure II-5: SDS-PAGE followed by immunoblot analysis of IRF3 and HIV gag in SupT1 cells infected with HIV_{LAI} (MOI 1) for the indicated timepoints. Black arrow indicates the mature form of HIV gag protein (p24).

To further characterize the AR-1 mAb, we measured AR-1 immunoreactivity on extracts prepared from SupT1 cells stably expressing an shRNA that specifically knocks down IRF3 expression (Figure II-6). We found that the AR-1 mAb could detect IRF3 in control cells harboring non-targeting shRNA but had no reactivity to cell extracts prepared from cells with specific IRF3 knockdown. Moreover, we examined the species-specific reactivity of the AR-1 mAb by conducting immunoblot analysis of various mouse, human, and non-human primate cell extracts. We found that the AR-1 mAb reacts to human and rhesus macaque but not mouse IRF3 (Figure II-7). The AR-1 mAb also reacts to IRF3 from Vero cells, an African green monkey-derived cell line (Figure II-7), although with lower signal strength compared to the human and rhesus macaque bands. Full-length protein sequence analysis using ClustalW [220] and Jalview [221] of human, macaque, Vero cell, and mouse IRF3 (Figure II-8) showed that the N-terminal half of IRF3 contains regions of dissimilarity between the human and mouse sequences but

regions of high similarity between the human, macaque, and Vero cell sequences, suggesting that the N-terminus of IRF3 might determine the antibody specificity between species. We therefore assessed AR-1 detection of human IRF3 truncation mutants. We found that while the AR-1 mAb reacts efficiently to full-length IRF3, it fails to detect recombinant IRF3 Δ N (Figure II-9) lacking amino acids 9-133. Amino acids 9-133 contain the DNA-binding domain of IRF3 [213]; thus the AR-1 mAb recognizes an epitope within the DNA-binding domain of IRF3. Since human, macaque, and Vero cell IRF3 sequences of amino acids 9-133 are nearly identical, the reduced reactivity of the AR-1 mAb to Vero cells IRF3 relative to the human and macaque IRF3 (Figure II-7) is likely due to the relative lower abundance of IRF3 in Vero cells compared to human and macaque cells, as has been previously reported [222].

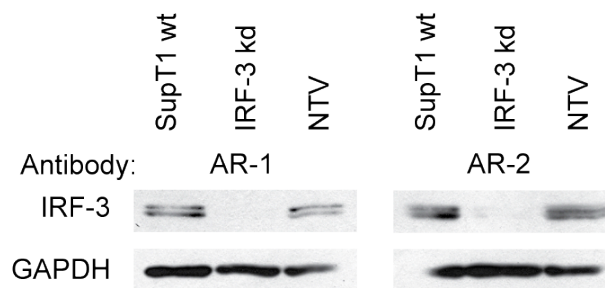


Figure II-6: SDS-PAGE followed by immunoblot analysis of extracts of SupT1 cells, wild type (wt) or stably expressing shRNA to IRF3 (IRF3 kd) or non-targeting vector (NTV).

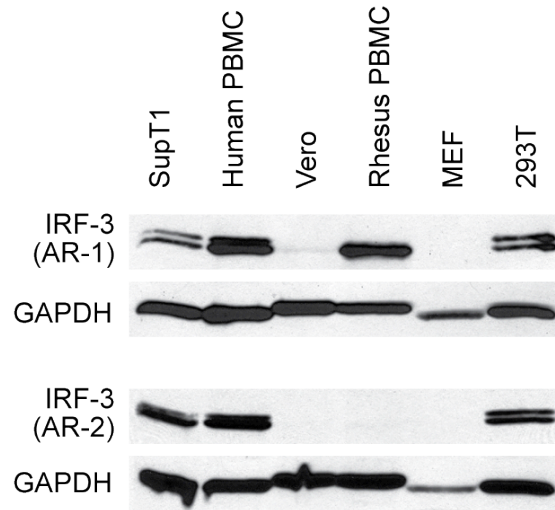


Figure II-7: SDS-PAGE followed by immunoblot analysis of IRF3 in human (SupT1, human PBMC, and 293T), African green monkey (Vero), rhesus macaque, and mouse, using the indicated antibodies.

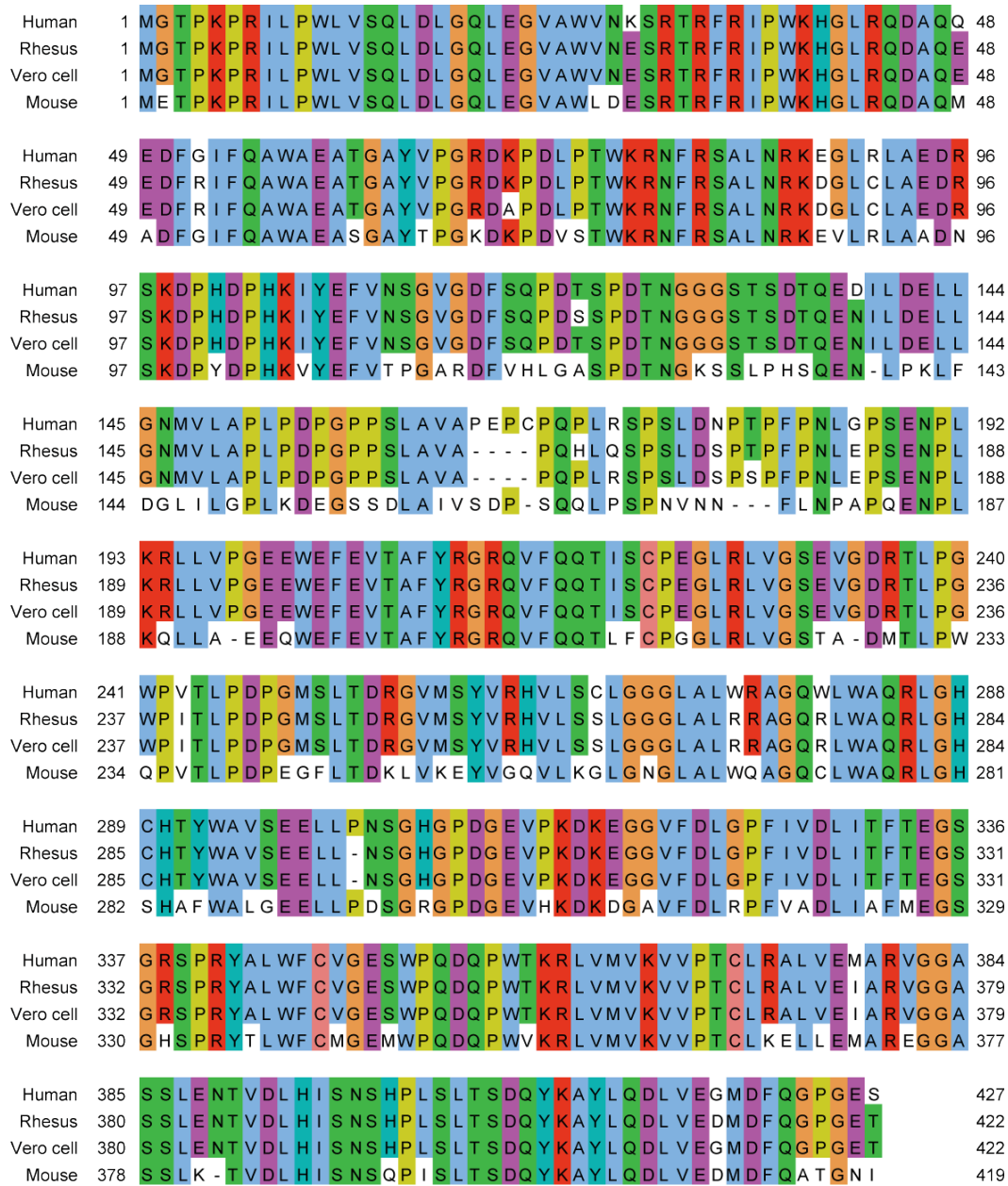


Figure II-8: Sequence alignment using ClustalW of reference protein sequences for IRF3 from human (NCBI Reference Sequence NP_001562.1), rhesus macaque (NP_001129269.1), Vero cell ([222]) and mouse (NP_058545.1), visualized in Jalview. Identical amino acids between at least two species are colored.

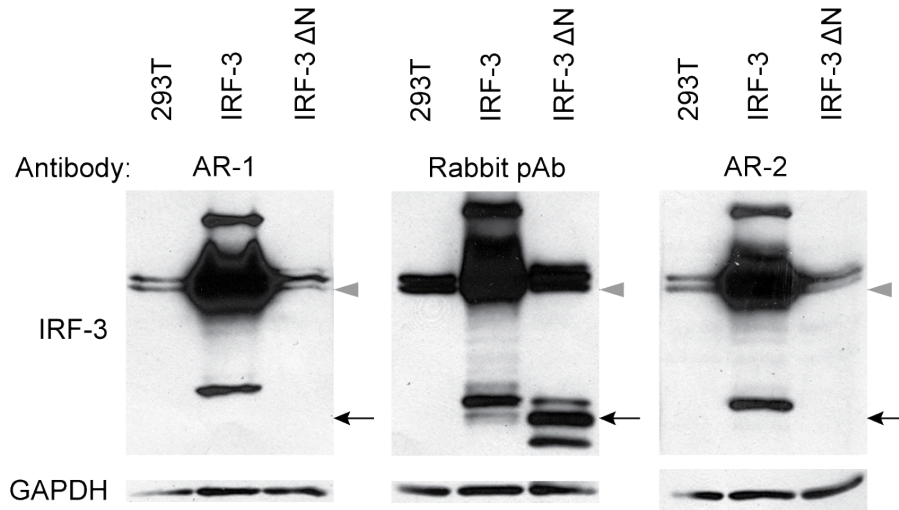


Figure II-9: SDS-PAGE followed by immunoblot analysis of IRF3 in 293Ts that were mock transfected or transiently transfected for 36 hrs with BL-CMV-IRF3 or BL-CMV-IRF3ΔN. For IRF3, the band corresponding to resting full-length IRF3 (grey triangle) and the three bands corresponding to IRF3ΔN (black arrow) are indicated.

Our data indicate that the AR-1 mAb can detect denatured endogenous and recombinant human IRF3, and is therefore useful as a reagent for immunoblot assay. To determine if AR-1 can detect IRF3 protein in its native, three-dimensional conformation, we tested the ability of the AR-1 mAb to detect native, non-denatured IRF3 *in situ* by immunofluorescence microscopy. When used as a primary antibody to stain uninfected TZM-bl cells (a HeLa-derived cell line), the AR-1 mAb detected the cytosolic/resting form of IRF3 (Figure II-10, bottom). In cells that had been infected with 200 HAU/mL SenV for 18 hours, the AR-1 mAb detected the nuclear/active forms of IRF3 (Figure II-10, top, and [200]). Importantly, however, the AR-1 mAb provided a much stronger signal of IRF3 staining above background in infected cells in which IRF3 had translocated to the nucleus, suggesting either that IRF3 signal intensity increases when the antigen is concentrated in a smaller area of the cell, or that AR-1 could specifically detect native, active IRF3 more efficiently than it detects the resting IRF3 isoform.

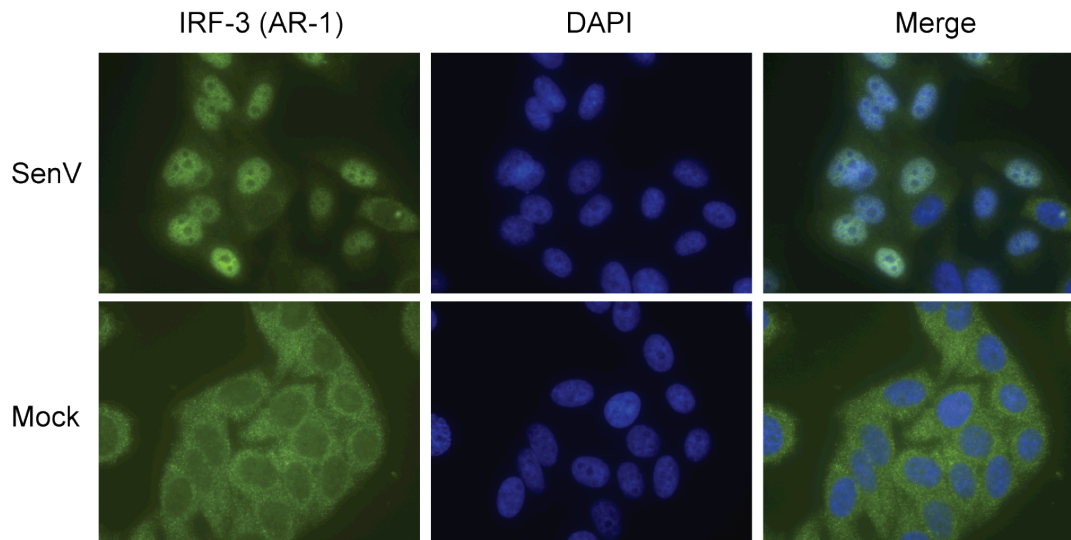


Figure II-10: Immunofluorescence analysis of IRF3 (AR-1 mAb, green) and nuclei (DAPI, blue) in T2M-bl cells infected with SenV for 18 hrs.

To further characterize the ability of the AR-1 mAb to detect native IRF3, we assessed IRF3 localization in a highly sensitive flow cytometry assay developed in our laboratory. This assay allows high-throughput analysis of IRF3 protein levels and activation state on a per-cell and quantitative basis. We permeabilized cells and used the Amnis ImageStream instrument for assessment of IRF3 by AR-1 mAb immunostaining. We examined IRF3 in uninfected SupT1 cells and in cells infected for 16 hrs with SenV. Colocalization of IRF3 and the nuclear stain DAPI was apparent in SupT1 cells infected with SenV (Figure II-11, bottom). Analysis of infected cultures revealed the presence of cells harboring resting/cytoplasmic IRF3 as well as those harboring nuclear/active IRF3 responding to the SenV infection (Figure II-11, top). For further analysis using conventional flow cytometry, we directly conjugated the AR-1 mAb to AlexaFluor647 fluorophore to facilitate direct immunostaining of cells. An antibody concentration sensitive to IRF3 knock-down in SupT1 cells was determined by titration analysis, and was applied to our assay (Figure II-12). Upon performing flow cytometry analysis on SenV-

infected SupT1 cells, we found that virus-infected cells displayed an overall increase in IRF3 fluorescence (Figure II-13), and this occurred concomitant with the appearance of activated IRF3 isoforms as assessed in parallel by denaturing immunoblot assay of extracts from the same cells (Figure II-14). Moreover, the typical depletion and recovery of IRF3 that occurs after virus infection (Figure II-2) was not detected by flow cytometry over a 24-hour SenV timecourse, suggesting that the AR-1 mAb is specific to the activated but not the resting IRF3 isoform in the context of native, non-denaturing assay conditions.

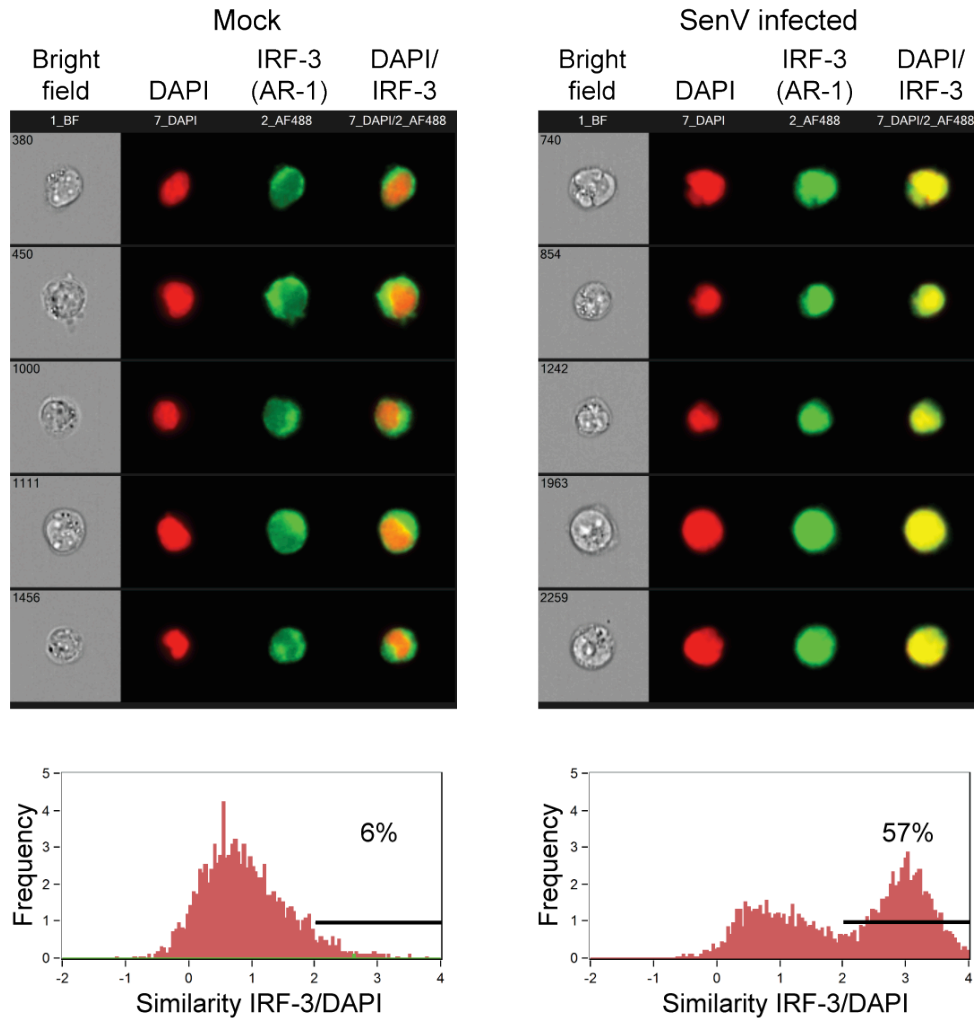


Figure II-11: ImageStream analysis of IRF3 (AR-1 mAb, green) and nuclei (DAPI, red) in SupT1 cells mock or SenV-infected for 18 hrs. Representative brightfield, red, green, and red/green merge images are shown (top). Analysis of IRF3/DAPI colocalization on the whole population is quantified (bottom). The percentage of cells with similarity values above an arbitrary value of 2 is shown.

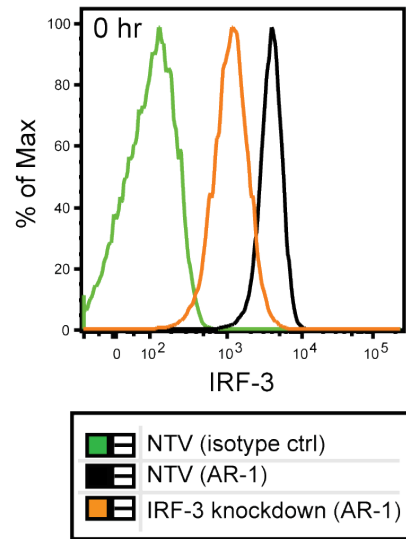


Figure II-12: Flow cytometry analysis of SupT1 cells using isotype control antibody or AR-1 mAb (IRF3).

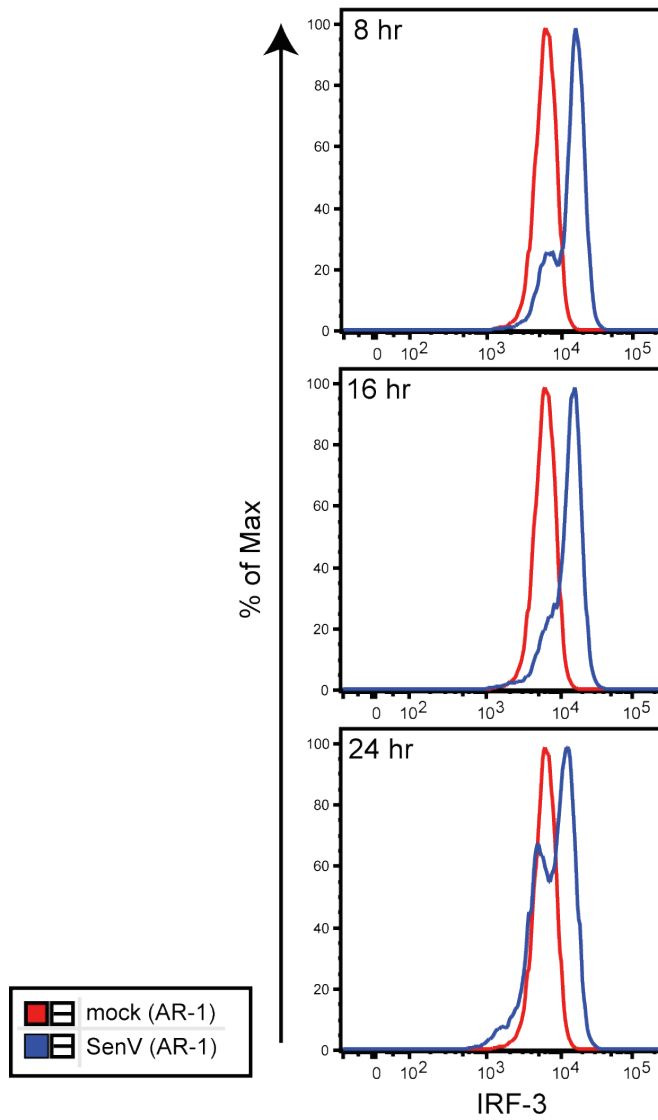


Figure II-13: Flow cytometry analysis of IRF3 in SupT1 cells infected with SenV for the indicated timepoints. Mock refers to 0 hrs of infection.

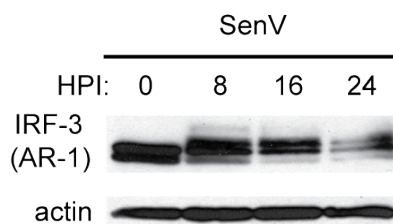


Figure II-14: SDS-PAGE followed by immunoblot analysis of IRF3 in the same cells used in Figure II-13.

To confirm whether or not the AR-1 mAb preferentially detected active IRF3 under native conditions, we compared the relative sensitivity of the AR-1 mAb for resting vs. active IRF3 by native PAGE and immunoblot analysis. In the SenV-infected SupT1 cell lysate, the AR-1 mAb was highly specific to the active/dimeric IRF3 isoform but did not react to the resting/monomeric isoform by native PAGE, though both isoforms were detected by SDS-PAGE and immunoblot analysis (Figure II-15 and Figure II-17). To facilitate a specific flow cytometry assay of total IRF3 protein, including both active and resting IRF3 isoforms, we sought to develop a mAb that could bind to native resting/monomeric IRF3 as well reacting to IRF3 in its active/dimeric isoform. We therefore tested supernatants from additional anti-IRF3 mAb-producing hybridoma clones from our original screen in order to identify a novel mAb that could recognize IRF3 isoforms under native conditions. This testing revealed an additional clone producing antibody that reacted well to the resting/monomeric IRF3 isoform (clone 2, Figure Figure II-16), as well as other clones (clones 3-5) that shared the AR-1 mAb specificity for dimeric IRF3 in native conditions. Antibody from the newly-identified clone #2, designated AR-2, detected IRF3 activation, turnover, and recovery within lysates from SenV-infected cells (see Figure II-2, bottom panel). The AR-2 mAb was specific for IRF3, as it did not detect IRF3 in lysate from cells with a stable knock-down of IRF3 mRNA expression (Figure II-6). Similar to

the AR-1 mAb, the AR-2 mAb detected full-length IRF3 but not IRF3 Δ N protein (Figure II-9). However, the AR-2 mAb was found to be human-specific and did not recognize non-human primate IRF3 (Figure II-7). Thus, the AR-2 mAb offers a novel reagent for immunodetection of both resting and active IRF3 isoforms, while the AR-1 mAb provides a novel mAb reagent for the specific detection of native, active IRF3 and is amenable to high throughput flow cytometric assessment of IRF3 activation state.

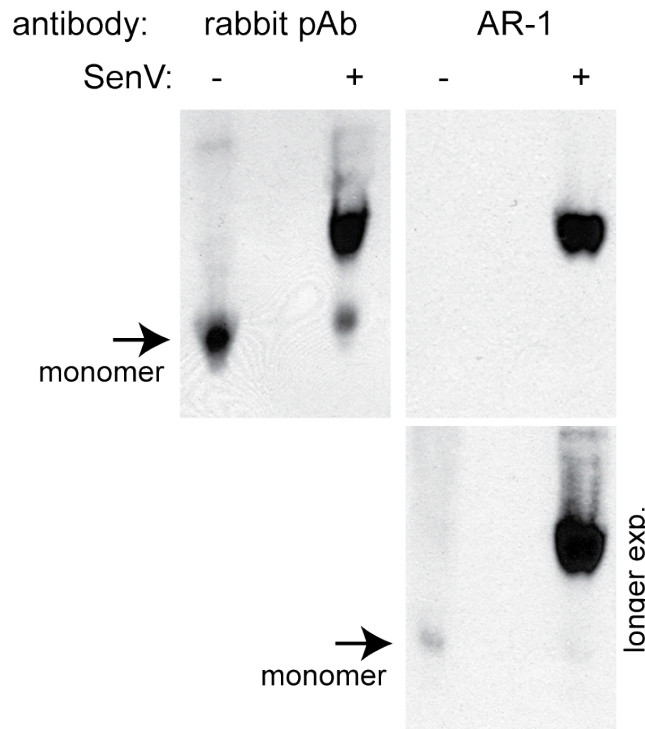


Figure II-15: Native PAGE followed by immunoblot analysis for IRF3 in SupT1 cells infected with SenV for 18 hrs. A rabbit polyclonal antibody or AR-1 mAb was used to detect IRF3. Arrows indicate monomeric IRF3. Short (top) and long (bottom) film exposures are shown.

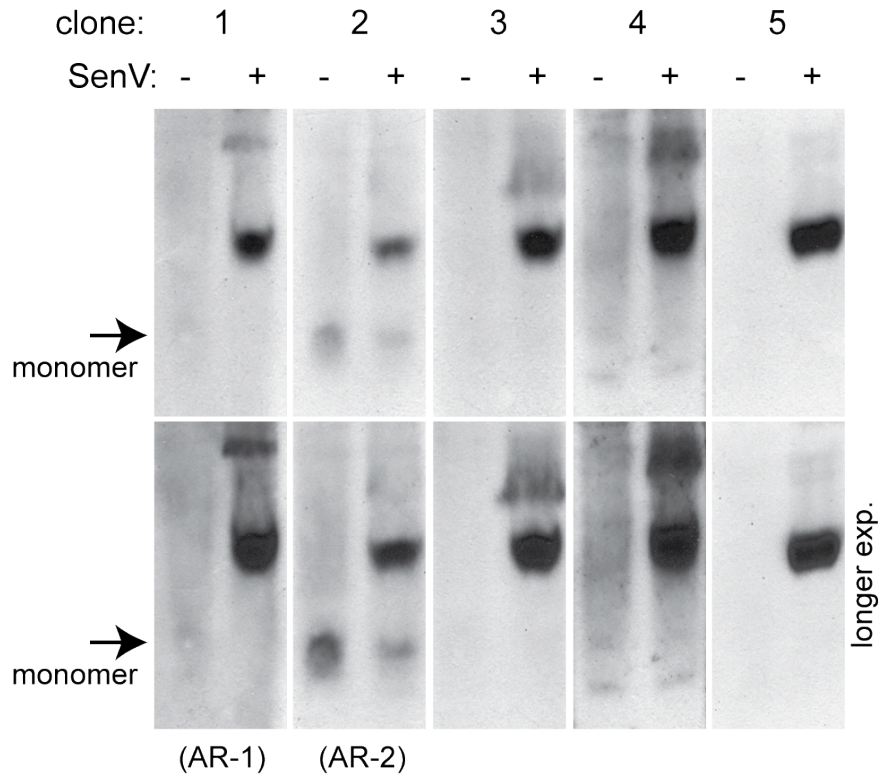


Figure II-16: Native PAGE followed by immunoblot analysis for IRF3 using supernatants from five hybridoma clones. Clone number 1 represents AR-1 mAb, while clone number 2 represents AR-2 mAb. Short and long film exposures of each immunoblot assay are shown as in 4A.

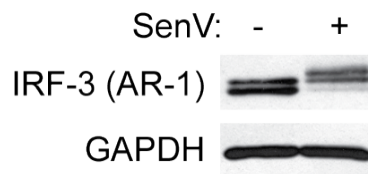


Figure II-17: SDS-PAGE followed by immunoblot analysis for IRF3 (AR-1) for loading control.

CONCLUSIONS

We have described two novel mouse monoclonal antibodies to human IRF3, designated AR-1 and AR-2, and we have developed a novel flow cytometric assay using the AR-1 mAb for

high throughput assessment of IRF3 activation state. In analyses of native IRF3 protein, the AR-1 mAb was found to specifically recognize active/dimeric IRF3, while the AR-2 mAb can detect both resting/monomeric IRF3 and active/dimeric IRF3. The AR-1 mAb detects human and nonhuman primate IRF3, while AR-2 mAb detection of IRF3 is restricted to human. The AR-1 mAb is therefore a useful reagent for the detection of activated human IRF3 by intracellular staining and flow cytometry. A summary of the characteristic properties of the two new reagents is depicted in Table II-1. The AR-2 mAb may prove useful for high-throughput assessment of resting and active IRF3 levels in a variety of cells types. These mAbs applied to our flow cytometry assay and other conventional assessments of IRF3 status can provide insights into virus activation and regulation of human and macaque IRF3 protein during infection. In clinical and research specimens, these reagents will allow for rapid screening of IRF3 agonists for antiviral and immunomodulatory drug development.

Table II-1: Summary of new monoclonal antibody properties. TBD, to be determined.

Antibody	Detects total IRF3 after SDS-PAGE	Detects monomeric IRF3 after native PAGE	Cross reacts with non-human primate	Detects epitope in DNA-binding domain	Detects IRF3 activation by flow cytometry
AR-1	Yes	Very weakly	Yes	Yes	Yes
AR-2	Yes	Yes	No	Yes	TBD

ACKNOWLEDGMENTS

We thank the Antibody Development Facility and John P. McNevin at the Fred Hutchinson Cancer Research Center for technical assistance, and Dr. Stacy M. Horner for critical

reading of the manuscript. The following reagents were obtained through the NIH AIDS Research and Reference Reagent Program, Division of AIDS, NIAID, NIH: TZM-bl from Dr. John C. Kappes, Dr. Xiaoyun Wu and Tranzyme, Inc; GHOST R3/X4/R5 from Dr. Vineet N. KewalRamani and Dr. Dan R. Littman; mAb to HIV-1 p24 (AG3.0) from Jonathan Allan; CEM-ss cells from Peter L. Nara. This work was supported by grants from the UW Medical Scientist Training Program (5T32GM007266-34) and the UW STD/AIDS Training Grant Program (T32 AI07140-32) to A.R. and by NIH grants R01DA024563, R01AI060389, and U19AI08319 to M.G.

ADDENDUM

Since publication of this project, we stabilized the AR-2 hybridomas, produced and purified antibody, and tested it for use on denatured and native protein. SDS-PAGE and immunoblot using purified AR-2 mAb was identical to blots published above. The AR-2 mAb was then tested on native IRF3 in an immunofluorescence assay on SenV-infected TZM-bl cells, as shown for AR-1 in Figure II-10. The resultant staining is shown in Figure II-18. Surprisingly, although the AR-2 mAb recognizes non-denatured IRF3 protein by native PAGE, the antibody demonstrates a subtle qualitative increase in perinuclear staining but does not demonstrate the full nuclear translocation (colocalization with DAPI) seen with AR-1 (or other anti-IRF3 antibody) staining. As a result, AR-2 was not tested further for suitability in flow cytometry or Imagestream applications.

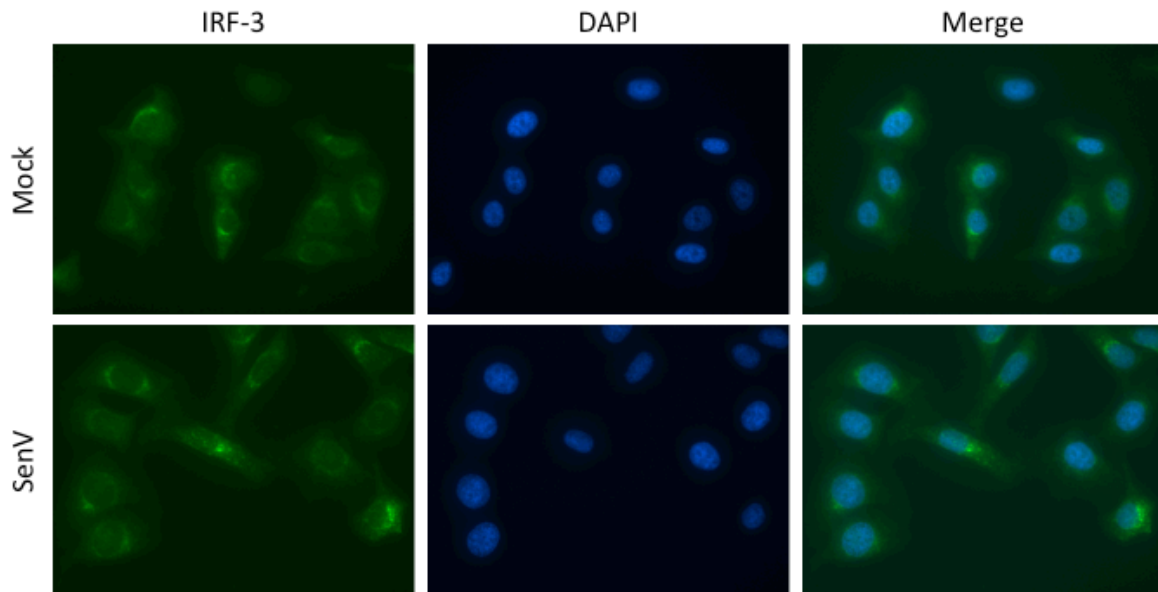


Figure II-18: Immunofluorescence analysis of IRF3 (AR-2 mAb, green) and nuclei (DAPI, blue) in TZM-bl cells infected with SenV for 18 hrs.

III. VPU IS NECESSARY AND SUFFICIENT TO INHIBIT IRF3 FUNCTION

This chapter will be combined with chapter IV as a manuscript.

ABSTRACT

Human immunodeficiency virus 1 (HIV-1) infection continues to be a major public health problem, with 34 million people infected worldwide. Cell-intrinsic innate immune defenses are essential for the control of HIV-1 infection, and are evaded by the virus to establish successful infection. Interferon regulatory factor 3 (IRF3) is a central transcription factor of innate immune signaling that is activated by cellular pattern recognition receptors in response to the presence of non-self molecules. Activation of IRF3 induces the expression of antiviral and immunomodulatory genes whose products can suppress HIV-1 infection within target cells and regulate the adaptive immune response to infection, and we have found that during acute infection HIV-1 evades innate antiviral immunity through the actions of HIV-1 viral protein *v* (Vpu), which interacts with IRF3 and inhibits its activity. Vpu blocked both IRF3- and NF κ B-dependent activities at the IFN- β promoter. These findings led us to hypothesize that Vpu blocks IRF3 activation to prevent IRF3 from carrying out the necessary biochemical steps to drive antiviral gene expression. We investigated these steps, and found that IRF3 and Vpu form a stable complex during infection of CD4⁺ T cells with HIV-1. Using truncation and deletion mutants of recombinant IRF3, we mapped the binding epitope for Vpu on IRF3 to a region of IRF3 protein called the IRF association domain. This domain is the site necessary for homodimerization of IRF3 molecules after activation and interaction with transcriptional

cofactors, so we hypothesized that Vpu alters IRF3 dimerization and cofactor interaction. Indeed, when we examined the IRF3 activation pathway in the presence of Vpu to identify the site of the Vpu-induced block in IRF3 activity, we found that Vpu inhibited IRF3 dimerization and CBP binding. We predict that Vpu antagonism of IRF3-directed innate immunity may be a key step in HIV-1 pathogenesis during acute infection.

INTRODUCTION

Microbial infection is sensed by pattern recognition receptors (PRRs) that recognize foreign pathogen-associated molecular patterns (PAMPs) [207]. Downstream of PRRs, signaling cascades lead to the transcription of genes that mediate an antimicrobial state, and several PRRs signal to the activation of IRF3. When activated, IRF3 directly drives the transcription of several genes with key antiviral functions including interferon- β (IFN- β) [114]. Signaling by IFN- β , both in an autocrine and paracrine manner, leads to the expression of hundreds of interferon-stimulated genes (ISGs) [113]. ISG products inhibit viral replication through a diverse set of mechanisms, and factors known to restrict HIV-1 infection are interferon stimulated (e.g. APOBEC3G and tetherin/BST2 [223], schlafen 11 [142]), but most ISGs have yet to be characterized. In order to support replication, viruses have developed mechanisms to block the induction of the innate antiviral response, the function of specific ISGs, or both.

IRF3 is constitutively expressed in virtually all cells [77] and encodes a ~55 kDa protein that contains a DNA-binding domain (DBD), nuclear export signal, IRF-association domain (IAD), and a C-terminal serine-rich region [99, 211]. The serine-rich region contains several phosphorylation sites, some of which are phosphorylated in the resting state. Activation-specific phosphorylation occurs at certain residues, such as S396, after which IRF3 dimerizes,

translocates to the nucleus, and associates with the necessary coactivator CBP/p300 to drive gene transcription [92-94]. IRF3-dependent gene transcription normally ends upon ubiquitination of IRF-3 and proteasome-dependent degradation [103, 104].

When activated, IRF3 directs a response that suppresses HIV-1 infection in CD4+ T cells and macrophages [106]. To counter these antiviral actions of IRF3, HIV-1 directs the degradation of IRF3 [106, 194]. This IRF3 degradation results in suppression of innate immune defenses that allow the virus to replicate and persist unchecked by host cell-intrinsic antiviral defenses. IRF3 degradation overall supports HIV-1 infection and therefore may contribute to the development of AIDS [106, 194]. Other examples of direct [151, 176, 178] and indirect [157, 173] inhibition of IRF3 by viruses have been observed. Direct antagonism of anti-HIV ISGs has also been reported. For example, tetherin cannot function as an inhibitor of viral release when targeted away from the cell surface and degraded through the actions of Vpu [68]. In addition, we previously reported that Vpu is responsible for trafficking of IRF3 to the lysosome, preventing innate immune signaling, particularly as measured by IFN- β promoter activity [168]. Further, we reported that infection of macrophages with Vpu-deficient HIV-1 leads to the induction of IRF3-dependent genes, while infection with Vpu-expressing virus does not [167]. However, Hotter and colleagues reported that Vpu alone is not sufficient to induce degradation of IRF3, and that Vpu inhibited the activity of NF κ B [195]. The authors suggested that suppression of IFN- β therefore is the result of Vpu inhibition of NF κ B activity and not due to IRF3 depletion [195]. This suggestion is based on the concept that both IRF3 and NF κ B are components of the IFN- β enhanceosome, a complex of proteins that drives the enhancer element, which is the DNA sequence -102 to -47 bp from the transcription start site for the IFN- β gene [107].

Activation of the IFN- β enhancer occurs at a low rate in resting cells [108], while strong activation involves the cooperation of several factors: NF κ B, an IRF3 dimer, an IRF7 dimer, and AP-1 [109]. Though IRF7 is an ISG, enough IRF7 is basally expressed to participate in the earliest activation of the IFN- β promoter [111]. The DNA-binding proteins are stabilized by interactions with CBP/p300 in a structure called the enhanceosome [107]. In addition, IRF3 and IRF7 are sufficient to drive virus-dependent IFN- β production in the absence of NF κ B and AP-1, while NF κ B and AP-1 may be responsible for the weak basal promoter activity [112]. NF κ B binds to the PRDII domain of the IFN- β enhancer, while the IRFs bind to PRDIII and I [107]. NF κ B activity is necessary for transcription of the latent HIV-1 genome after integration, though during later stages of infection (virion accumulation in the cell), the antiviral ISG tetherin may function as an inducer of innate immunity, as interaction between tetherin and HIV-1 virions drives NF κ B-dependent signaling [70]. Degradation of tetherin by Vpu may link Vpu to decreases in IFN- β activity [195]. However, the ability of Vpu to inhibit transcription of promoters activated by IRF3 but not NF κ B (promoters that can be found upstream of IRF3-dependent genes) has not been thoroughly evaluated.

Assessment of IRF3 function and viral inhibition of IRF3 is effectively measured by promoter luciferase activity. Studies of IFN- β by Vpu and Vpu-expressing HIV-1 genomes have revealed that Vpu imparts control of IRF3 function at early timepoints after infection [167, 168]. In addition, through microarray analysis of IRF3-dependent genes, a block in IRF3-dependent signaling can already be observed at 8 and 16 hrs post infection of macrophages with Vpu-expressing HIV-1 as compared to Vpu-deficient virus [167], suggesting a role for Vpu in inhibition of IRF3 function early in infection. However, degradation of IRF3 does not occur until later timepoints [106, 205], indicating that HIV-1 regulation of IRF3 is a multi-component

process that likely includes Vpu/IRF3 binding, possible cofactor regulation, and IRF3 degradation. However, the ability of Vpu to interact with IRF3 during HIV-1 infection of CD4+ T cells has not been examined.

In the experiments described in this chapter, we use dual luciferase assays to reveal the inhibition of NF κ B and IRF3 activities by 3 different Vpu constructs. Vpu from NL4-3 and WITO viral clones was able to inhibit the expression of luciferase driven by promoters containing IRF3 binding sites, NF κ B binding sites, or both. In addition, when infecting differentiated THP-1 cells with HIV-1, Vpu was necessary to inhibit the expression of IRF3-driven genes of innate antiviral immunity.

MATERIALS AND METHODS

Cells and transfections

293T, HEK-293, and TZM-bl cells were cultured in cDMEM: DMEM supplemented with 10% heat-inactivated FBS, L-glutamine, HEPES, sodium pyruvate, MEM non-essential amino acids, and antibiotics. THP-1 cells were cultured in cRPMI: RPMI supplemented with 10% heat-inactivated FBS, L-glutamine, HEPES, sodium pyruvate, and antibiotics. THP-1 cells were differentiated into macrophages using 100 μ M PMA. The following reagent was obtained through the NIH AIDS Reagent Program: TZM-bl from Dr. John C. Kappes, Dr. Xiaoyun Wu and Tranzyme, Inc. Transfections of cells were performed using Fugene 6 transfection reagent (Roche) according to the manufacturer's suggested protocol, except for generation of HIV-1_{JR-CSF} and HIV-1_{JR-CSF A/C} stocks, which used the calcium phosphate method.

Plasmids

Firefly luciferase constructs with the following promoters were used, and have been described previously: IFN- β [224], single IRF3 binding site only [78], IFN- β PRDII domain [224], and five NF κ B binding sites only [225]. In addition, the IFN- β promoter luciferase construct from [224] with mutated NF κ B DNA-binding site (GGGAAATTCC → TGGCAATTCA; labeled IFN- β Δ NF κ B) was generously gifted by Dr. Daniel Sauter. For all experiments, a renilla luciferase construct under the control of the constitutively active thymidine kinase promoter, pGL4.74 RL-TK (Promega), was transfected with a ratio of 10:1 firefly to renilla. The codon-optimized NL4-3 Vpu plasmid [226] was obtained from the NIH AIDS Reagent Program (pcDNA-Vphu from Dr. Stephan Bour and Dr. Klaus Strebel), while the Q23-17 Vpu [227] was a gift from Dr. Michael Emerman. The WITO Vpu construct [228, 229] was kindly gifted by Dr. Daniel Sauter.

Dual luciferase assay and statistics

Cells were plated at 3×10^5 cells per well of a 6-well plate and transfected 18 hours later with 2 μ g DNA per well. For luciferase assay transfections including both Vpu and IRF3 constructs, 400 ng IFN-B-luciferase (firefly), 40 ng pGL4.74 RL-TK, 390 ng IRF3 construct, and 1170 ng Vpu construct were used. For the other luciferase assay transfections, 500 ng IFN-B or other promoter luciferase (firefly), 50 ng RL-TK, and 1,450 ng Vpu were used. For dose responses, the amount of Vpu was 1450, 725, or 362.5 ng, with vector DNA as filler. Eighteen hours after transfection, cells were trypsinized, counted, and plated at 2×10^4 cells per well in a 48-well plate. For all experiments, ≥ 3 biological replicates were used. Cells were infected in the 48-well plate with 200 HAU/mL SenV Cantell strain (Charles River Laboratories) 24 hours after

transfection. Cells were lysed 18 hours after SenV infection and lysates transferred to 96-well plates for analysis with dual luciferase assay reagents (Promega). All data are presented as the ratio of firefly luciferase to renilla luciferase, and the ratios are normalized to an arbitrary vector-transfected, mock-infected sample in each experiment. Data were analyzed using Prism software (GraphPad) with two-tailed Student's *t*-test or two-way ANOVA with Bonferroni post-tests as appropriate.

Viral stocks and infections

HIV-1_{JR-CSF} and HIV-1_{JR-CSF A/C} stocks were made in 293T cells that were transfected with the JR-CSF plasmid or the JR-CSF A/C plasmid containing a stop codon instead of the Vpu translation initiation codon [168], and titered on TZM-bl cells to determine concentration of infectious virus. Sendai virus (SenV) strain Cantell was acquired from Charles River Laboratory.

Targeted genomics and data analysis

RNA extraction and preparation is described in [167]. Briefly, RNA was extracted and amplified, and mRNA was analyzed using an Illumina human HT12 array. Quality control was performed using R, and probes not expressed were removed. Bioinformatics analyses were performed as described in [230]. Briefly, functional analysis was performed using DAVID and Ingenuity Pathway Analysis (IPA) [231, 232]. Multiple test correction was performed on the IPA-generated *P* value using the Benjamini-Hochberg method.

RESULTS

We first confirmed our previous finding that Vpu is sufficient to block induction of the IFN- β promoter by SenV. SenV infection provides a RIG-I-specific stimulus that signals through

IRF3 and NFκB to activate IFN-β transcription. Upon cotransfection of HIV-1 viral clone NL4-3 Vpu, IFN-β promoter luciferase (firefly) and TK promoter luciferase (renilla) and various IRF3 constructs, Vpu inhibits IFN-β promoter activity (Figure III-1). This block occurs in the activity of endogenous IRF3, and is intact but diminished when IRF3 is overexpressed. When constitutively active IRF3 5D is expressed, NL4-3 Vpu transfection blocks SenV-induced IFN-β promoter activity, suggesting NL4-3 Vpu acts against endogenous IRF3 or other components of the IFN-β enhanceosome (such as NFκB) but not against IRF3 5D. IRF3 ΔN is a dominant negative variant that dimerizes with IRF3 but lacks the DNA-binding domain, preventing transcriptional activity. During SenV infection, IFN-β promoter activity in ΔN-transfected samples represents maximal inhibition of IRF3 signaling.

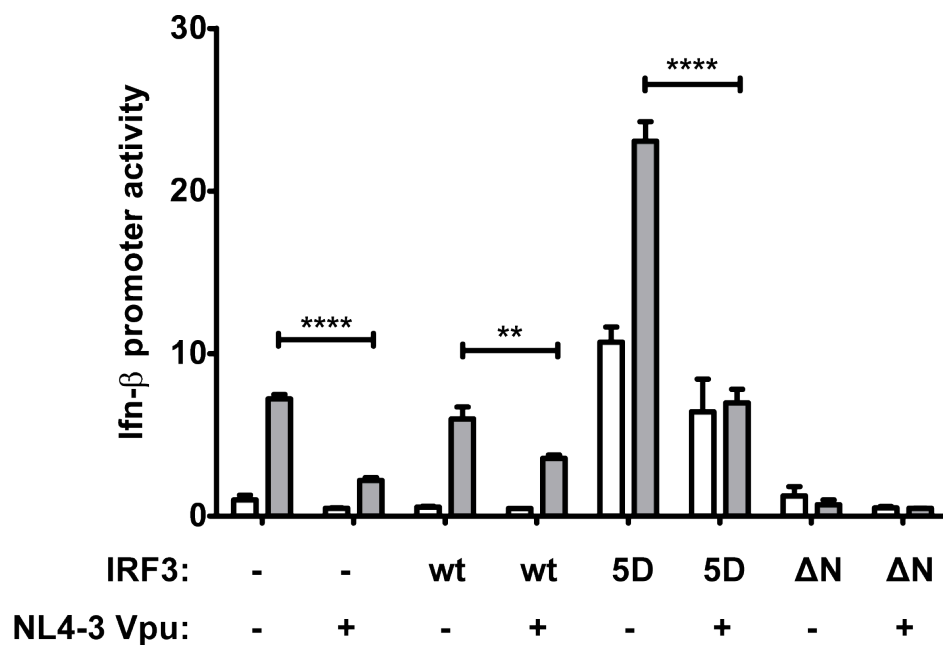


Figure III-1: NL4-3 Vpu inhibits IFN-β promoter activity. Fold induction of IFN-β promoter (as represented by firefly to renilla luciferase activity ratio) after transfection with IRF3 and Vpu constructs, followed by infection with SenV. White bars represent mock-infected cell lysates; grey bars represent SenV-infected cell lysates. Data represented as mean ± standard deviation (SD). $N \geq 3$ biological replicates. Two-tailed Student's *t*-test

was used to compare Vpu-transfected samples to vector-transfected for each condition. **** $P \leq 0.0001$; ** $P \leq 0.01$.

To determine whether or not the Vpu-induced inhibition of the IFN- β promoter is restricted to NL4-3 Vpu, we tested Vpu from Q23-17, a primary HIV-1 subtype A isolate obtained from a woman 1 year post seroconversion [227]. Vpu from this isolate was also able to block IFN- β promoter induction (Figure III-2). Unlike with NL4-3 Vpu, overexpression of IRF3 was unable to partially rescue suppression of promoter induction by Q23-17 Vpu. In addition, Q23-17 Vpu was able to inhibit IRF3 5D activation of the IFN- β promoter in the absence of SenV infection, suggesting more potent inhibition or inhibition of multiple components of the IFN- β enhanceosome. Thus, inhibition of IFN- β promoter activity is not restricted to NL4-3 Vpu.

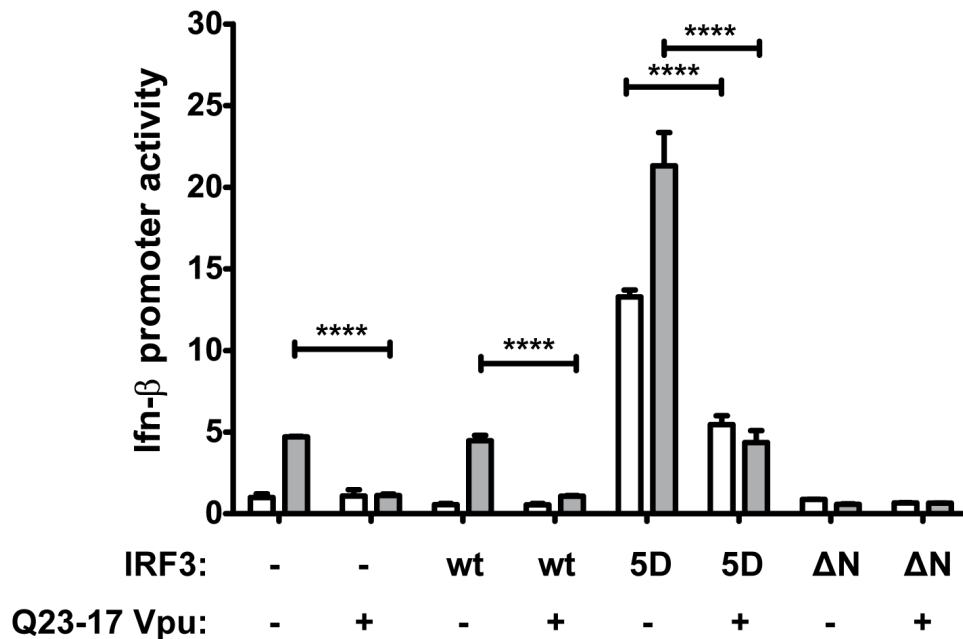


Figure III-2: Q23-17 Vpu inhibits IFN- β promoter activity. Fold induction of IFN- β promoter (as represented by firefly to renilla luciferase activity ratio) after transfection with IRF3 and Vpu constructs, followed by infection with SenV. White bars represent mock-infected cell lysates; grey bars represent SenV-infected cell lysates. Data represented

as mean \pm SD. $N \geq 3$ biological replicates. Two-tailed Student's *t*-test was used to compare Vpu-transfected samples to vector-transfected for each condition. **** $P \leq 0.0001$.

We then varied the transfected amount of NL4-3 Vpu, and found that the inhibition of SenV-induced IFN- β promoter activity is dependent on the dose of Vpu, as shown in Figure III-3. For this and subsequent experiments, we added WITO Vpu [228, 229] because it is derived from a founder variant of HIV-1 group M subtype B and therefore, as compared to Vpu from NL4-3 and Q23-17 clones, most representative of early infection [195]. When using equal amounts of Vpu DNA, WITO Vpu provided stronger inhibition of IFN- β promoter activity than NL4-3 Vpu.

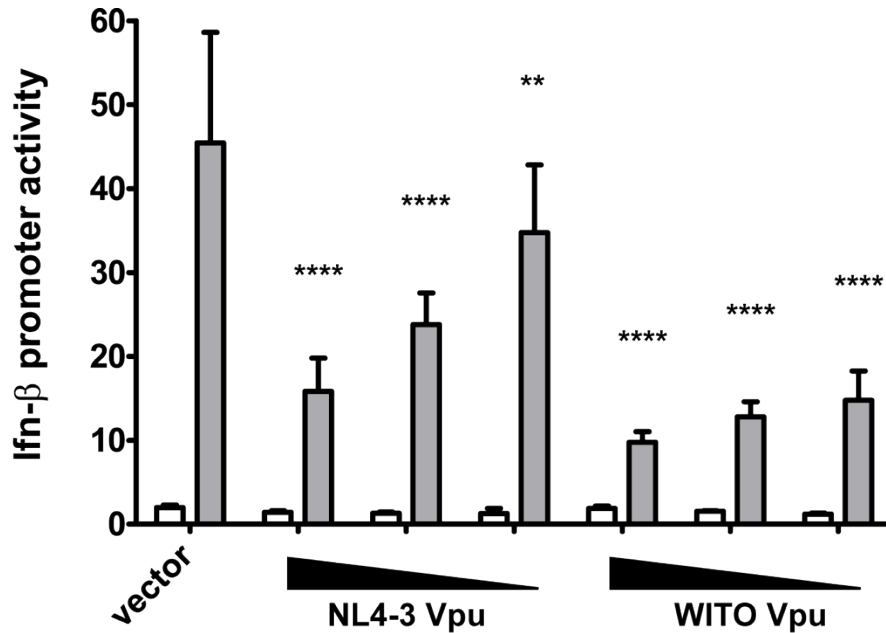


Figure III-3: Vpu from NL4-3 and WITO inhibit IFN- β promoter activity in a dose-dependent manner. Fold induction of IFN- β promoter (as represented by firefly to renilla luciferase activity ratio) after transfection with a dose response of NL4-3 and WITO Vpu constructs, followed by infection with SenV. The decreased doses represent 2- and 4-fold reductions in Vpu plasmid with vector plasmid added to maintain equal DNA amounts. White bars represent mock-infected cell lysates; grey bars represent SenV-infected cell lysates. Data represented as mean \pm SD. $N \geq 3$ biological replicates. Two-way ANOVA with Bonferroni post-tests was used. ** $P \leq 0.0001$; ** $P \leq 0.01$.**

We sought to determine whether the block in IFN- β promoter activation was due only to the ability of Vpu to block NF κ B-dependent enhancement of the IFN- β promoter, as suggested by Hotter and colleagues [195]. We first tested the ability of the Vpu proteins to block NF κ B-dependent signaling in the absence of IRF3-dependent enhancement. As shown in Figure III-4, during SenV infection, both NL4-3 Vpu and WITO Vpu were able to block NF κ B-dependent signaling to promoters containing 5 NF κ B binding sites only (left panel) or the PRDII sequence from the IFN- β promoter, which contains 1 NF κ B binding site but not IRF3 binding sites (right panel). With regard to these promoters, transfection of WITO Vpu DNA led to better inhibition of SenV-induced promoter activity than transfection of NL4-3 Vpu DNA. Thus, Vpu blocks NF κ B activity, which may contribute to the inhibition of IFN- β promoter activity. We then tested whether expression of the NL4-3 and WITO Vpu proteins could block IRF3-dependent signaling in the absence of NF κ B-dependent enhancement. For these experiments, we used a luciferase construct driven by a single IRF3 binding site, as well as the IFN- β promoter luciferase construct used in previous experiments (Figure III-1, Figure III-2, and Figure III-3) but this time with mutated NF κ B binding sites. Upon SenV infection, both NL4-3 Vpu and WITO Vpu were able to block IRF3-dependent promoter activation (Figure III-5). In contrast to their effects on the activity of the NF κ B and PRDII promoters, when tested on IRF3-only plasmids, NL4-3 Vpu was slightly better at inhibiting SenV-induced promoter activity as compared to WITO Vpu. Thus, in contrast to previously-published results [195], Vpu expression is sufficient to block IRF3 activity, indicating that inhibition of IFN- β promoter activity may involve actions by Vpu to block the activities of both NF κ B and IRF3.

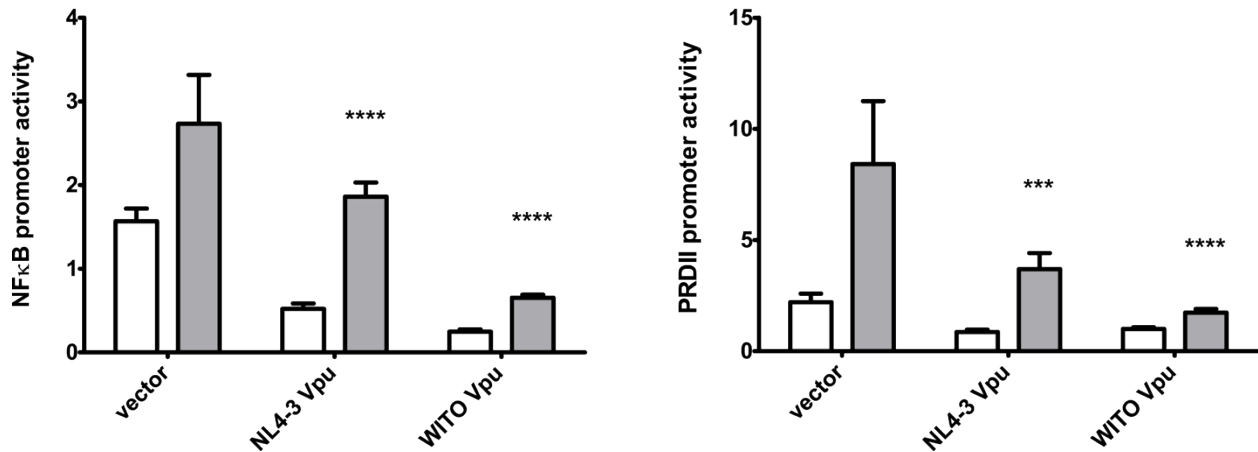


Figure III-4: Vpu from NL4-3 and WITO inhibit NFκB activity. Fold induction of limited promoters (as represented by firefly to renilla luciferase activity ratio) containing five NFκB binding sites (left) or PRDII sequence (right) after transfection with NL4-3 and WITO Vpu constructs, followed by infection with SenV. White bars represent mock-infected cell lysates; grey bars represent SenV-infected cell lysates. Data represented as mean ± SD. $N \geq 3$ biological replicates. Two-way ANOVA with Bonferroni post-tests was used. **** $P \leq 0.0001$; *** $P \leq 0.001$.

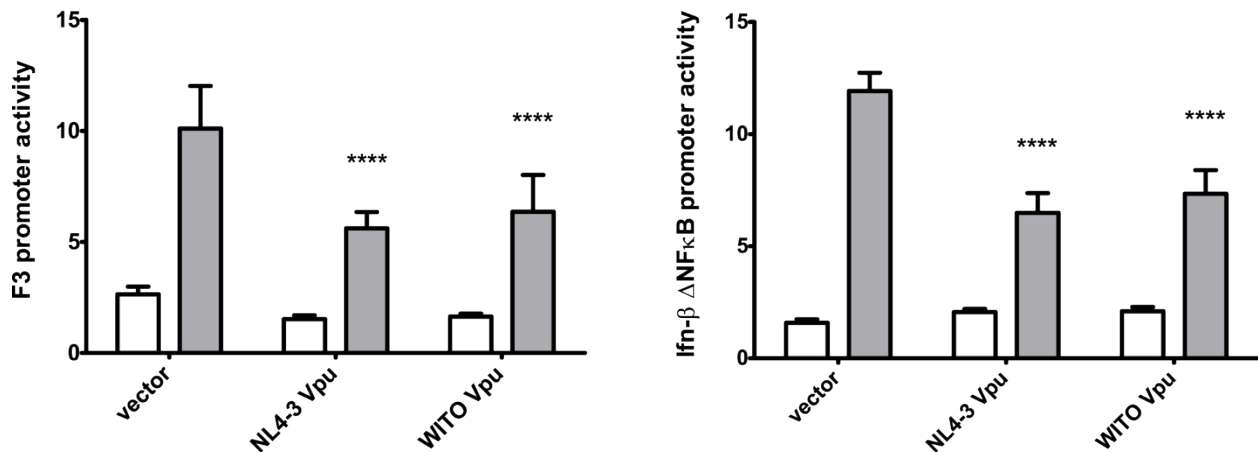


Figure III-5: Vpu from NL4-3 and WITO inhibit IRF3 activity. Fold induction (as represented by firefly to renilla luciferase activity ratio) of limited promoters containing a single IRF3 binding site (left) or the IFN-β promoter with mutated NFκB DNA-binding site (right) after transfection with NL4-3 and WITO Vpu constructs, followed by infection with SenV. White bars represent mock-infected cell lysates; grey bars represent SenV-infected cell lysates. Data represented as mean ± SD. $N \geq 3$ biological replicates. Two-way ANOVA with Bonferroni post-tests was used **** $P \leq 0.0001$.

In addition to being sufficient to block SenV-induced IRF3-dependent promoter activity, Vpu is necessary to inhibit the expression of many genes during viral infection of PMA-differentiated THP-1 cells, which model CD4⁺ macrophages [167]. We aimed to determine the biological processes altered by Vpu during infection at early timepoints, as well as the relationships between the top 25 altered genes and IRF3, using DAVID bioinformatics and Ingenuity Pathway Analysis (IPA). Since in previous work we observed that HIV-1_{JR-CSF} provirus inhibited IFN- β promoter luciferase activity better than other Vpu-expressing proviruses we tested [168], we infected PMA-differentiated THP-1 cells with HIV-1_{JR-CSF} virus generated in 293T cells from provirus encoding normal JR-CSF or a point mutation generating a stop codon in place of the Vpu start codon (HIV-1_{JR-CSF A/C}) at equal MOIs, and processed cell lysates for RNA microarray analysis at 8 h and 16 h post infection. We then applied IPA to those genes that differed ≥ 1.5 fold between HIV-1_{JR-CSF A/C}-infected and mock-infected cells, and are known to be IRF3-driven. The A/C mutation-associated, IRF3-regulated genes are displayed in Figure III-6, and the number of genes and statistical strength for each GO category are displayed in Figure III-1. Of the genes regulated by the Vpu-deficient virus, none are induced by the wild type virus at 8 hours, with a small fraction induced by the wild type virus at 16 hours post infection. Based on this analysis, infection with HIV-1 that contains Vpu significantly reduces the expression of IRF3-dependent genes that are associated with the immune response to viruses, protein kinase cascades, and transcriptional regulation.

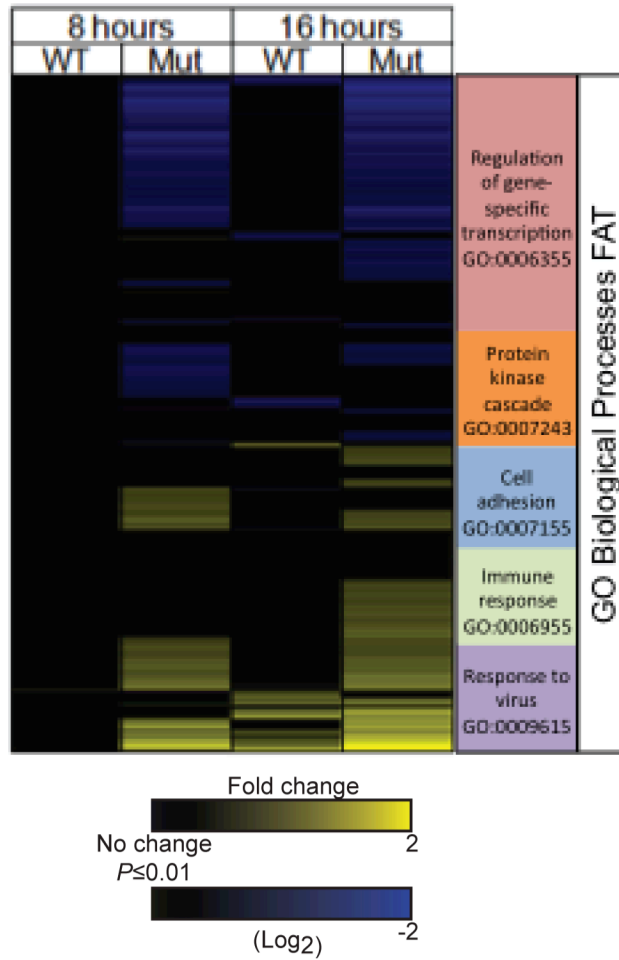


Figure III-6: Hierarchical clustering of differentially expressed genes between HIV-1_{JR-CSF} and HIV-1_{JR-CSF A/C} infected samples. Differentially expressed genes are shown as $\log_{10}(\text{ratio})$ of infected to mock-infected. Genes whose expression was significantly different in HIV-1_{JR-CSF A/C} relative to mock-infected cells are depicted in the heat map (1.5 fold; $P \leq 0.01$).

Table III-1: Number of genes annotated with each GO term and the associated *P* values for genes of a certain GO category to be differentially regulated by HIV-1 ± Vpu.

GO Term	Starting # of genes	# of genes recognized by DAVID	# of genes from top 25	<i>P</i>-value
Regulation of gene-specific transcription	360	330	10	5.8E-4
Protein kinase cascade	153	140	11	7.4E-4
Cell adhesion	132	125	12	1.6E-2
Immune response	128	119	15	1.2E-4
Response to virus	161	131	20	1.6E-21

Using these data, the top 25 genes that were upregulated during infection with the Vpu-deficient virus (HIV-1_{JR-CSF A/C}) were extracted and queried for interaction with IRF3 using IPA. All of the genes queried interacted with IRF3 directly or indirectly. A network was constructed around IRF3 with these genes (Figure III-7), and this network describes a signature of IRF3-regulated genes that are upregulated by Vpu-deficient viral infection, but not by wild type virus.

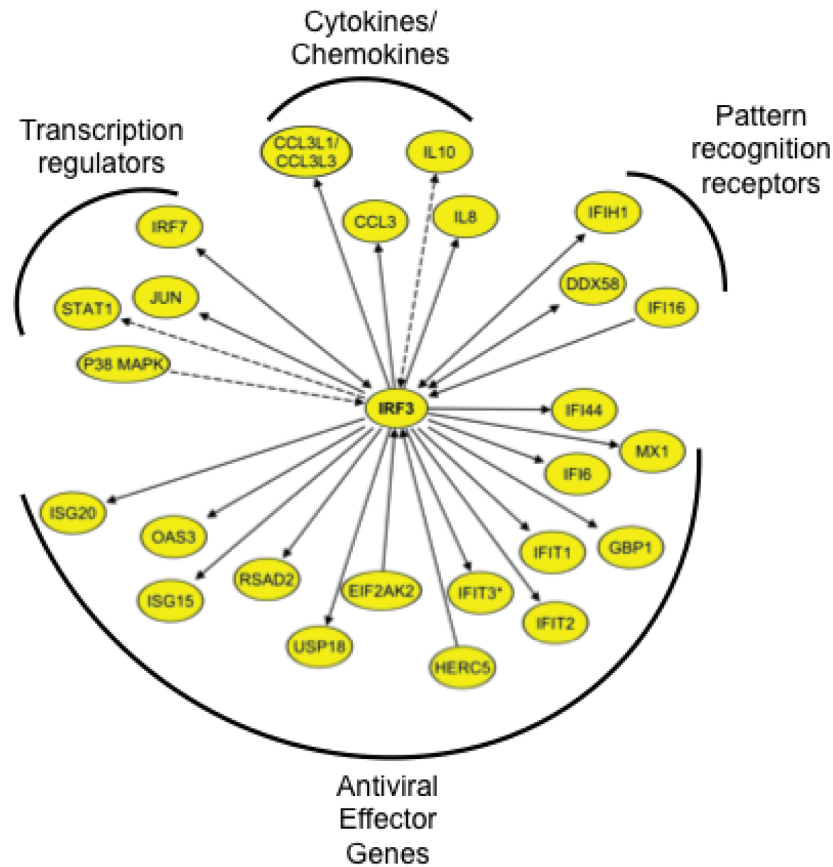


Figure III-7: Network analysis of the top 25 genes upregulated during HIV-1_{JR-CSF A/C} infection with biological function indicated. Solid arrows indicate direct interaction between those proteins/genes has been reported, dashed lines indicate indirect interaction (interaction through 1 or more proteins).

Taken together, the results from promoter activity experiments and THP-1 infection with targeted genomics analysis indicate that Vpu is necessary and sufficient to inhibit innate immune induction by decreasing the ability of IRF3 to drive gene expression. This inhibition could be due to degradation of IRF3 by Vpu, or by inhibition of the IRF3 activation process. At the early timepoints used in the above experiments, Vpu is not sufficient to completely deplete IRF3 levels in the cell, suggesting that Vpu is acting to inhibit IRF3 activation. Thus, these results warrant further investigation of the IRF3 activation process in the context of Vpu.

DISCUSSION

In previous studies of IRF3 antagonism by HIV-1, Vif, Vpr, and Vpu have been implicated in degradation of IRF3 [106, 194], while in one report, no degradation of IRF3 was seen during infection with clonal viruses, with or without Vif, Vpr, or Vpu [195]. As it stands, the degradation of IRF3 is reproducible during infection of CD4⁺ T cells with replication-competent, non-clonal HIV-1 [106, 168, 194, 205]. We have further demonstrated that Vpu is necessary for inhibition of IRF3-dependent gene expression during HIV-1 infection, as HIV-1_{JR-CSF} strains that differ only in a single point mutation in the Vpu start codon induce dramatically different levels of IRF3-dependent genes when infecting THP-1 cells [167]. Hotter and colleagues did not find a link between Vpu and reduced IRF3 expression, and further suggest that the defect in IFN- β transcription may be IRF3-independent [195], but do not consider our results in [167] that contradict this hypothesis.

In this study, we found that Vpu antagonizes IRF3 and NF κ B, resulting in decreased IFN- β gene expression. In agreement with results reported by Hotter and colleagues [195], when using the NF κ B-luc and PRDII-luc constructs, we found that Vpu from NL4-3 and WITO is able to inhibit NF κ B activity specifically, suggesting one role for Vpu in inhibition of IFN- β induction. In the context of infection, inhibition of NF κ B by Vpu would seemingly prevent transcription of integrated provirus and inhibit viral replication, as the HIV-1 LTR contains binding sites for NF κ B and other transcription factors that are important for viral gene expression [233, 234]. If enough HIV-1 mRNA and genomic RNA transcripts are produced prior to antagonism of NF κ B by Vpu, perhaps a decrease in HIV-1 LTR activity could prevent over accumulation of cytoplasmic viral nucleic acid and concomitant PRR signaling. It is also

possible that Vpu antagonizes the sensing of virions by tetherin during the latter stages of infection [70] through actions against both tetherin and NFκB.

In contrast to the report by Hotter and colleagues [195], when using constructs that have IRF3 binding sites but not NFκB binding sites (F3-luc and IFN-β ΔNFκB-luc), we observed that Vpu from NL4-3 and WITO was able to significantly inhibit IRF3 activity. Thus, inhibition of IFN-β promoter activity by Vpu is not due simply to antagonism of NFκB; rather, our results point to a multi-pronged approach by Vpu in inhibition of IFN-β promoter induction. This idea is consistent with findings that a single virus may antagonize multiple steps in the type I IFN response pathway. As induction of IFN-β requires the cooperation of several transcription factors, all of which are required for maximal induction [110], interference with multiple components of the IFN-β enhanceosome by HIV-1 Vpu may ensure the low rates of IFN-β transcriptions seen during infection [127].

In addition, pathway analysis of the top 25 genes induced in PMA-differentiated THP-1 cells infected with Vpu-deficient HIV-1 identifies IRF3-dependent genes associated with the innate immune response and the immune response to viruses. These results suggest that though Vpu may reduce the ability of tetherin to activate NFκB [70], and though Vpu may not decrease IRF3 expression in some systems [195], Vpu may still be necessary and sufficient to antagonize IRF3-dependent innate antiviral immunity. It is possible that other viral proteins play roles in suppressing innate immune induction by directly or indirectly inhibiting IRF3, IRF7, or NFκB function, and a screen of combinations of HIV-1 genes or gene deletions may reveal cooperativity in signaling inhibition.

CONCLUSIONS

The results presented in this chapter indicate that Vpu is necessary and sufficient to inhibit the ability of IRF3 to drive gene transcription. The antagonism of IRF3 function during acute infection may contribute to innate immune dysfunction in patients and may facilitate productive infection of initial target cells. Based on these experiments, I investigated the mechanism by which Vpu inhibits IRF3 activity.

IV. VPU BINDS IRF3 AND INHIBITS ITS DIMERIZATION AND CBP INTERACTION

This chapter will be combined with chapter III as a manuscript.

INTRODUCTION

As illustrated in Figure II-1, after viral infection resting IRF3 in the cytosol is phosphorylated, upon which it forms homodimers, translocates to the nucleus, and associates with cofactors to drive transcription of a set of genes including IFN- β . Previous structural studies of IRF3 predict the functions of the different protein domains in the activation process [99], as modeled in Figure IV-1. Upon activation by phosphorylation, the C-terminal inhibitory domain is predicted to be electrostatically repelled from the DNA-binding domain (DBD) and IRF association domain (IAD). This relief of inhibition allows the DBD to bind DNA and the IAD to promote protein-protein interactions, specifically homodimerization and then CBP interaction.

Since Vpu blocks the ability of IRF3 to drive transcription, we aimed to determine which step or steps in the IRF3 activation pathway Vpu is targeting. In the experiments described in this chapter, we show IRF3 and Vpu form a stable complex. We further show that Vpu binds IRF3 in the IAD, which then results in inhibition of IRF3 dimerization and CBP binding. These studies define the mechanism by which Vpu antagonizes innate immune signaling.

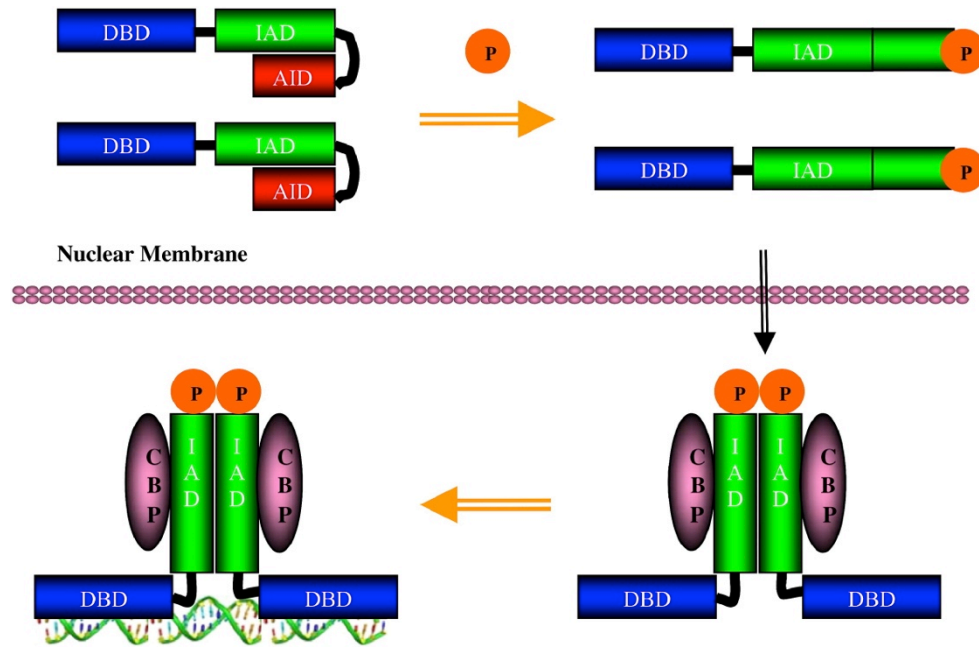


Figure IV-1: Model of IRF3 protein domains during the activation process (Fig. 4 from [235], used by permission – copyright license #3192260093436).

MATERIALS AND METHODS

Cells and transfections

293T, HEK-293, and GHOST R3/X4/X5 cells were cultured in cDMEM: DMEM supplemented with 10% heat-inactivated FBS, L-glutamine, HEPES, sodium pyruvate, MEM non-essential amino acids, and antibiotics. SupT1 and CEM-ss cells were cultured in cRPMI: RPMI supplement with 10% heat-inactivated FBS, L-glutamine, HEPES, sodium pyruvate, and antibiotics. Transfection of cells was performed using Fugene 6 transfection reagent (Roche) according to the manufacturer's suggested protocol. The following reagents were obtained through the NIH AIDS Research and Reference Reagent Program, Division of AIDS, NIAID, NIH: GHOST R3/X4/R5 from Dr. Vineet N. KewalRamani and Dr. Dan R. Littman; CEM-ss cells from Peter L. Nara.

Plasmids

To generate IRF3 constructs, the following approach was used: the oligonucleotide 5'-GAGAGCGGCCGCGGGAACCCCAAAGCCACGGATCCTGCCCTCTAGAGAGAGTTTAAACGAGA-3' and its reverse complement were annealed and, along with the pEF-Tak vector [28] digested with NotI and PmeI. The small fragment was ligated into the cut pEF-Tak backbone, thus introducing downstream of the 2xFLAG sequence the first 26 nucleotides of the IRF3 cDNA sequence including a BamHI site followed by an XbaI site. This enabled the subcloning of the wild type IRF3 gene from pEF-p50IRF-3 [94] into the now-modified pEF-Tak (called pEFTak mod AR) by digesting both with BamHI and XbaI, and after ligation of the digested IRF3 into the modified pEF-Tak, the resultant construct was named pEF-Tak-IRF3. This process was repeated with pEF-p50IRF-3 5D to generate pEF-Tak-IRF3 5D. To generate truncation mutants, truncation sites were chosen based on the IRF3 truncation mutants used in [213]. Recombinant PCR using Advantage HF 2 polymerase (Clontech) was performed using a protocol with 5 cycles using an annealing temperature of 50°C annealing followed by 20 cycles using an annealing temperature of 60°C. For C-terminal truncations, pEF-Tak-IRF3 was used with a forward oligo upstream of the NotI site and reverse oligos containing the truncation site sequence, a stop codon, and a PmeI site. For N-terminal truncations, fragments were amplified out of pCMV-BL-IRF3ΔN [213]. The PCR fragments and pEF-Tak were digested with NotI and PmeI and ligated to generate pEF-Tak-IRF3 1-407, 1-394, 1-357, 1-328, 1-240, ΔN, ΔN-328, and ΔN-240. New constructs were verified by sequencing. Sequences and constructs are available on request.

Viral stocks and infections

HIV-1_{LAI} was propagated in CEM-ss cells using standard procedures. Briefly, CEM-ss cells were infected with low passage HIV-1_{LAI} at an MOI of 0.01. Mock infections represent addition of CEM-ss conditioned media. HIV-1 was titered on GHOST cells to determine concentration of infectious virus. When chloroquine was used, cells were pretreated for 12 hours with 10 μ M chloroquine (from 25 mM aqueous stock). Sendai virus (SenV) strain Cantell was obtained from Charles River Laboratory, and was used at 200 HAU/mL.

Immunoprecipitation and immunoblot

Immunoprecipitations (IPs) were performed using protein G Dynal beads (Life Technologies). Cells were incubated in lysis buffer + inhibitors with IP antibody for 16 hrs at 4°C. Beads were washed and added to bound lysate for 1 hr at 4°C, after which beads and lysate were washed x3 before being boiled for 10 min at 70°C in 4X loading buffer. SDS-PAGE (sodium dodecyl sulfate-polyacrylamide gel electrophoresis) and immunoblot analysis were performed using standard procedures. Pre-cast TGX gels (Bio-Rad) or freshly-poured gels were used. Native PAGE was adapted from [218] to use 7.5% TGX gels, which were run for 30 min at 30 mA/gel. Antibodies used in this study: mouse α IRF3 clone AR1 [205], rabbit α IRF3 (FL-425, Santa Cruz), rabbit α Vpu [236] (from Klaus Strebel, NIH AIDS Research and Reference Reagent Program), mouse α FLAG (M2, Sigma), rabbit α CBP (A-22, Santa Cruz), and rabbit IgG (Abcam). For immunoblot detection, HRP-conjugated antibodies (Jackson ImmunoResearch) were used followed by development using ECL or ECL 2 reagents (Pierce) and imaging on X-ray film. Densitometry was performed using ImageJ software (NIH).

RESULTS

We previously reported that Vpu and FLAG-IRF3 interact using an anti-FLAG agarose bead immunoprecipitation approach [168]. For epitope mapping experiments, we generated a new FLAG-IRF3 construct (see Materials and Methods) and switched to more-sensitive protein G magnetic beads. Thus, we first asked whether exogenous IRF3 and Vpu form a stable complex in 293T cells. We transfected cells with NL4-3 Vpu and FLAG-IRF3 prior to SenV infection. Cells were lysed and IRF3 was IPed using anti-FLAG antibody. Immunoblot of input lysate and the IPed complex with FLAG and Vpu antibodies is shown in Figure IV-2. Compared to vector-transfected cells, IP of IRF3-transfected cells showed an interaction with Vpu that was not altered by SenV infection.

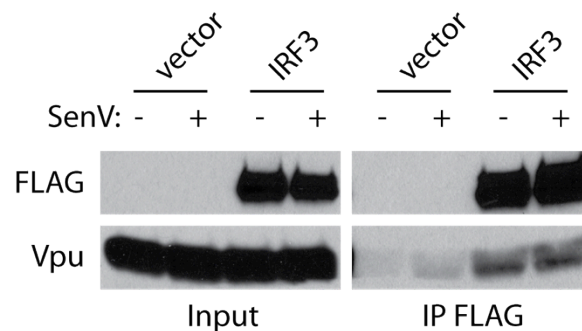


Figure IV-2: Overexpressed Vpu and IRF3 form a stable complex. IP of IRF3 and Vpu using FLAG antibody was performed in 293T cells transfected with FLAG vector or FLAG-IRF3 along with NL4-3 Vpu for 30 hrs. Cells were then infected with SenV (+) or mock infected (-) for 18 hrs prior to harvest. Input cell lysates (left) and FLAG IPed lysates (right) are shown.

While our studies revealed a colocalization of IRF3 and Vpu in HIV-1-infected cells [168], analysis of the direct binding between IRF3 and Vpu using IP had only been done in the context of overexpressed Vpu. To determine whether IRF3 and Vpu interact when physiologically expressed during an actual HIV-1 infection, we infected SupT1 cells with HIV_{LAI} for 24 hours. Since IRF3 levels are decreased at 24 hours in this system when using

higher MOIs [168, 205], we used a low MOI and treated cells with chloroquine (CQ) to inhibit lysosome-mediated IRF3 degradation [168]. IP with IRF3 antibody revealed interaction with Vpu, but only in CQ-treated cells (Figure IV-3). These data demonstrate that IRF3 and Vpu indeed form a stable complex during infection of CD4+ T cells during HIV-1 infection.

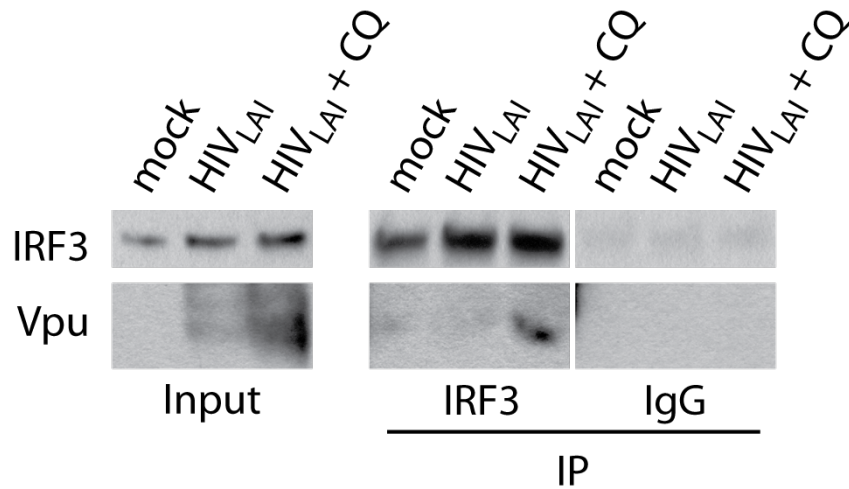


Figure IV-3: During HIV-1 infection, Vpu and endogenous IRF3 form a stable complex. IP of IRF3 and Vpu using IRF3 antibody or IgG control was performed in SupT1 cells infected for 24 hrs with HIV_{LAI} with or without chloroquine (CQ). For CQ infections, SupT1 cells were pretreated with CQ for 12 hrs prior to infection with HIV_{LAI}, at which point CQ was re-added. Input cell lysates (left) and IPed lysates (right) are shown. IRF3 IP and IgG IP images were taken from the same exposures of the same blots.

Having confirmed that IRF3 and Vpu interact within transfected and infected cells, we generated a panel of truncation mutants of IRF-3 to determine the binding epitope for Vpu on IRF3. NL4-3 Vpu and 2xFLAG-tagged IRF3 mutants were coexpressed in 293T cells for 48 hours and IPed with FLAG antibody (Figure IV-4). The expression of Vpu in input lysate from cells cotransfected with IRF3 5D is decreased at this timepoint as IRF3 5D strongly drives the expression of IRF3-dependent genes including several that inhibit protein translation.

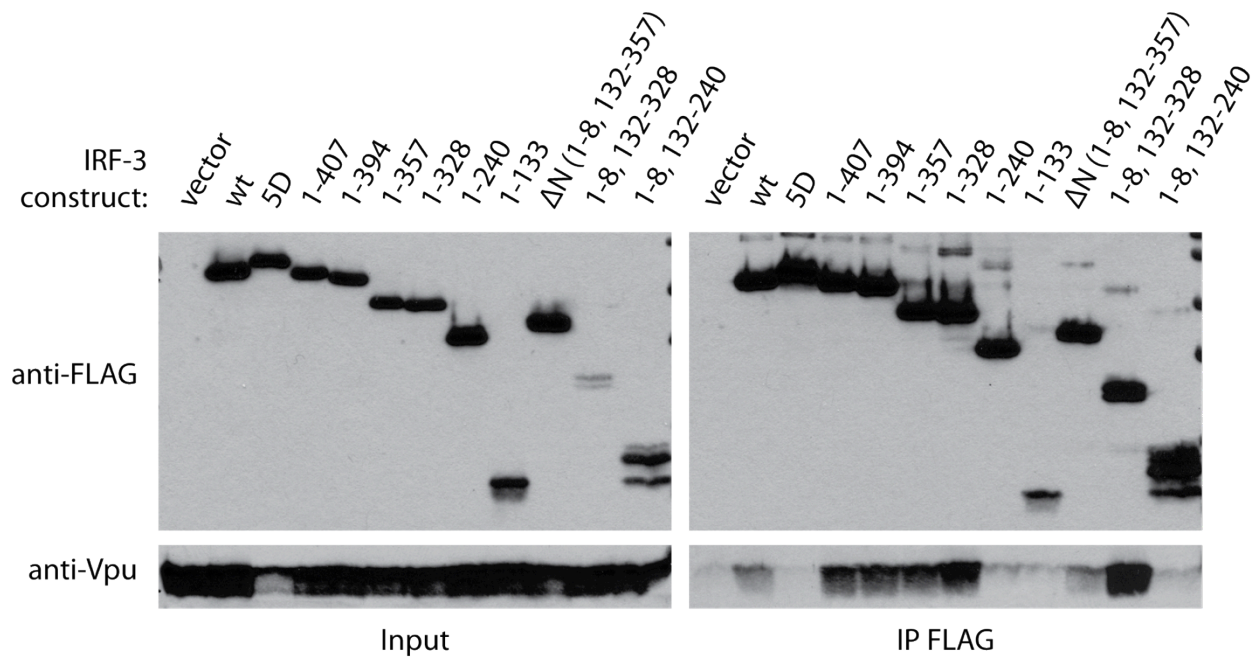


Figure IV-4: NL4-3 Vpu binds to IRF3 between amino acids 240 and 328. IP of IRF3 mutants and coexpressed NL4-3 Vpu using FLAG antibody was performed in 293T cells transfected with the indicated FLAG-IRF3 constructs along with NL4-3 Vpu for 48hrs. Full-length, wild type (wt) IRF3 has amino acids 1-427, IRF3 5D is full-length and constitutively active, and the amino acids contained in each truncation mutant are indicated. Input cell lysate (left) and IPed lysate (right) are shown.

The IRF3 mutants used to precipitate Vpu are shown diagrammatically in Figure IV-5, with a summary of the amount of Vpu pulled down by the various mutants (column, right). The various domains of the IRF3 protein are indicated. Upon expression of progressively C-terminal truncated IRF3 mutants, we observed that a construct containing amino acids 1-328 was able to pull down Vpu while a construct containing amino acids 1-240 was not, suggesting that Vpu binds to IRF3 between amino acids 240 and 328. This putative 88 amino acid binding site was supported by immunoprecipitations performed using IRF3 constructs derived from IRF3 Δ N.

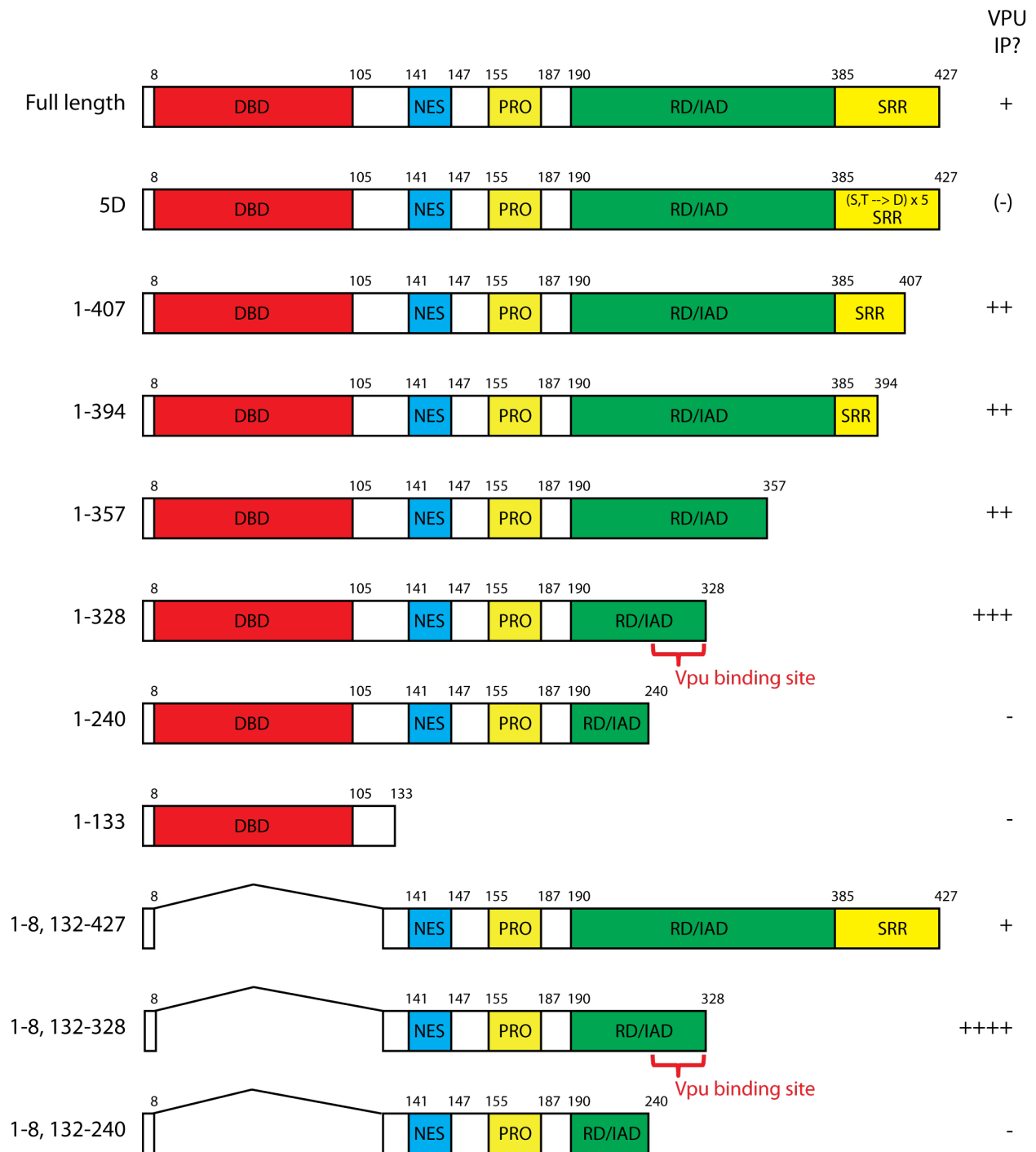


Figure IV-5: Schematic of IRF3 mutants used in Figure IV-4. A summary of the binding results from Figure IV-4 is indicated in the column on the right. The Vpu binding site is indicated in red. DBD, DNA-binding domain; NES, nuclear export sequence; PRO, proline-rich region; RD/IAD, regulatory domain/IRF association domain; SRR, serine-rich region.

Based on functional and structural data, the IAD is hypothesized to mediate the protein-protein interactions during IRF3 homodimerization and heterodimerization with IRF7, as well as association with CBP [99, 211, 237]. Given the evidence that Vpu binds to IRF3 in the IAD, we hypothesized that Vpu would prevent IRF3 multimerization and CBP binding. To determine if Vpu blocks IRF3 dimerization, we transfected 293 cells with NL4-3 Vpu for 24 hrs prior to infecting them with SenV. In order to avoid detection of IRF3 dimerization in untransfected cells, we used exogenous FLAG-IRF3, and assumed both Vpu and IRF3 constructs would be delivered to the same cell at a high rate. Cells were lysed 18 hrs after SenV-infection and analyzed by native gel electrophoresis, where higher-order IRF3 forms migrate more slowly (middle and upper bands) as compared to monomeric IRF3 (lower band) (Figure IV-6). Vector control was used in this experiment, as well as a positive control for inhibition of IRF3 dimerization, the NS3/4A protease from HCV, and its vector control. Infection with SenV of cells transfected with pcDNA showed increased IRF3 dimerization and higher-order multimerization relative to Vpu-transfected cells. The total amount of FLAG-IRF3 did not appear to be decreased in Vpu-cotransfected cells relative to vector-cotransfected cells (Figure IV-6, middle blot).

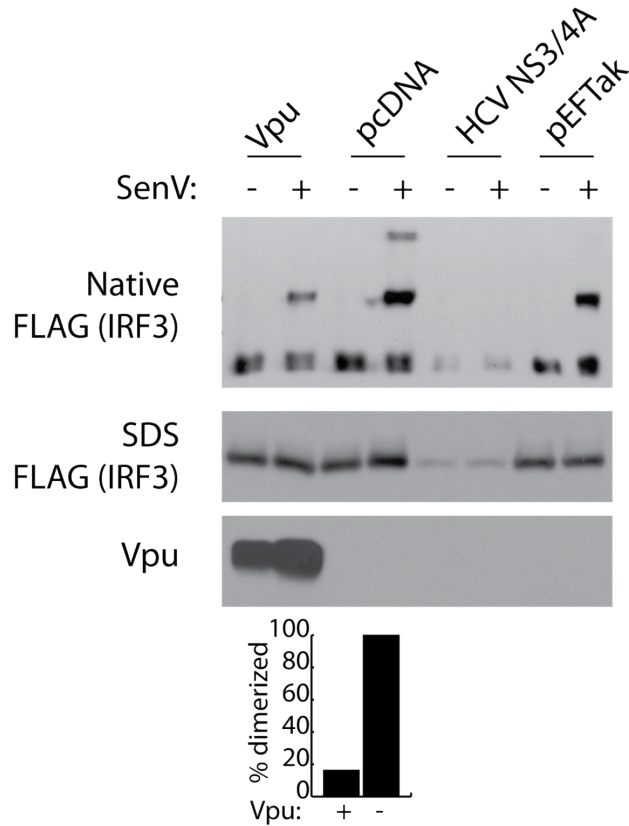


Figure IV-6: IRF3 multimerization is reduced in cells expressing NL4-3 Vpu. Native and SDS PAGE followed by immunoblot for FLAG (marking IRF3 on native and SDS gels) and Vpu (on SDS gel) was performed in 293 cells infected with SenV (+) or mock infected (-). Densitometry of IRF3 dimer during SenV infection (middle band on native blot), as a percentage of pcDNA-transfected cells, is represented in the bar graph (bottom).

Since Vpu prevented multimerization of IRF3, and since dimerization is a precursor to interaction with CBP, we hypothesized that Vpu transfection would prevent interaction between CBP and IRF3. Again, we used exogenous IRF3 to restrict our IRF3 analysis to Vpu-transfected cells. 293 cells were transfected with Vpu and FLAG-IRF3 and infected with SenV as in Figure IV-6. This time, cell lysates were IPed with CBP antibody and complexes were probed for IRF3 and Vpu. As shown in Figure IV-7, Vpu expression decreased the amount of FLAG-IRF3 bound to CBP in response to SenV infection.

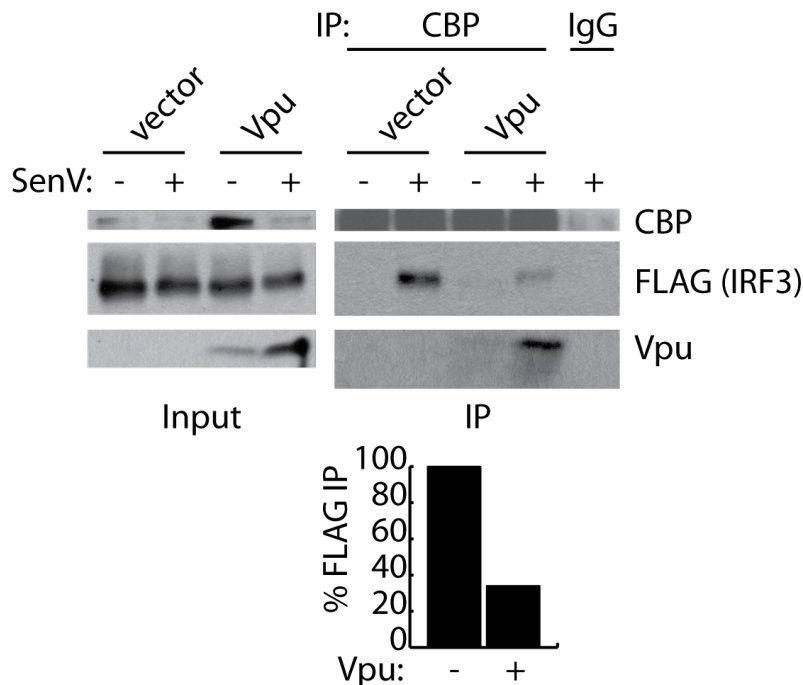


Figure IV-7: IRF3 interaction with CBP is reduced in cells expressing Vpu. IP using CBP antibody or IgG control was performed in 293 cells transfected with NL4-3 Vpu and FLAG-IRF3 and infected with SenV (+) or mock infected (-). Input cell lysates (left) and IPed lysates (right) are shown. Densitometry of FLAG-IRF3 IPed by CBP antibody during SenV infection, as a percentage of pcDNA-transfected cells, is represented in the bar graph (bottom).

DISCUSSION

Based on data presented in chapter III, we determined the mechanism of Vpu inhibition of IRF3 function. We have confirmed that Vpu and IRF3 interact during overexpression in 293T cells using a new IRF3 construct and a different IP method (magnetic beads). In contrast to our previous findings, where SenV enhanced the IP of Vpu by IRF3 [168], SenV infection did not appear to alter the interaction between IRF3 and Vpu. This may be due to an increase in sensitivity of the IP using magnetic beads. We now report that the two proteins interact during HIV-1 infection of CD4+ T cells, though this interaction is not detectable in the absence of the lysosome inhibitor CQ, supporting a role for targeting of IRF3 to the lysosome during infection.

Using a panel of IRF3 truncation and deletion mutants, we then mapped the interaction site on IRF3 to an 88 amino acid epitope in the IAD of IRF3. Since the IAD mediates IRF3/IRF3 and IRF3/CBP interactions, we explored the ability of IRF3 to form these interactions in the presence of Vpu, which would presumably interfere with IAD function. In IRF3 dimerization studies using native protein techniques, we show that Vpu expression reduces IRF3 dimerization in response to SenV infection. Further, Vpu expression prevented IRF3 from SenV-induced interaction with its necessary coactivator CBP. Interestingly, the amount of Vpu that precipitated with CBP increased in the presence of SenV, suggesting that during SenV infection, Vpu may interfere with the interaction between IRF3 and CBP, and may itself then bind to CBP. Importantly, the dimerization and CBP interaction experiments performed in this study used Vpu from the NL4-3 clone, which comes from the Bru3 HIV-1 isolate, or the same parent virus as our HIV_{LAI} stock. The generalizability to other Vpu proteins of inhibition of dimerization and CBP interaction remains to be seen.

The inhibition of IRF3/CBP interaction is a mechanism shared by other unrelated viruses: the respiratory syncytial virus NS1 protein binds IRF3 and prevents recruitment of CBP, though in that case dimerization is not affected [176], and the Kaposi's Sarcoma-associated herpesvirus vIRF-1 protein acts as a dummy substrate to bind and sequester CBP away from IRF3 [173]. However, as with other viruses, HIV-1 may employ yet undiscovered methods to antagonize IRF3-dependent and independent induction and function of innate immunity, and our results do not exclude those possibilities. For example, the antiviral action of IRF3 has recently been expanded to include the induction of apoptosis in infected cells in an IFN-independent manner [89]. This activity requires the interaction of IRF3 and the apoptosis-promoting protein Bax in the cytosol, and could also be antagonized by HIV-1 to prevent cell death during productive

infection. And, it is not clear if liberation of CBP from IRF3 interaction in the nucleus affects HIV-1 replication processes, such as integration or viral gene expression, which may rely on the histone deacetylation function of CBP.

Though the nucleic acid PAMP(s) for HIV-1 are not yet fully defined, it is clear that, as is the case for other pathogenic viruses, HIV-1 antagonizes innate immunity. The antagonism of IRF3, a central transcription factor in the innate antiviral immune response, may be critical to the ability of the virus to establish infection in the initial target cells, which for mucosal transmission is intra-epithelial CD4⁺ T cells. Mucosal transmission of HIV-1 fails more often than it succeeds, and this may be due to an innate antiviral immune response that is successful most of the time. Further study of the mechanisms by which HIV-1 antagonizes innate immunity will help inform the development of vaccines, adjuvants, and drugs that increase the innate antiviral response to acute HIV-1 infection.

CONCLUSIONS

In this chapter, we presented experiments that define a novel mechanism by which Vpu antagonizes IRF3 function. Vpu binds IRF3 in the IAD, and as a result is able to inhibit IRF3 dimerization and CBP interaction in response to SenV infection. This abrogation of normal IRF3 function may be a key step in deactivating the innate intracellular immune response during the earliest stages of HIV-1 infection. Therapies that preserve innate immune signaling in the initial target cells of infection may facilitate the prevention of infectious focus formation and the rejection of infection by the host.

V. CONCLUSIONS AND FUTURE DIRECTIONS

HIV-1 remains a major global health problem, and is the leading cause of adult death in sub-Saharan Africa [14], despite decades of research into the biology and treatment of this retrovirus. The ability of the virus to subvert or evade the innate and adaptive immune response has exceeded the abilities of modern vaccine candidates and antiretroviral therapies to respectively either prevent infection or provide a sterilizing cure. To date, the only examples of complete eradication of the virus come from lethal radiation and allogeneic stem cell transplant from a CCR5-negative donor, intense antiretroviral therapy of an infected newborn from birth, or initiation of combination antiretroviral therapy during acute infection [182-184]. As these options are not available to the majority of HIV-infected patients, attention has remained focused on studying the early events of infection, identifying the mechanisms by which HIV-1 evades innate immunity to survive in the host long enough to latently infect therapy-inaccessible reservoirs, and developing vaccines and therapies that improve the ability of the innate immune system to block HIV-1 infection. The work in this thesis comprises the development of new tools to study IRF3 activation and depletion during viral infection, and the discovery of a new mechanism of IRF3 antagonism by HIV-1 Vpu.

DEVELOPMENT OF MONOCLONAL ANTIBODIES AGAINST IRF3

We have described two novel mouse monoclonal antibodies to human IRF3, designated AR-1 and AR-2, and we have developed a novel flow cytometric assay using the AR-1 mAb for high throughput assessment of IRF3 activation state. In analyses of native IRF3 protein, the AR-1 mAb was found to specifically recognize active/dimeric IRF3, while the AR-2 mAb can detect

both resting/monomeric IRF3 and active/dimeric IRF3. After SDS-PAGE, the AR-1 mAb detects rhesus macaque IRF3 in primary cell lysate and has not yet been tested against native protein by immunofluorescence or immunohistochemistry. Even if, as is the case for human IRF3, the AR-1 mAb were to only recognize activated rhesus macaque IRF3 in native protein assays, this would be useful in the macaque/SIV animal model of HIV infection. For example, the ability of SIV to activate IRF3 in mucosal target cells could be studied. The identification of SIV strains, vaccine candidates, or infection conditions that demonstrate increased IRF3 activation *in vivo* could provide highly valuable information for the development of treatment or prevention strategies against HIV.

As we have reported, the AR-1 mAb can be used as a high-throughput reagent for measurement of IRF3 activation by conventional flow cytometry. This property could be leveraged in a number of research applications. In mixed cultures *in vitro* or peripheral blood samples *ex vivo*, cells exhibiting IRF3 activation can be isolated from other cells for multi-epitope phenotyping using flow cytometry. As a result, use of the AR-1 mAb in flow cytometry would allow the study of acute and subtle shifts in IRF3 activation in mixed populations of cells, which is currently a challenge due to the technical difficulties of native PAGE and phospho-flow cytometry. In addition, the AR-1 mAb could be combined with an antibody against total IRF3 for two-dimensional analysis of IRF3 activation and turnover in human cells infected *in vivo*, *ex vivo*, or *in vitro*, with a variety of viruses. IRF3 plays a central and early role in the innate intracellular immune response, and many viruses use various mechanisms to antagonize IRF3 function, but surely more mechanisms remain to be discovered.

VPU IS NECESSARY AND SUFFICIENT TO INHIBIT IRF3 FUNCTION

IRF3 activation strongly inhibits HIV-1 replication, and IRF3 is degraded but not activated during HIV-1 infection of SupT1 cells [106]. Vpu alone inhibits IRF3 activity, and while we ascribed Vpu-mediated inhibition of IRF3 to the ability of Vpu to target IRF3 to the lysosome [168], another group could not find IRF3 depletion in the presence of Vpu [195]. Thus, we investigated whether Vpu may antagonize IRF3 via an additional mechanism independent of degradation. We used Vpu expression constructs from multiple HIV-1 clones and promoter-luciferase constructs containing binding sites for IRF3, NF κ B, or the entire IFN- β enhanceosome, and discovered that Vpu inhibits the activities of IRF3 and NF κ B independently in response to SenV infection.

For all of the studies of HIV-1 antagonism of IRF3-dependent signaling, SenV has been used as a stimulus after HIV-1 gene transfection or virus infection. Sendai virus is a mouse paramyxovirus, and is therefore a negative sense ssRNA virus, that replicates in the cytoplasm and signals through RIG-I to MAVS, which activates TBK1, which then phosphorylates and activates IRF3. There is evidence that HIV-1 replication produces PAMPs that stimulate IRF3 activation, and while RIG-I has been identified as an HIV-1 PRR in one study [66], other studies have suggested RNA:DNA hybrids, ssDNA, and dsDNA as cytosolic replication intermediates that activate IRF3 through a cytosolic DNA sensor [65, 67]. With the recent discovery of the cytosolic DNA sensor cGAS, which signals through STING and not MAVS, it may be informative to activate IRF3 with a STING-dependent stimulus (such as cGAMP) to see if the activation of IRF3 through STING is affected by HIV-1 protein expression. In addition, the panel of luciferase constructs studied in chapter III could be tested with full-length and accessory gene-deleted proviral constructs to determine the necessity of Vpu and other HIV-1 proteins to inhibit IRF3-dependent, NF κ B-dependent, and IFN- β promoter activity. An alternative approach to

promoter-luciferase induction assays would be to use chromatin immunoprecipitation for IRF3 and NFκB in the context of innate immune activation after putative antagonist expression.

The Vpu proteins we used came from NL4-3, Q23-17, and WITO viruses. The Q23-17 Vpu was used for one set of IFN-β experiments, while the WITO Vpu was used for studies involving multiple promoters. The WITO Vpu comes from a transmitter/founder strain of M group HIV-1 and is therefore most representative of acute infection. For future studies, other transmitter/founder HIV-1 Vpu proteins could be tested, as well as Vpu proteins from different Vpu-containing SIV strains. A preliminary screen of Vpu proteins for IFN-β promoter activity in Vero cells, which come from African green monkey and therefore express a non-human primate IRF3, revealed broad activity of Vpu proteins against IRF3 function. The abilities of these different Vpus to antagonize IRF3 and NFκB functions can be tested to reveal insight into the evolutionary conservation of innate immune suppression by lentiviruses. Further, it is unknown whether HIV-2, which does not encode a Vpu gene, or various SIV strains lacking Vpu, encode factors that block IRF3 function and IFN-β promoter activity.

VPU BINDS IRF3 AND INHIBITS ITS DIMERIZATION AND CBP INTERACTION

Through immunoprecipitation studies, we confirmed that Vpu and IRF3 interact during overexpression in 293 cells, mapped the interaction to an 88 amino acid stretch in the IAD of IRF3, and reported that the two proteins interact during HIV-1_{LAI} infection of CD4⁺ T cells. We did not, however, report the use of clonal viruses with or without Vpu for IP studies, and may wish to perform such infections in the presence of CQ to preserve Vpu-IRF3 interactions. In IRF3 dimerization studies using native gels, we showed that Vpu expression reduces IRF3 dimerization in response to SenV infection. Further, Vpu expression prevented IRF3 from

interacting with its necessary coactivator CBP. Taken together, these results indicate that Vpu blocks IRF3 function independent of IRF3 depletion. It is not clear if liberation of CBP from IRF3 interaction affects HIV-1 replication processes, such as integration or viral gene expression. To explore the actions of other accessory genes, IPs for CBP from CD4+ T cells infected with HIV-1 and then infected with SenV or stimulated with another IRF3 activation signal could reveal effects on CBP/IRF3 interaction at early or late timepoints that may or may not precede IRF3 depletion. The advantage to this approach would be the applicability of replication-competent, clonal viruses generated from proviruses with defects in various HIV-1 genes.

There is evidence that phosphorylation of Vpu, on residues S52 and S56, is required for interaction with β TrCP to downmodulate surface expression of CD4 and tetherin, and that IRF3 may interact more strongly with Vpu when itself is phosphorylated. However, in the current work, S52,56N Vpu bound just as strongly as wild type Vpu to IRF3 (data not shown), and SenV infection did not seem to enhance the IRF3/Vpu interaction; though, transfection of plasmids activates the DNA response, perhaps providing a baseline level of IRF3 activation. If phosphorylation of IRF3 or Vpu is important for interaction during HIV-1 infection, treatment of cells with calyculin-A can preserve phosphorylation of proteins, which is notoriously labile. In addition, treatment of cells with the crosslinking agent DSP can fix protein-protein interactions prior to cell lysis and IP, further stabilizing weaker interactions.

IRF3 is a cytosolic protein that is recruited to membrane-bound adaptors like MAVS or STING during activation processes. Unlike IRF3, Vpu is a transmembrane protein, so presumably the interaction between IRF3 and Vpu occurs at a membrane interface, in association with innate immune signaling complex formation. Forms of MAVS, a transmembrane protein,

have been identified on the mitochondria, mitochondria-associated endoplasmic reticulum (ER) membrane (MAM), and peroxisomes, while STING has been localized to the nucleus-associated ER membrane. It is not clear whether IRF3 trafficking to the immediate proximity of upstream signaling adaptors is required for IRF3-dependent signaling, nor has the sub-cellular membrane localization of Vpu been resolved. To identify the localization of IRF3 during Vpu transfection and HIV-1 transfection, membrane fractionation techniques could be used, with fraction identification as described in [32].

During the IRF3 activation cycle, homodimerization occurs after phosphorylation but prior to nuclear translocation, while CBP binding occurs after nuclear translocation. In this work, we described how Vpu expression inhibits IRF3 dimerization as well as CBP binding. Thus, Vpu likely also inhibits translocation of IRF3 to the nucleus. Indeed, a defect in IRF3 nuclear translocation has been observed in HIV-1-infected macrophages and THP-1 cells [127, 167]. The effect of Vpu expression alone on IRF3 phosphorylation after SenV infection is also unknown, though a lack of IRF3 phosphorylation during infection with Vpu-expressing HIV-1 in THP-1 cells relative to Vpu-deficient virus has been observed [167]. To answer these questions, the amount of cotransfected FLAG-IRF3 needs to be carefully titered, and nuclear and cytoplasmic fractions need to be immunoprecipitated for FLAG-IRF3 prior to S396 phosphoblotting to eliminate background signal from endogenous IRF3. Activated IRF3 also plays a role in promoting apoptosis during viral infection that is separate from its role in inducing IFN- β expression, and this role has not been evaluated in the context of viral infection or Vpu expression.

Vpu is a class IA viroporin, as it is suspected to form an oligomeric ion channel [238, 239]. Another viroporin, influenza M2, activates the NLRP3 inflammasome by disturbing ion gradients [240], and the ability of Vpu to activate inflammasomes in target cells through its viroporin activity has not been examined. However, small molecule inhibitors of Vpu pore function do not prevent antagonism of tetherin, suggesting that this pore-forming ability of Vpu is not involved in interaction at least with tetherin [241], and maybe other host proteins. The residues of Vpu responsible for interaction with tetherin have been mapped to the transmembrane domain of Vpu [242], but the interaction with IRF3 is likely mediated through the cytoplasmic domain. Inhibitors of Vpu-mediated tetherin inhibition are under investigation [243], but additional screens may be necessary to identify candidates that block Vpu-mediated IRF3 inhibition.

Such inhibitors could be used in topical preparations applied to target mucosa to prevent inhibition of innate immune signaling and thus lower the rate of acquisition of HIV-1. And, since the common vaccine adjuvant alum works in part by stimulating IRF3-dependent innate immunity [244], Vpu-deficient HIV-1 strains or Vpu-expressing HIV-1 strains delivered with potent Vpu inhibitors may be a strategy worth pursuing for the development of an effective preventative HIV-1 vaccine by enhancing innate immune signaling during the vaccine response. Disruption of the Vpu/IRF3 interface during acute infection or latent reactivation of infected cells might also promote protective cell-intrinsic antiviral defenses and infected cell apoptosis, thus reducing viral set point or viral load. Since one of the few instances of curative HIV-1 treatment involved combination antiretroviral therapy during acute infection [184], inhibitors that prevent Vpu antagonism of IRF3 could play a role in furthering cure efforts.

The antagonism of IRF3 by HIV-1 may play an important role in the development of advanced HIV disease, or AIDS, and this antagonism may be critically important during acute infection. From studies of non-progressing SIV infections in natural hosts, there is evidence that neither acute CD4+ T cell depletion in gut-associated lymphoid tissue nor exuberant acute innate immune activation necessarily lead to advanced disease. While these measurements are more difficult to take at precise times during acute infection in humans, it is possible that IRF3 antagonism is a key determinant of infection in cell types critical to disease progression. It is not known whether SIV strains that infect non-natural hosts and lead to disease progression antagonize innate immune induction relative to non-progressing infections. A currently favored hypothesis for the cause of HIV-1 disease progression is one of chronic immune activation, possibly caused by chronic loss or dysfunction of gut immune cells and barrier integrity and microbial translocation [245, 246]. In addition, chronic stimulation of pDCs with virus or infected cell debris may contribute to chronic elevation of systemic interferon levels and immune cell dysfunction. Acute inhibition of IRF3-mediated innate immune signaling by HIV-1 may precipitate chronic immune activation through these or other mechanisms.

In Charles Janeway's 1989 discussion on the nature of innate immunity, he predicted that: "A virus that did not induce costimulator activity and also did not infect dendritic cells might be particularly dangerous" [2]. Through mechanisms described here, HIV-1 antagonizes innate immune induction in target cells and has evolved to inefficiently infect dendritic cells. In addition, HIV-1 latently infects target cells to remain hidden from the immune system, and directly antagonizes restriction factors. As a consequence, viral infection is not effectively cleared from infected cells, and the innate and adaptive immune systems are not properly

activated and trained. Interventions to boost the innate immune response to HIV-1 may be necessary to stop the spread of the HIV-1 pandemic.

VI. REFERENCES

1. Medzhitov, R., *Approaching the asymptote: 20 years later*. Immunity, 2009. **30**(6): p. 766-75.
2. Janeway, C.A., Jr., *Approaching the asymptote? Evolution and revolution in immunology*. Cold Spring Harb Symp Quant Biol, 1989. **54 Pt 1**: p. 1-13.
3. Iwasaki, A. and R. Medzhitov, *Toll-like receptor control of the adaptive immune responses*. Nat Immunol, 2004. **5**(10): p. 987-95.
4. Iwasaki, A. and R. Medzhitov, *Regulation of adaptive immunity by the innate immune system*. Science, 2010. **327**(5963): p. 291-5.
5. Collin, M., N. McGovern, and M. Haniffa, *Human dendritic cell subsets*. Immunology, 2013.
6. Lubber, C.A., J. Cox, H. Lauterbach, B. Fancke, et al., *Quantitative proteomics reveals subset-specific viral recognition in dendritic cells*. Immunity, 2010. **32**(2): p. 279-89.
7. Poulin, L.F., M. Salio, E. Griessinger, F. Anjos-Afonso, et al., *Characterization of human DNGR-1+ BDCA3+ leukocytes as putative equivalents of mouse CD8alpha+ dendritic cells*. J Exp Med, 2010. **207**(6): p. 1261-71.
8. Stetson, D.B. and R. Medzhitov, *Type I interferons in host defense*. Immunity, 2006. **25**(3): p. 373-81.
9. Schoggins, J.W., S.J. Wilson, M. Panis, M.Y. Murphy, et al., *A diverse range of gene products are effectors of the type I interferon antiviral response*. Nature, 2011.
10. Welsh, R.M., K. Bahl, H.D. Marshall, and S.L. Urban, *Type I interferons and antiviral CD8 T-cell responses*. PLoS Pathog, 2012. **8**(1): p. e1002352.
11. Tough, D.F., *Modulation of T-cell function by type I interferon*. Immunol Cell Biol, 2012. **90**(5): p. 492-7.
12. Michallet, M.C., G. Rota, K. Maslowski, and G. Guarda, *Innate receptors for adaptive immunity*. Curr Opin Microbiol, 2013.
13. Suthar, M.S., H.J. Ramos, M.M. Brassil, J. Netland, et al., *The RIG-I-like receptor LGP2 controls CD8(+) T cell survival and fitness*. Immunity, 2012. **37**(2): p. 235-48.
14. Lozano, R., M. Naghavi, K. Foreman, S. Lim, et al., *Global and regional mortality from 235 causes of death for 20 age groups in 1990 and 2010: a systematic analysis for the Global Burden of Disease Study 2010*. Lancet, 2012. **380**(9859): p. 2095-128.
15. Kawai, T. and S. Akira, *The role of pattern-recognition receptors in innate immunity: update on Toll-like receptors*. Nat Immunol, 2010. **11**(5): p. 373-84.
16. Botos, I., D.M. Segal, and D.R. Davies, *The structural biology of Toll-like receptors*. Structure, 2011. **19**(4): p. 447-59.

17. Akira, S., S. Uematsu, and O. Takeuchi, *Pathogen recognition and innate immunity*. Cell, 2006. **124**(4): p. 783-801.
18. Kawai, T. and S. Akira, *Innate immune recognition of viral infection*. Nat Immunol, 2006. **7**(2): p. 131-7.
19. Heil, F., H. Hemmi, H. Hochrein, F. Ampenberger, et al., *Species-specific recognition of single-stranded RNA via toll-like receptor 7 and 8*. Science, 2004. **303**(5663): p. 1526-9.
20. Lee, H.K., J.M. Lund, B. Ramanathan, N. Mizushima, and A. Iwasaki, *Autophagy-dependent viral recognition by plasmacytoid dendritic cells*. Science, 2007. **315**(5817): p. 1398-401.
21. Dreux, M., U. Garaigorta, B. Boyd, E. Decembre, et al., *Short-range exosomal transfer of viral RNA from infected cells to plasmacytoid dendritic cells triggers innate immunity*. Cell Host Microbe, 2012. **12**(4): p. 558-70.
22. Takahashi, K., S. Asabe, S. Wieland, U. Garaigorta, et al., *Plasmacytoid dendritic cells sense hepatitis C virus-infected cells, produce interferon, and inhibit infection*. Proc Natl Acad Sci U S A, 2010. **107**(16): p. 7431-6.
23. Jiang, F., A. Ramanathan, M.T. Miller, G.Q. Tang, et al., *Structural basis of RNA recognition and activation by innate immune receptor RIG-I*. Nature, 2011. **479**(7373): p. 423-7.
24. Myong, S., S. Cui, P.V. Cornish, A. Kirchofer, et al., *Cytosolic viral sensor RIG-I is a 5'-triphosphate-dependent translocase on double-stranded RNA*. Science, 2009. **323**(5917): p. 1070-4.
25. Kato, H., O. Takeuchi, E. Mikamo-Satoh, R. Hirai, et al., *Length-dependent recognition of double-stranded ribonucleic acids by retinoic acid-inducible gene-1 and melanoma differentiation-associated gene 5*. J Exp Med, 2008. **205**(7): p. 1601-10.
26. Peisley, A., M.H. Jo, C. Lin, B. Wu, et al., *Kinetic mechanism for viral dsRNA length discrimination by MDA5 filaments*. Proc Natl Acad Sci U S A, 2012. **109**(49): p. E3340-9.
27. Yoneyama, M., M. Kikuchi, K. Matsumoto, T. Imaizumi, et al., *Shared and unique functions of the DExD/H-box helicases RIG-I, MDA5, and LGP2 in antiviral innate immunity*. J Immunol, 2005. **175**(5): p. 2851-8.
28. Saito, T., R. Hirai, Y.M. Loo, D. Owen, et al., *Regulation of innate antiviral defenses through a shared repressor domain in RIG-I and LGP2*. Proc Natl Acad Sci U S A, 2007. **104**(2): p. 582-7.
29. Saito, T., D.M. Owen, F. Jiang, J. Marcotrigiano, and M. Gale, Jr., *Innate immunity induced by composition-dependent RIG-I recognition of hepatitis C virus RNA*. Nature, 2008. **454**(7203): p. 523-7.
30. Schnell, G., Y.M. Loo, J. Marcotrigiano, and M. Gale, Jr., *Uridine composition of the poly-U/UC tract of HCV RNA defines non-self recognition by RIG-I*. PLoS Pathog, 2012. **8**(8): p. e1002839.

31. Liu, H.M., Y.M. Loo, S.M. Horner, G.A. Zornetzer, et al., *The mitochondrial targeting chaperone 14-3-3epsilon regulates a RIG-I translocon that mediates membrane association and innate antiviral immunity*. Cell Host Microbe, 2012. **11**(5): p. 528-37.
32. Horner, S.M., H.M. Liu, H.S. Park, J. Briley, and M. Gale, Jr., *Mitochondrial-associated endoplasmic reticulum membranes (MAM) form innate immune synapses and are targeted by hepatitis C virus*. Proc Natl Acad Sci U S A, 2011. **108**(35): p. 14590-5.
33. Paz, S., Q. Sun, P. Nakhaei, R. Romieu-Mourez, et al., *Induction of IRF-3 and IRF-7 phosphorylation following activation of the RIG-I pathway*. Cell Mol Biol (Noisy-le-grand), 2006. **52**(1): p. 17-28.
34. Loo, Y.M., J. Fornek, N. Crochet, G. Bajwa, et al., *Distinct RIG-I and MDA5 signaling by RNA viruses in innate immunity*. J Virol, 2008. **82**(1): p. 335-45.
35. Kawai, T., K. Takahashi, S. Sato, C. Coban, et al., *IPS-1, an adaptor triggering RIG-I- and Mda5-mediated type I interferon induction*. Nat Immunol, 2005. **6**(10): p. 981-8.
36. Gitlin, L., W. Barchet, S. Gilfillan, M. Cella, et al., *Essential role of mda-5 in type I IFN responses to polyriboinosinic:polyribocytidylic acid and encephalomyocarditis picornavirus*. Proc Natl Acad Sci U S A, 2006. **103**(22): p. 8459-64.
37. Sun, Q., L. Sun, H.H. Liu, X. Chen, et al., *The specific and essential role of MAVS in antiviral innate immune responses*. Immunity, 2006. **24**(5): p. 633-42.
38. Suthar, M.S., D.Y. Ma, S. Thomas, J.M. Lund, et al., *IPS-1 is essential for the control of West Nile virus infection and immunity*. PLoS Pathog, 2010. **6**(2): p. e1000757.
39. Malathi, K., B. Dong, M. Gale, Jr., and R.H. Silverman, *Small self-RNA generated by RNase L amplifies antiviral innate immunity*. Nature., 2007. .
40. Goubau, D., S. Deddouche, and E.S.C. Reis, *Cytosolic sensing of viruses*. Immunity, 2013. **38**(5): p. 855-69.
41. Cho, J.A., A.H. Lee, B. Platzer, B.C. Cross, et al., *The unfolded protein response element IRE1alpha senses bacterial proteins invading the ER to activate RIG-I and innate immune signaling*. Cell Host Microbe, 2013. **13**(5): p. 558-69.
42. Kufer, T.A. and P.J. Sansonetti, *NLR functions beyond pathogen recognition*. Nat Immunol, 2011. **12**(2): p. 121-8.
43. Ting, J.P., J.A. Duncan, and Y. Lei, *How the noninflammasome NLRs function in the innate immune system*. Science, 2010. **327**(5963): p. 286-90.
44. Stetson, D.B., J.S. Ko, T. Heidmann, and R. Medzhitov, *Trex1 prevents cell-intrinsic initiation of autoimmunity*. Cell, 2008. **134**(4): p. 587-98.
45. Rice, G.I., J. Bond, A. Asipu, R.L. Brunette, et al., *Mutations involved in Aicardi-Goutieres syndrome implicate SAMHD1 as regulator of the innate immune response*. Nat Genet, 2009. **41**(7): p. 829-32.
46. Goncalves, A., E. Karayel, G.I. Rice, K.L. Bennett, et al., *SAMHD1 is a nucleic-acid binding protein that is mislocalized due to aicardi-goutieres syndrome-associated mutations*. Hum Mutat, 2012. **33**(7): p. 1116-22.

47. Crow, Y.J., B.E. Hayward, R. Parmar, P. Robins, et al., *Mutations in the gene encoding the 3'-5' DNA exonuclease TREX1 cause Aicardi-Goutieres syndrome at the AGS1 locus*. Nat Genet, 2006. **38**(8): p. 917-20.
48. Ishii, K.J., T. Kawagoe, S. Koyama, K. Matsui, et al., *TANK-binding kinase-1 delineates innate and adaptive immune responses to DNA vaccines*. Nature, 2008. **451**(7179): p. 725-9.
49. Chiu, Y.H., J.B. Macmillan, and Z.J. Chen, *RNA polymerase III detects cytosolic DNA and induces type I interferons through the RIG-I pathway*. Cell, 2009. **138**(3): p. 576-91.
50. Zhang, Z., B. Yuan, M. Bao, N. Lu, et al., *The helicase DDX41 senses intracellular DNA mediated by the adaptor STING in dendritic cells*. Nat Immunol, 2011. **12**(10): p. 959-65.
51. Unterholzner, L., S.E. Keating, M. Baran, K.A. Horan, et al., *IFI16 is an innate immune sensor for intracellular DNA*. Nat Immunol, 2010. **11**(11): p. 997-1004.
52. Yang, P., H. An, X. Liu, M. Wen, et al., *The cytosolic nucleic acid sensor LRRFIP1 mediates the production of type I interferon via a beta-catenin-dependent pathway*. Nat Immunol, 2010. **11**(6): p. 487-94.
53. Zhang, X., T.W. Brann, M. Zhou, J. Yang, et al., *Cutting edge: Ku70 is a novel cytosolic DNA sensor that induces type III rather than type I IFN*. J Immunol, 2011. **186**(8): p. 4541-5.
54. Ishikawa, H., Z. Ma, and G.N. Barber, *STING regulates intracellular DNA-mediated, type I interferon-dependent innate immunity*. Nature, 2009. **461**(7265): p. 788-92.
55. Sun, L., J. Wu, F. Du, X. Chen, and Z.J. Chen, *Cyclic GMP-AMP synthase is a cytosolic DNA sensor that activates the type I interferon pathway*. Science, 2013. **339**(6121): p. 786-91.
56. Wu, J., L. Sun, X. Chen, F. Du, et al., *Cyclic GMP-AMP is an endogenous second messenger in innate immune signaling by cytosolic DNA*. Science, 2013. **339**(6121): p. 826-30.
57. Civril, F., T. Deimling, C.C. de Oliveira Mann, A. Ablasser, et al., *Structural mechanism of cytosolic DNA sensing by cGAS*. Nature, 2013.
58. Burdette, D.L., K.M. Monroe, K. Sotelo-Troha, J.S. Iwig, et al., *STING is a direct innate immune sensor of cyclic di-GMP*. Nature, 2011. **478**(7370): p. 515-8.
59. Parvatiyar, K., Z. Zhang, R.M. Teles, S. Ouyang, et al., *The helicase DDX41 recognizes the bacterial secondary messengers cyclic di-GMP and cyclic di-AMP to activate a type I interferon immune response*. Nat Immunol, 2012. **13**(12): p. 1155-61.
60. Ablasser, A., M. Goldeck, T. Cavlar, T. Deimling, et al., *cGAS produces a 2'-5'-linked cyclic dinucleotide second messenger that activates STING*. Nature, 2013.
61. Gao, P., M. Ascano, Y. Wu, W. Barchet, et al., *Cyclic [G(2',5')pA(3',5')p] Is the Metazoan Second Messenger Produced by DNA-Activated Cyclic GMP-AMP Synthase*. Cell, 2013. **153**(5): p. 1094-107.

62. Diner, E.J., D.L. Burdette, S.C. Wilson, K.M. Monroe, et al., *The Innate Immune DNA Sensor cGAS Produces a Noncanonical Cyclic Dinucleotide that Activates Human STING*. Cell Rep, 2013. **3**(5): p. 1355-61.
63. Arrildt, K.T., S.B. Joseph, and R. Swanstrom, *The HIV-1 env protein: a coat of many colors*. Curr HIV/AIDS Rep, 2012. **9**(1): p. 52-63.
64. Pertel, T., S. Hausmann, D. Morger, S. Zuger, et al., *TRIM5 is an innate immune sensor for the retrovirus capsid lattice*. Nature, 2011. **472**(7343): p. 361-5.
65. Doitsh, G., M. Cavrois, K.G. Lassen, O. Zepeda, et al., *Abortive HIV infection mediates CD4 T cell depletion and inflammation in human lymphoid tissue*. Cell, 2010. **143**(5): p. 789-801.
66. Berg, R.K., J. Melchjorsen, J. Rintahaka, E. Diget, et al., *Genomic HIV RNA induces innate immune responses through RIG-I-dependent sensing of secondary-structured RNA*. PLoS One, 2012. **7**(1): p. e29291.
67. Yan, N., A.D. Regalado-Magdos, B. Stiggelbout, M.A. Lee-Kirsch, and J. Lieberman, *The cytosolic exonuclease TREX1 inhibits the innate immune response to human immunodeficiency virus type 1*. Nat Immunol, 2010. **11**(11): p. 1005-13.
68. Neil, S.J., T. Zang, and P.D. Bieniasz, *Tetherin inhibits retrovirus release and is antagonized by HIV-1 Vpu*. Nature, 2008. **451**(7177): p. 425-30.
69. Perez-Caballero, D., T. Zang, A. Ebrahimi, M.W. McNatt, et al., *Tetherin inhibits HIV-1 release by directly tethering virions to cells*. Cell, 2009. **139**(3): p. 499-511.
70. Galao, R.P., A. Le Tortorec, S. Pickering, T. Kueck, and S.J. Neil, *Innate sensing of HIV-1 assembly by Tetherin induces NFkappaB-dependent proinflammatory responses*. Cell Host Microbe, 2012. **12**(5): p. 633-44.
71. Coiras, M., M.R. Lopez-Huertas, M. Perez-Olmeda, and J. Alcamí, *Understanding HIV-1 latency provides clues for the eradication of long-term reservoirs*. Nat Rev Microbiol, 2009. **7**(11): p. 798-812.
72. Beignon, A.S., K. McKenna, M. Skoberne, O. Manches, et al., *Endocytosis of HIV-1 activates plasmacytoid dendritic cells via Toll-like receptor-viral RNA interactions*. J Clin Invest, 2005. **115**(11): p. 3265-75.
73. Lepelley, A., S. Louis, M. Sourisseau, H.K. Law, et al., *Innate sensing of HIV-infected cells*. PLoS Pathog, 2011. **7**(2): p. e1001284.
74. Iwasaki, A., *Innate immune recognition of HIV-1*. Immunity, 2012. **37**(3): p. 389-98.
75. Goujon, C., V. Arfi, T. Pertel, J. Luban, et al., *Characterization of simian immunodeficiency virus SIVSM/human immunodeficiency virus type 2 Vpx function in human myeloid cells*. J Virol, 2008. **82**(24): p. 12335-45.
76. Honda, K., A. Takaoka, and T. Taniguchi, *Type I interferon [corrected] gene induction by the interferon regulatory factor family of transcription factors*. Immunity, 2006. **25**(3): p. 349-60.

77. Au, W.C., P.A. Moore, W. Lowther, Y.T. Juang, and P.M. Pitha, *Identification of a member of the interferon regulatory factor family that binds to the interferon-stimulated response element and activates expression of interferon-induced genes*. Proc Natl Acad Sci U S A, 1995. **92**(25): p. 11657-61.
78. Lin, R., P. Genin, Y. Mamane, and J. Hiscott, *Selective DNA binding and association with the CREB binding protein coactivator contribute to differential activation of alpha/beta interferon genes by interferon regulatory factors 3 and 7*. Mol Cell Biol, 2000. **20**(17): p. 6342-53.
79. Honda, K. and T. Taniguchi, *IRFs: master regulators of signalling by Toll-like receptors and cytosolic pattern-recognition receptors*. Nat Rev Immunol, 2006. **6**(9): p. 644-58.
80. Fujii, Y., T. Shimizu, M. Kusumoto, Y. Kyogoku, et al., *Crystal structure of an IRF-DNA complex reveals novel DNA recognition and cooperative binding to a tandem repeat of core sequences*. EMBO J, 1999. **18**(18): p. 5028-41.
81. Negishi, H., Y. Fujita, H. Yanai, S. Sakaguchi, et al., *Evidence for licensing of IFN-gamma-induced IFN regulatory factor 1 transcription factor by MyD88 in Toll-like receptor-dependent gene induction program*. Proc Natl Acad Sci U S A, 2006. **103**(41): p. 15136-41.
82. Sgarbanti, M., A. Borsetti, N. Moscufo, M.C. Bellocchi, et al., *Modulation of human immunodeficiency virus 1 replication by interferon regulatory factors*. J Exp Med, 2002. **195**(10): p. 1359-70.
83. Sgarbanti, M., A.L. Remoli, G. Marsili, B. Ridolfi, et al., *IRF-1 is required for full NF-kappaB transcriptional activity at the human immunodeficiency virus type 1 long terminal repeat enhancer*. J Virol, 2008. **82**(7): p. 3632-41.
84. Harada, H., K. Willison, J. Sakakibara, M. Miyamoto, et al., *Absence of the type I IFN system in EC cells: transcriptional activator (IRF-1) and repressor (IRF-2) genes are developmentally regulated*. Cell, 1990. **63**(2): p. 303-12.
85. Harada, H., M. Kitagawa, N. Tanaka, H. Yamamoto, et al., *Anti-oncogenic and oncogenic potentials of interferon regulatory factors-1 and -2*. Science, 1993. **259**(5097): p. 971-4.
86. Marecki, S. and M.J. Fenton, *The role of IRF-4 in transcriptional regulation*. J Interferon Cytokine Res, 2002. **22**(1): p. 121-33.
87. Takaoka, A., H. Yanai, S. Kondo, G. Duncan, et al., *Integral role of IRF-5 in the gene induction programme activated by Toll-like receptors*. Nature, 2005. **434**(7030): p. 243-9.
88. Kondo, S., B.C. Schutte, R.J. Richardson, B.C. Bjork, et al., *Mutations in IRF6 cause Van der Woude and popliteal pterygium syndromes*. Nat Genet, 2002. **32**(2): p. 285-9.
89. Chattopadhyay, S., M. Yamashita, Y. Zhang, and G.C. Sen, *The IRF-3/Bax-mediated apoptotic pathway, activated by viral cytoplasmic RNA and DNA, inhibits virus replication*. J Virol, 2011. **85**(8): p. 3708-16.

90. Chattopadhyay, S., V. Fensterl, Y. Zhang, M. Veleparambil, et al., *Role of interferon regulatory factor 3-mediated apoptosis in the establishment and maintenance of persistent infection by Sendai virus*. J Virol, 2013. **87**(1): p. 16-24.
91. Stawowczyk, M., S. Van Scoy, K.P. Kumar, and N.C. Reich, *The interferon stimulated gene 54 promotes apoptosis*. J Biol Chem, 2011. **286**(9): p. 7257-66.
92. Bergstroem, B., I.B. Johnsen, T.T. Nguyen, L. Hagen, et al., *Identification of a novel in vivo virus-targeted phosphorylation site in interferon regulatory factor-3 (IRF3)*. J Biol Chem, 2010. **285**(32): p. 24904-14.
93. Panne, D., S.M. McWhirter, T. Maniatis, and S.C. Harrison, *Interferon regulatory factor 3 is regulated by a dual phosphorylation-dependent switch*. J Biol Chem, 2007. **282**(31): p. 22816-22.
94. Yoneyama, M., W. Suhara, Y. Fukuhara, M. Fukuda, et al., *Direct triggering of the type I interferon system by virus infection: activation of a transcription factor complex containing IRF-3 and CBP/p300*. EMBO J, 1998. **17**(4): p. 1087-95.
95. Sharma, S., B.R. tenOever, N. Grandvaux, G.P. Zhou, et al., *Triggering the interferon antiviral response through an IKK-related pathway*. Science, 2003. **300**(5622): p. 1148-51.
96. Fitzgerald, K.A., S.M. McWhirter, K.L. Faia, D.C. Rowe, et al., *IKKepsilon and TBK1 are essential components of the IRF3 signaling pathway*. Nat Immunol, 2003. **4**(5): p. 491-6.
97. Lin, R., J. Lacoste, P. Nakhaei, Q. Sun, et al., *Dissociation of a MAVS/IPS-1/VISA/Cardif-IKKepsilon molecular complex from the mitochondrial outer membrane by hepatitis C virus NS3-4A proteolytic cleavage*. J Virol, 2006. **80**(12): p. 6072-83.
98. Tanaka, Y. and Z.J. Chen, *STING specifies IRF3 phosphorylation by TBK1 in the cytosolic DNA signaling pathway*. Sci Signal, 2012. **5**(214): p. ra20.
99. Qin, B.Y., C. Liu, S.S. Lam, H. Srinath, et al., *Crystal structure of IRF-3 reveals mechanism of autoinhibition and virus-induced phosphoactivation*. Nat Struct Biol, 2003. **10**(11): p. 913-21.
100. Shukla, H., P. Vaitiekunas, A.K. Majumdar, A.I. Dragan, et al., *The linker of the interferon response factor 3 transcription factor is not unfolded*. Biochemistry, 2012. **51**(32): p. 6320-7.
101. Kim, H. and B. Seed, *The transcription factor MafB antagonizes antiviral responses by blocking recruitment of coactivators to the transcription factor IRF3*. Nat Immunol, 2010. **11**(8): p. 743-50.
102. Sears, N., G.C. Sen, G.R. Stark, and S. Chattopadhyay, *Caspase-8-mediated cleavage inhibits IRF-3 protein by facilitating its proteasome-mediated degradation*. J Biol Chem, 2011. **286**(38): p. 33037-44.
103. Saitoh, T., A. Tun-Kyi, A. Ryo, M. Yamamoto, et al., *Negative regulation of interferon-regulatory factor 3-dependent innate antiviral response by the prolyl isomerase Pin1*. Nat Immunol, 2006. **7**(6): p. 598-605.

104. Zhang, M., Y. Tian, R.P. Wang, D. Gao, et al., *Negative feedback regulation of cellular antiviral signaling by RBCK1-mediated degradation of IRF3*. Cell Res, 2008. **18**(11): p. 1096-104.
105. Kubota, T., M. Matsuoka, T.H. Chang, P. Taylor, et al., *Virus infection triggers SUMOylation of IRF3 and IRF7, leading to the negative regulation of type I interferon gene expression*. J Biol Chem, 2008. **283**(37): p. 25660-70.
106. Doehle, B.P., F. Hladik, J.P. McNevin, M.J. McElrath, and M. Gale, Jr., *Human immunodeficiency virus type 1 mediates global disruption of innate antiviral signaling and immune defenses within infected cells*. J Virol, 2009. **83**(20): p. 10395-405.
107. Panne, D., *The enhanceosome*. Curr Opin Struct Biol, 2008. **18**(2): p. 236-42.
108. Taniguchi, T. and A. Takaoka, *A weak signal for strong responses: interferon-alpha/beta revisited*. Nat Rev Mol Cell Biol, 2001. **2**(5): p. 378-86.
109. Panne, D., T. Maniatis, and S.C. Harrison, *An atomic model of the interferon-beta enhanceosome*. Cell, 2007. **129**(6): p. 1111-23.
110. Kim, T.K. and T. Maniatis, *The mechanism of transcriptional synergy of an in vitro assembled interferon-beta enhanceosome*. Mol Cell, 1997. **1**(1): p. 119-29.
111. Honda, K., H. Yanai, H. Negishi, M. Asagiri, et al., *IRF-7 is the master regulator of type-I interferon-dependent immune responses*. Nature, 2005. **434**(7034): p. 772-7.
112. Balachandran, S. and A.A. Beg, *Defining emerging roles for NF-kappaB in antiviral responses: revisiting the interferon-beta enhanceosome paradigm*. PLoS Pathog, 2011. **7**(10): p. e1002165.
113. Der, S.D., A. Zhou, B.R. Williams, and R.H. Silverman, *Identification of genes differentially regulated by interferon alpha, beta, or gamma using oligonucleotide arrays*. Proc Natl Acad Sci U S A, 1998. **95**(26): p. 15623-8.
114. Andersen, J., S. VanScoy, T.F. Cheng, D. Gomez, and N.C. Reich, *IRF-3-dependent and augmented target genes during viral infection*. Genes Immun, 2008. **9**(2): p. 168-75.
115. Lin, R., C. Heylbroeck, P. Genin, P.M. Pitha, and J. Hiscott, *Essential role of interferon regulatory factor 3 in direct activation of RANTES chemokine transcription*. Mol Cell Biol, 1999. **19**(2): p. 959-66.
116. Guo, J., D.J. Hui, W.C. Merrick, and G.C. Sen, *A new pathway of translational regulation mediated by eukaryotic initiation factor 3*. EMBO J, 2000. **19**(24): p. 6891-9.
117. Pichlmair, A., C. Lassnig, C.A. Eberle, M.W. Gorna, et al., *IFIT1 is an antiviral protein that recognizes 5'-triphosphate RNA*. Nat Immunol, 2011. **12**(7): p. 624-30.
118. Grandvaux, N., M.J. Servant, B. tenOever, G.C. Sen, et al., *Transcriptional profiling of interferon regulatory factor 3 target genes: direct involvement in the regulation of interferon-stimulated genes*. J Virol, 2002. **76**(11): p. 5532-9.
119. Yang, Z., H. Liang, Q. Zhou, Y. Li, et al., *Crystal structure of ISG54 reveals a novel RNA binding structure and potential functional mechanisms*. Cell Res, 2012. **22**(9): p. 1328-38.

120. Amini-Bavil-Olyaei, S., Y.J. Choi, J.H. Lee, M. Shi, et al., *The antiviral effector IFITM3 disrupts intracellular cholesterol homeostasis to block viral entry*. Cell Host Microbe, 2013. **13**(4): p. 452-64.
121. Li, K., R.M. Markosyan, Y.M. Zheng, O. Golfetto, et al., *IFITM proteins restrict viral membrane hemifusion*. PLoS Pathog, 2013. **9**(1): p. e1003124.
122. Schafer, S.L., R. Lin, P.A. Moore, J. Hiscott, and P.M. Pitha, *Regulation of type I interferon gene expression by interferon regulatory factor-3*. J Biol Chem, 1998. **273**(5): p. 2714-20.
123. Okumura, F., A.J. Okumura, K. Uematsu, S. Hatakeyama, et al., *Activation of double-stranded RNA-activated protein kinase (PKR) by interferon-stimulated gene 15 (ISG15) modification down-regulates protein translation*. J Biol Chem, 2013. **288**(4): p. 2839-47.
124. Espert, L., G. Degols, C. Gongora, D. Blondel, et al., *ISG20, a new interferon-induced RNase specific for single-stranded RNA, defines an alternative antiviral pathway against RNA genomic viruses*. J Biol Chem, 2003. **278**(18): p. 16151-8.
125. Espert, L., G. Degols, Y.L. Lin, T. Vincent, et al., *Interferon-induced exonuclease ISG20 exhibits an antiviral activity against human immunodeficiency virus type 1*. J Gen Virol, 2005. **86**(Pt 8): p. 2221-9.
126. Seo, J.Y., R. Yaneva, and P. Cresswell, *Viperin: a multifunctional, interferon-inducible protein that regulates virus replication*. Cell Host Microbe, 2011. **10**(6): p. 534-9.
127. Nasr, N., S. Maddocks, S.G. Turville, A.N. Harman, et al., *HIV-1 infection of human macrophages directly induces viperin which inhibits viral production*. Blood, 2012. **120**(4): p. 778-88.
128. Wang, N., Q. Dong, J. Li, R.K. Jangra, et al., *Viral induction of the zinc finger antiviral protein is IRF3-dependent but NF-kappaB-independent*. J Biol Chem, 2010. **285**(9): p. 6080-90.
129. Gao, G., X. Guo, and S.P. Goff, *Inhibition of retroviral RNA production by ZAP, a CCH-type zinc finger protein*. Science, 2002. **297**(5587): p. 1703-6.
130. Yan, H., K. Krishnan, J.T. Lim, L.G. Contillo, and J.J. Krolewski, *Molecular characterization of an alpha interferon receptor 1 subunit (IFNAR1) domain required for TYK2 binding and signal transduction*. Mol Cell Biol, 1996. **16**(5): p. 2074-82.
131. Li, X., S. Leung, I.M. Kerr, and G.R. Stark, *Functional subdomains of STAT2 required for preassociation with the alpha interferon receptor and for signaling*. Mol Cell Biol, 1997. **17**(4): p. 2048-56.
132. Fu, X.Y., C. Schindler, T. Improta, R. Aebersold, and J.E. Darnell, Jr., *The proteins of ISGF-3, the interferon alpha-induced transcriptional activator, define a gene family involved in signal transduction*. Proc Natl Acad Sci U S A, 1992. **89**(16): p. 7840-3.
133. Lin, R., Y. Mamane, and J. Hiscott, *Multiple regulatory domains control IRF-7 activity in response to virus infection*. J Biol Chem, 2000. **275**(44): p. 34320-7.

134. Schoggins, J.W., S.J. Wilson, M. Panis, M.Y. Murphy, et al., *A diverse range of gene products are effectors of the type I interferon antiviral response*. Nature, 2011. **472**(7344): p. 481-5.
135. Ozato, K., D.M. Shin, T.H. Chang, and H.C. Morse, 3rd, *TRIM family proteins and their emerging roles in innate immunity*. Nat Rev Immunol, 2008. **8**(11): p. 849-60.
136. Rajsbaum, R., J.P. Stoye, and A. O'Garra, *Type I interferon-dependent and -independent expression of tripartite motif proteins in immune cells*. Eur J Immunol, 2008. **38**(3): p. 619-30.
137. Sheehy, A.M., N.C. Gaddis, J.D. Choi, and M.H. Malim, *Isolation of a human gene that inhibits HIV-1 infection and is suppressed by the viral Vif protein*. Nature, 2002. **418**(6898): p. 646-50.
138. Peng, G., K.J. Lei, W. Jin, T. Greenwell-Wild, and S.M. Wahl, *Induction of APOBEC3 family proteins, a defensive maneuver underlying interferon-induced anti-HIV-1 activity*. J Exp Med, 2006. **203**(1): p. 41-6.
139. Mohanram, V., A.E. Skold, S.M. Bachle, S.K. Pathak, and A.L. Spetz, *IFN-alpha induces APOBEC3G, F, and A in immature dendritic cells and limits HIV-1 spread to CD4+ T cells*. J Immunol, 2013. **190**(7): p. 3346-53.
140. Woods, M.W., J.N. Kelly, C.J. Hattlmann, J.G. Tong, et al., *Human HERC5 restricts an early stage of HIV-1 assembly by a mechanism correlating with the ISGylation of Gag*. Retrovirology, 2011. **8**: p. 95.
141. Meurs, E.F., Y. Watanabe, S. Kadereit, G.N. Barber, et al., *Constitutive expression of human double-stranded RNA-activated p68 kinase in murine cells mediates phosphorylation of eukaryotic initiation factor 2 and partial resistance to encephalomyocarditis virus growth*. J Virol, 1992. **66**(10): p. 5805-14.
142. Li, M., E. Kao, X. Gao, H. Sandig, et al., *Codon-usage-based inhibition of HIV protein synthesis by human schlafen 11*. Nature, 2012. **491**(7422): p. 125-8.
143. Yang, K., H.X. Shi, X.Y. Liu, Y.F. Shan, et al., *TRIM21 is essential to sustain IFN regulatory factor 3 activation during antiviral response*. J Immunol, 2009. **182**(6): p. 3782-92.
144. Allouch, A., C. Di Primio, E. Alpi, M. Lusic, et al., *The TRIM family protein KAP1 inhibits HIV-1 integration*. Cell Host Microbe, 2011. **9**(6): p. 484-95.
145. Stremlau, M., C.M. Owens, M.J. Perron, M. Kiessling, et al., *The cytoplasmic body component TRIM5alpha restricts HIV-1 infection in Old World monkeys*. Nature, 2004. **427**(6977): p. 848-53.
146. Ye, J. and T. Maniatis, *Negative regulation of interferon-beta gene expression during acute and persistent virus infections*. PLoS One, 2011. **6**(6): p. e20681.
147. Lee, H.R., M.H. Kim, J.S. Lee, C. Liang, and J.U. Jung, *Viral interferon regulatory factors*. J Interferon Cytokine Res, 2009. **29**(9): p. 621-7.

148. Laurent-Rolle, M., E.F. Boer, K.J. Lubick, J.B. Wolfinger, et al., *The NS5 protein of the virulent West Nile virus NY99 strain is a potent antagonist of type I interferon-mediated JAK-STAT signaling*. J Virol, 2010. **84**(7): p. 3503-15.
149. Zhang, Z., Z. Zheng, H. Luo, J. Meng, et al., *Human bocavirus NP1 inhibits IFN-beta production by blocking association of IFN regulatory factor 3 with IFNB promoter*. J Immunol, 2012. **189**(3): p. 1144-53.
150. Unterstab, G., S. Ludwig, A. Anton, O. Planz, et al., *Viral targeting of the interferon- β -inducing Traf family member-associated NF- κ B activator (TANK)-binding kinase-1*. Proc Natl Acad Sci U S A, 2005. **102**(38): p. 13640-5.
151. Hilton, L., K. Moganeradj, G. Zhang, Y.H. Chen, et al., *The NPro product of bovine viral diarrhea virus inhibits DNA binding by interferon regulatory factor 3 and targets it for proteasomal degradation*. J Virol, 2006. **80**(23): p. 11723-32.
152. Aguirre, S., A.M. Maestre, S. Pagni, J.R. Patel, et al., *DENV inhibits type I IFN production in infected cells by cleaving human STING*. PLoS Pathog, 2012. **8**(10): p. e1002934.
153. Basler, C.F., A. Mikulasova, L. Martinez-Sobrido, J. Paragas, et al., *The Ebola virus VP35 protein inhibits activation of interferon regulatory factor 3*. J Virol, 2003. **77**(14): p. 7945-56.
154. Cardenas, W.B., Y.M. Loo, M. Gale, Jr., A.L. Hartman, et al., *Ebola virus VP35 protein binds double-stranded RNA and inhibits alpha/beta interferon production induced by RIG-I signaling*. J Virol, 2006. **80**(11): p. 5168-78.
155. Bentz, G.L., R. Liu, A.M. Hahn, J. Shackelford, and J.S. Pagano, *Epstein-Barr virus BRLF1 inhibits transcription of IRF3 and IRF7 and suppresses induction of interferon-beta*. Virology, 2010. **402**(1): p. 121-8.
156. Wang, J.T., S.L. Doong, S.C. Teng, C.P. Lee, et al., *Epstein-Barr virus BGLF4 kinase suppresses the interferon regulatory factor 3 signaling pathway*. J Virol, 2009. **83**(4): p. 1856-69.
157. Foy, E., K. Li, C. Wang, R. Sumpter, Jr., et al., *Regulation of interferon regulatory factor-3 by the hepatitis C virus serine protease*. Science, 2003. **300**(5622): p. 1145-8.
158. Loo, Y.M., D.M. Owen, K. Li, A.K. Erickson, et al., *Viral and therapeutic control of IFN-beta promoter stimulator 1 during hepatitis C virus infection*. Proc Natl Acad Sci U S A, 2006. **103**(15): p. 6001-6.
159. Meylan, E., J. Curran, K. Hofmann, D. Moradpour, et al., *Cardif is an adaptor protein in the RIG-I antiviral pathway and is targeted by hepatitis C virus*. Nature, 2005. **437**(7062): p. 1167-72.
160. Li, K., E. Foy, J.C. Ferreon, M. Nakamura, et al., *Immune evasion by hepatitis C virus NS3/4A protease-mediated cleavage of the Toll-like receptor 3 adaptor protein TRIF*. Proc Natl Acad Sci U S A, 2005. **102**(8): p. 2992-7.

161. Orzalli, M.H., N.A. DeLuca, and D.M. Knipe, *Nuclear IFI16 induction of IRF-3 signaling during herpesviral infection and degradation of IFI16 by the viral ICP0 protein.* Proc Natl Acad Sci U S A, 2012. **109**(44): p. E3008-17.
162. Melroe, G.T., L. Silva, P.A. Schaffer, and D.M. Knipe, *Recruitment of activated IRF-3 and CBP/p300 to herpes simplex virus ICP0 nuclear foci: Potential role in blocking IFN-beta induction.* Virology, 2007. **360**(2): p. 305-21.
163. McNatt, M.W., T. Zang, and P.D. Bieniasz, *Vpu binds directly to tetherin and displaces it from nascent virions.* PLoS Pathog, 2013. **9**(4): p. e1003299.
164. Van Damme, N., D. Goff, C. Katsura, R.L. Jorgenson, et al., *The interferon-induced protein BST-2 restricts HIV-1 release and is downregulated from the cell surface by the viral Vpu protein.* Cell Host Microbe, 2008. **3**(4): p. 245-52.
165. Douglas, J.L., K. Viswanathan, M.N. McCarroll, J.K. Gustin, et al., *Vpu directs the degradation of the human immunodeficiency virus restriction factor BST-2/Tetherin via a {beta}TrCP-dependent mechanism.* J Virol, 2009. **83**(16): p. 7931-47.
166. Magadan, J.G., F.J. Perez-Victoria, R. Sougrat, Y. Ye, et al., *Multilayered mechanism of CD4 downregulation by HIV-1 Vpu involving distinct ER retention and ERAD targeting steps.* PLoS Pathog, 2010. **6**(4): p. e1000869.
167. Doehle, B.P., K. Chang, L. Fleming, J. McNevin, et al., *Vpu-deficient HIV strains stimulate innate immune signaling responses in target cells.* J Virol, 2012. **86**(16): p. 8499-506.
168. Doehle, B.P., K. Chang, A. Rustagi, J. McNevin, et al., *Vpu mediates depletion of interferon regulatory factor 3 during HIV infection by a lysosome-dependent mechanism.* J Virol, 2012. **86**(16): p. 8367-74.
169. Sheehy, A.M., N.C. Gaddis, and M.H. Malim, *The antiretroviral enzyme APOBEC3G is degraded by the proteasome in response to HIV-1 Vif.* Nat Med, 2003. **9**(11): p. 1404-7.
170. Solis, M., P. Nakhaei, M. Jalalirad, J. Lacoste, et al., *RIG-I-mediated antiviral signaling is inhibited in HIV-1 infection by a protease-mediated sequestration of RIG-I.* J Virol, 2011. **85**(3): p. 1224-36.
171. Jaworska, J., A. Gravel, K. Fink, N. Grandvaux, and L. Flamand, *Inhibition of transcription of the beta interferon gene by the human herpesvirus 6 immediate-early 1 protein.* J Virol, 2007. **81**(11): p. 5737-48.
172. Yu, Y., S.E. Wang, and G.S. Hayward, *The KSHV immediate-early transcription factor RTA encodes ubiquitin E3 ligase activity that targets IRF7 for proteasome-mediated degradation.* Immunity, 2005. **22**(1): p. 59-70.
173. Lin, R., P. Genin, Y. Mamane, M. Sgarbanti, et al., *HHV-8 encoded vIRF-1 represses the interferon antiviral response by blocking IRF-3 recruitment of the CBP/p300 coactivators.* Oncogene, 2001. **20**(7): p. 800-11.
174. Fuld, S., C. Cunningham, K. Klucher, A.J. Davison, and D.J. Blackbourn, *Inhibition of interferon signaling by the Kaposi's sarcoma-associated herpesvirus full-length viral interferon regulatory factor 2 protein.* J Virol, 2006. **80**(6): p. 3092-7.

175. Joo, C.H., Y.C. Shin, M. Gack, L. Wu, et al., *Inhibition of interferon regulatory factor 7 (IRF7)-mediated interferon signal transduction by the Kaposi's sarcoma-associated herpesvirus viral IRF homolog vIRF3*. J Virol, 2007. **81**(15): p. 8282-92.
176. Ren, J., T. Liu, L. Pang, K. Li, et al., *A novel mechanism for the inhibition of interferon regulatory factor-3-dependent gene expression by human respiratory syncytial virus NS1 protein*. J Gen Virol, 2011. **92**(Pt 9): p. 2153-9.
177. DeFilippis, V. and K. Fruh, *Rhesus cytomegalovirus particles prevent activation of interferon regulatory factor 3*. J Virol, 2005. **79**(10): p. 6419-31.
178. Barro, M. and J.T. Patton, *Rotavirus nonstructural protein 1 subverts innate immune response by inducing degradation of IFN regulatory factor 3*. Proc Natl Acad Sci U S A, 2005. **102**(11): p. 4114-9.
179. Zhu, H., C. Zheng, J. Xing, S. Wang, et al., *Varicella-zoster virus immediate-early protein ORF61 abrogates the IRF3-mediated innate immune response through degradation of activated IRF3*. J Virol, 2011. **85**(21): p. 11079-89.
180. Cohen, M.S., G.M. Shaw, A.J. McMichael, and B.F. Haynes, *Acute HIV-1 Infection*. N Engl J Med, 2011. **364**(20): p. 1943-54.
181. Salazar-Gonzalez, J.F., M.G. Salazar, B.F. Keele, G.H. Learn, et al., *Genetic identity, biological phenotype, and evolutionary pathways of transmitted/founder viruses in acute and early HIV-1 infection*. J Exp Med, 2009. **206**(6): p. 1273-89.
182. Allers, K., G. Hutter, J. Hofmann, C. Loddenkemper, et al., *Evidence for the cure of HIV infection by CCR5Delta32/Delta32 stem cell transplantation*. Blood, 2011. **117**(10): p. 2791-9.
183. Dolgin, E., *New, intensive trials planned on heels of Mississippi HIV 'cure'*. Nat Med, 2013. **19**(4): p. 380-1.
184. Saez-Cirion, A., C. Bacchus, L. Hocqueloux, V. Avettand-Fenoel, et al., *Post-treatment HIV-1 controllers with a long-term virological remission after the interruption of early initiated antiretroviral therapy ANRS VISCONTI Study*. PLoS Pathog, 2013. **9**(3): p. e1003211.
185. Lahouassa, H., W. Daddacha, H. Hofmann, D. Ayinde, et al., *SAMHD1 restricts the replication of human immunodeficiency virus type 1 by depleting the intracellular pool of deoxynucleoside triphosphates*. Nat Immunol, 2012. **13**(3): p. 223-8.
186. Manel, N., B. Hogstad, Y. Wang, D.E. Levy, et al., *A cryptic sensor for HIV-1 activates antiviral innate immunity in dendritic cells*. Nature, 2010. **467**(7312): p. 214-7.
187. Dragin, L., L.A. Nguyen, H. Lahouassa, A. Sourisce, et al., *Interferon block to HIV-1 transduction in macrophages despite SAMHD1 degradation and high deoxynucleoside triphosphates supply*. Retrovirology, 2013. **10**: p. 30.
188. Cribier, A., B. Descours, A.L. Valadao, N. Laguette, and M. Benkirane, *Phosphorylation of SAMHD1 by cyclin A2/CDK1 regulates its restriction activity toward HIV-1*. Cell Rep, 2013. **3**(4): p. 1036-43.

189. White, T.E., A. Brandariz-Nunez, J.C. Valle-Casuso, S. Amie, et al., *The retroviral restriction ability of SAMHD1, but not its deoxynucleotide triphosphohydrolase activity, is regulated by phosphorylation*. Cell Host Microbe, 2013. **13**(4): p. 441-51.
190. Baldauf, H.M., X. Pan, E. Erikson, S. Schmidt, et al., *SAMHD1 restricts HIV-1 infection in resting CD4(+) T cells*. Nat Med, 2012. **18**(11): p. 1682-7.
191. Stremlau, M., M. Perron, M. Lee, Y. Li, et al., *Specific recognition and accelerated uncoating of retroviral capsids by the TRIM5alpha restriction factor*. Proc Natl Acad Sci U S A, 2006. **103**(14): p. 5514-9.
192. Lu, J., Q. Pan, L. Rong, W. He, et al., *The IFITM proteins inhibit HIV-1 infection*. J Virol, 2011. **85**(5): p. 2126-37.
193. Kaiser, S.M., H.S. Malik, and M. Emerman, *Restriction of an extinct retrovirus by the human TRIM5alpha antiviral protein*. Science, 2007. **316**(5832): p. 1756-8.
194. Okumura, A., T. Alce, B. Lubyova, H. Ezelle, et al., *HIV-1 accessory proteins VPR and Vif modulate antiviral response by targeting IRF-3 for degradation*. Virology, 2008. **373**(1): p. 85-97.
195. Hotter, D., F. Kirchhoff, and D. Sauter, *HIV-1 Vpu Does Not Degrade Interferon Regulatory Factor 3*. J Virol, 2013. **87**(12): p. 7160-5.
196. Matusali, G., M. Potesta, A. Santoni, C. Cerboni, and M. Doria, *The human immunodeficiency virus type 1 Nef and Vpu proteins downregulate the natural killer cell-activating ligand PVR*. J Virol, 2012. **86**(8): p. 4496-504.
197. Shah, A.H., B. Sowrirajan, Z.B. Davis, J.P. Ward, et al., *Degranulation of natural killer cells following interaction with HIV-1-infected cells is hindered by downmodulation of NTB-A by Vpu*. Cell Host Microbe, 2010. **8**(5): p. 397-409.
198. Hardy, G.A., S. Sieg, B. Rodriguez, D. Anthony, et al., *Interferon-alpha is the primary plasma type-I IFN in HIV-1 infection and correlates with immune activation and disease markers*. PLoS One, 2013. **8**(2): p. e56527.
199. Li, Q., J.D. Estes, P.M. Schlievert, L. Duan, et al., *Glycerol monolaurate prevents mucosal SIV transmission*. Nature, 2009. **458**(7241): p. 1034-8.
200. Harman, A.N., J. Lai, S. Turville, S. Samarajiwa, et al., *HIV infection of dendritic cells subverts the IFN induction pathway via IRF-1 and inhibits type 1 IFN production*. Blood, 2011. **118**(2): p. 298-308.
201. Miller, E. and N. Bhardwaj, *Dendritic cell dysregulation during HIV-1 infection*. Immunol Rev, 2013. **254**(1): p. 170-89.
202. Bosinger, S.E., Q. Li, S.N. Gordon, N.R. Klatt, et al., *Global genomic analysis reveals rapid control of a robust innate response in SIV-infected sooty mangabeys*. J Clin Invest, 2009. **119**(12): p. 3556-72.
203. Harris, L.D., B. Tabb, D.L. Sodora, M. Paiardini, et al., *Downregulation of robust acute type I interferon responses distinguishes nonpathogenic simian immunodeficiency virus (SIV) infection of natural hosts from pathogenic SIV infection of rhesus macaques*. J Virol, 2010. **84**(15): p. 7886-91.

204. Powers, K.A., A.C. Ghani, W.C. Miller, I.F. Hoffman, et al., *The role of acute and early HIV infection in the spread of HIV and implications for transmission prevention strategies in Lilongwe, Malawi: a modelling study*. *Lancet*, 2011. **378**(9787): p. 256-68.
205. Rustagi, A., B.P. Doehle, M.J. McElrath, and M. Gale, Jr., *Two new monoclonal antibodies for biochemical and flow cytometric analyses of human interferon regulatory factor-3 activation, turnover, and depletion*. *Methods*, 2013. **59**(2): p. 225-32.
206. Sato, M., H. Suemori, N. Hata, M. Asagiri, et al., *Distinct and essential roles of transcription factors IRF-3 and IRF-7 in response to viruses for IFN-alpha/beta gene induction*. *Immunity*, 2000. **13**(4): p. 539-48.
207. Takeuchi, O. and S. Akira, *Pattern recognition receptors and inflammation*. *Cell*, 2010. **140**(6): p. 805-20.
208. Stetson, D.B. and R. Medzhitov, *Recognition of cytosolic DNA activates an IRF3-dependent innate immune response*. *Immunity*, 2006. **24**(1): p. 93-103.
209. Hornung, V., A. Ablasser, M. Charrel-Dennis, F. Bauernfeind, et al., *AIM2 recognizes cytosolic dsDNA and forms a caspase-1-activating inflammasome with ASC*. *Nature*, 2009. **458**(7237): p. 514-8.
210. Ablasser, A., F. Bauernfeind, G. Hartmann, E. Latz, et al., *RIG-I-dependent sensing of poly(dA:dT) through the induction of an RNA polymerase III-transcribed RNA intermediate*. *Nat Immunol*, 2009. **10**(10): p. 1065-72.
211. Lin, R., Y. Mamane, and J. Hiscott, *Structural and functional analysis of interferon regulatory factor 3: localization of the transactivation and autoinhibitory domains*. *Mol Cell Biol*, 1999. **19**(4): p. 2465-74.
212. Sumpter, R., Y.M. Loo, E. Foy, K. Li, et al., *Regulating intracellular antiviral defense and permissiveness to hepatitis C virus RNA replication through a cellular RNA helicase, RIG-I*. *J Virol*, 2005. **79**(5): p. 2689-99.
213. Lin, R., C. Heylbroeck, P.M. Pitha, and J. Hiscott, *Virus-dependent phosphorylation of the IRF-3 transcription factor regulates nuclear translocation, transactivation potential, and proteasome-mediated degradation*. *Mol Cell Biol*, 1998. **18**(5): p. 2986-96.
214. Yoneyama, M. and T. Fujita, *Function of RIG-I-like receptors in antiviral innate immunity*. *J Biol Chem*, 2007. **282**(21): p. 15315-8.
215. Yim, H.C., J.C. Li, J.S. Lau, and A.S. Lau, *HIV-1 Tat dysregulation of lipopolysaccharide-induced cytokine responses: microbial interactions in HIV infection*. *AIDS*, 2009. **23**(12): p. 1473-84.
216. Derdeyn, C.A., J.M. Decker, J.N. Sfakianos, X. Wu, et al., *Sensitivity of human immunodeficiency virus type 1 to the fusion inhibitor T-20 is modulated by coreceptor specificity defined by the V3 loop of gp120*. *J Virol*, 2000. **74**(18): p. 8358-67.
217. Mörner, A., A. Björndal, J. Albert, V.N. Kewalramani, et al., *Primary human immunodeficiency virus type 2 (HIV-2) isolates, like HIV-1 isolates, frequently use CCR5 but show promiscuity in coreceptor usage*. *J Virol*, 1999. **73**(3): p. 2343-9.

218. Iwamura, T., M. Yoneyama, K. Yamaguchi, W. Suhara, et al., *Induction of IRF-3/-7 kinase and NF-kappaB in response to double-stranded RNA and virus infection: common and unique pathways*. Genes Cells, 2001. **6**(4): p. 375-88.
219. Navarro, L. and M. David, *p38-dependent activation of interferon regulatory factor 3 by lipopolysaccharide*. J Biol Chem, 1999. **274**(50): p. 35535-8.
220. Larkin, M.A., G. Blackshields, N.P. Brown, R. Chenna, et al., *Clustal W and Clustal X version 2.0*. Bioinformatics, 2007. **23**(21): p. 2947-8.
221. Waterhouse, A.M., J.B. Procter, D.M. Martin, M. Clamp, and G.J. Barton, *Jalview Version 2--a multiple sequence alignment editor and analysis workbench*. Bioinformatics, 2009. **25**(9): p. 1189-91.
222. Chew, T., R. Noyce, S.E. Collins, M.H. Hancock, and K.L. Mossman, *Characterization of the interferon regulatory factor 3-mediated antiviral response in a cell line deficient for IFN production*. Mol Immunol, 2009. **46**(3): p. 393-9.
223. Cobos Jimenez, V., T. Booiman, S.W. de Taeye, K.A. van Dort, et al., *Differential expression of HIV-1 interfering factors in monocyte-derived macrophages stimulated with polarizing cytokines or interferons*. Sci Rep, 2012. **2**: p. 763.
224. Fredericksen, B., G.R. Akkaraju, E. Foy, C. Wang, et al., *Activation of the interferon-beta promoter during hepatitis C virus RNA replication*. Viral Immunol, 2002. **15**(1): p. 29-40.
225. Ishikawa, H. and G.N. Barber, *STING is an endoplasmic reticulum adaptor that facilitates innate immune signalling*. Nature, 2008. **455**(7213): p. 674-8.
226. Nguyen, K.L., M. Ilano, H. Akari, E. Miyagi, et al., *Codon optimization of the HIV-1 vpu and vif genes stabilizes their mRNA and allows for highly efficient Rev-independent expression*. Virology, 2004. **319**(2): p. 163-75.
227. Poss, M. and J. Overbaugh, *Variants from the diverse virus population identified at seroconversion of a clade A human immunodeficiency virus type 1-infected woman have distinct biological properties*. J Virol, 1999. **73**(7): p. 5255-64.
228. Sauter, D., M. Schindler, A. Specht, W.N. Landford, et al., *Tetherin-driven adaptation of Vpu and Nef function and the evolution of pandemic and nonpandemic HIV-1 strains*. Cell Host Microbe, 2009. **6**(5): p. 409-21.
229. Li, M., F. Gao, J.R. Mascola, L. Stamatatos, et al., *Human immunodeficiency virus type 1 env clones from acute and early subtype B infections for standardized assessments of vaccine-elicited neutralizing antibodies*. J Virol, 2005. **79**(16): p. 10108-25.
230. Suthar, M.S., M.M. Brassil, G. Blahnik, A. McMillan, et al., *A systems biology approach reveals that tissue tropism to West Nile virus is regulated by antiviral genes and innate immune cellular processes*. PLoS Pathog, 2013. **9**(2): p. e1003168.
231. Huang da, W., B.T. Sherman, and R.A. Lempicki, *Systematic and integrative analysis of large gene lists using DAVID bioinformatics resources*. Nat Protoc, 2009. **4**(1): p. 44-57.

232. Huang da, W., B.T. Sherman, and R.A. Lempicki, *Bioinformatics enrichment tools: paths toward the comprehensive functional analysis of large gene lists*. Nucleic Acids Res, 2009. **37**(1): p. 1-13.
233. Hiscott, J., H. Kwon, and P. Genin, *Hostile takeovers: viral appropriation of the NF-kappaB pathway*. J Clin Invest, 2001. **107**(2): p. 143-51.
234. Marsili, G., A.L. Remoli, M. Sgarbanti, E. Perrotti, et al., *HIV-1, interferon and the interferon regulatory factor system: an interplay between induction, antiviral responses and viral evasion*. Cytokine Growth Factor Rev, 2012. **23**(4-5): p. 255-70.
235. Chen, W. and W.E. Royer, Jr., *Structural insights into interferon regulatory factor activation*. Cell Signal, 2010. **22**(6): p. 883-7.
236. Maldarelli, F., M.Y. Chen, R.L. Willey, and K. Strebel, *Human immunodeficiency virus type 1 Vpu protein is an oligomeric type I integral membrane protein*. J Virol, 1993. **67**(8): p. 5056-61.
237. Au, W.C., W.S. Yeow, and P.M. Pitha, *Analysis of functional domains of interferon regulatory factor 7 and its association with IRF-3*. Virology, 2001. **280**(2): p. 273-82.
238. Nieva, J.L., V. Madan, and L. Carrasco, *Viroporins: structure and biological functions*. Nat Rev Microbiol, 2012. **10**(8): p. 563-74.
239. Cordes, F.S., A.D. Tustian, M.S. Sansom, A. Watts, and W.B. Fischer, *Bundles consisting of extended transmembrane segments of Vpu from HIV-1: computer simulations and conductance measurements*. Biochemistry, 2002. **41**(23): p. 7359-65.
240. Ichinohe, T., I.K. Pang, and A. Iwasaki, *Influenza virus activates inflammasomes via its intracellular M2 ion channel*. Nat Immunol, 2010. **11**(5): p. 404-10.
241. Kuhl, B.D., V. Cheng, D.A. Donahue, R.D. Sloan, et al., *The HIV-1 Vpu viroporin inhibitor BIT225 does not affect Vpu-mediated tetherin antagonism*. PLoS One, 2011. **6**(11): p. e27660.
242. Lim, E.S., H.S. Malik, and M. Emerman, *Ancient adaptive evolution of tetherin shaped the functions of Vpu and Nef in human immunodeficiency virus and primate lentiviruses*. J Virol, 2010. **84**(14): p. 7124-34.
243. Zhang, Q., Z. Liu, Z. Mi, X. Li, et al., *High-throughput assay to identify inhibitors of Vpu-mediated down-regulation of cell surface BST-2*. Antiviral Res, 2011. **91**(3): p. 321-9.
244. Marichal, T., K. Ohata, D. Bedoret, C. Mesnil, et al., *DNA released from dying host cells mediates aluminum adjuvant activity*. Nat Med, 2011. **17**(8): p. 996-1002.
245. Hatano, H., *Immune activation and HIV persistence: considerations for novel therapeutic interventions*. Curr Opin HIV AIDS, 2013. **8**(3): p. 211-6.
246. Canary, L.A., C.L. Vinton, D.R. Morcock, J.B. Pierce, et al., *Rate of AIDS progression is associated with gastrointestinal dysfunction in simian immunodeficiency virus-infected pigtail macaques*. J Immunol, 2013. **190**(6): p. 2959-65.

